Journal
of
The Franklin Institute
Devoted to Science and the Mechanic Arts

Vol. 235 MARCH, 1943 No. 3

THEORY OF SUSPENSION BRIDGES

BY

STEPHEN P. TIMOSHENKO

Professor of Theoretical and Applied Mechanics, Stanford University, California.

PART I.

INTRODUCTION.

In this paper various methods of analysis of suspension bridges are discussed together with their application to several particular bridges. In the first two articles, are discussed the cases of a perfectly flexible cable and of an unstiffened suspension bridge and equations for calculation of deflections and changes in cable tension produced by live load are developed. It is shown also that in the case of heavy long span suspension bridges, deflections produced by live load are very small and a stiffening truss is not required. In the third article, the fundamental equations for stiffened suspension bridges are derived and the errors introduced in these equations by various assumptions, usually made in the process of derivation, are discussed in detail. In the fourth article an analysis of a single span stiffened suspension bridge is given and it is shown that the derivation of the necessary equations is simplified by using the method of superposition. For the determination of the most unfavorable distribution of live load, the use of influence lines is recommended. In articles 5 and 6 the application of trigonometric series in calculating deflections is discussed and it is shown that by

(Note—The Franklin Institute is not responsible for the statements and opinions advanced by contributors in the JOURNAL.)

using these series not only the calculation of deflections and bending moments can be considerably simplified but also the calculation of cable tension produced by live load can be made with better accuracy. In article 7 the theory of a suspension bridge with a continuous stiffening truss is discussed and there are derived equations for cable tension produced by live load and for bending moments at the towers. The use of the method of superposition considerably simplifies the derivation of these equations. In the last article, the case of a stiffening truss of variable cross section is discussed and it is shown that by using trigonometric series this problem can be treated without much difficulty.

1. PARABOLIC FUNICULAR CURVE.

Assume that a uniform and perfectly flexible cable fixed at points A and B, Fig. 1, is submitted to the action of dis-

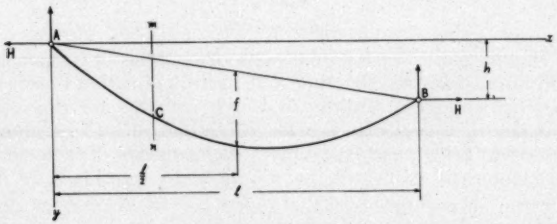

FIG. 1.

tributed vertical load. Then the ordinate y of any point C of the cable is obtained from the equation of moments with respect to C of forces to the left of this point which gives

$$\mathfrak{M}_x + H\frac{h}{l}x - Hy = 0. \qquad (a)$$

In this equation $\mathfrak{M}_x$ denotes the bending moment at the cross-section mn of a simply supported beam of span l and carrying the load acting on the cable. H is the horizontal component of the tensile force in the cable, and h is the difference in elevation of the ends of the cable. In the particular case when the load of intensity w is uniformly distributed along

the horizontal projection of the cable we have

$$\mathfrak{M}_x = \frac{wx}{2}(l - x)$$

and equation (*a*) gives

$$y = \frac{wx}{2H}(l - x) + \frac{h}{l}x \tag{1}$$

which shows that the funicular curve in this case is a parabola with vertical axis. If the ends of the cable are on the same level, we obtain

$$y = \frac{wx}{2H}(l - x). \tag{2}$$

Applying this equation to the mid-point of the cable, where the ordinate of the funicular curve represents the sag f, we obtain

$$f = \frac{wl^2}{8H} \quad \text{or} \quad H = \frac{wl^2}{8f}. \tag{3}$$

These equations hold also in the more general case shown in Fig. 1 if f is measured from the middle of the line AB joining the ends of the cable. In our further discussion the length s of the funicular curve will be required. It is obtained from the equation

$$s = \int_0^l (1 + y'^2)^{1/2} dx$$

Developing the expression under the integral sign into a series and substituting expression (2) for y, we obtain

$$s = l\left(1 + \frac{8}{3}\frac{f^2}{l^2} - \frac{32}{5}\frac{f^4}{l^4} + \frac{256}{7}\frac{f^6}{l^6} - \cdots\right).$$

In the case of flat parabolic curves, say $f/l \leqq 1/10$, we can take only the two first terms of the series and use the approximate formula:

$$s = l\left(1 + \frac{8}{3}\frac{f^2}{l^2}\right). \tag{4}$$

To establish the relation between the change in length of the curve and the change in its sag, we differentiate equation

(4), which gives

$$\Delta s = \frac{16}{3} \cdot \frac{f}{l} \Delta f \tag{5}$$

and

$$\Delta f = \frac{3}{16} \cdot \frac{l}{f} \Delta s. \tag{6}$$

To find the change Δf due to a rise in temperature of t degrees, we substitute $\Delta s = \epsilon l s$ into equation (6) and obtain

$$\Delta f = \frac{3}{16} \frac{l^2}{f} \epsilon t \left(1 + \frac{8}{3} \frac{f^2}{l^2} \right). \tag{7}$$

The elastic elongation of the cable is obtained from the equation

$$\Delta s = \int_0^s \frac{H}{A_c E_c} \frac{ds}{dx} ds = \int_0^l \frac{H}{A_c E_c} (1 + y'^2) dx$$

in which A_c is the cross-sectional area of the cable and E_c, its modulus of elasticity. Substituting equation (2) for y and integrating, we obtain

$$\Delta s = \frac{Hl}{A_c E_c} \left(1 + \frac{16}{3} \frac{f^2}{l^2} \right). \tag{8}$$

The corresponding change in sag, from equation (6), is *.

$$\Delta f = \frac{3}{16} \frac{Hl^2}{A_c E_c f} \left(1 + \frac{16}{3} \frac{f^2}{l^2} \right). \tag{9}$$

2. DEFLECTIONS OF UNSTIFFENED SUSPENSION BRIDGES.

In the case of a suspension bridge of large span the dead load uniformly distributed on a horizontal plane is usually many times larger than that uniformly distributed along the cables, and we can assume with sufficient accuracy that the curve of the cable under the action of dead load is a parabola. Let us consider now deflections in the cable produced by live load. As a first example we consider the symmetrical case in which the load of intensity p is uniformly distributed along the distance 2ξ of the span, Fig. 2. The full line indicates

* In the derivation of equations (7) and (9) it is assumed that the change Δf in sag is small and its effect on the horizontal tension H is neglected.

the shape of the cable under the action of dead load w only. Let f_w and H_w denote the corresponding values of the sag of the cable and of the horizontal component of the tensile force in the cable. The length of the cable then is

$$s = l\left(1 + \frac{8}{3}\frac{f_w^2}{l^2}\right) = l\left(1 + \frac{1}{24}\frac{w^2l^2}{H_w^2}\right). \qquad (b)$$

After application of live load p the shape of the cable will be as shown by the dotted line ACD. It consists of two parabolic curves AC and CD having a common tangent at C.

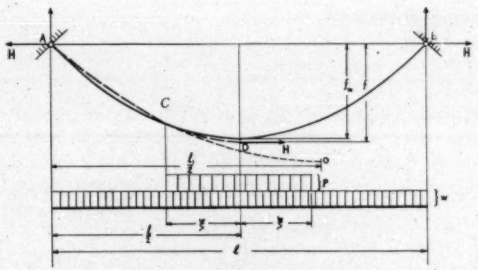

FIG. 2.

The curve CD carries the load of intensity $w + p$ and the curve AC carries the load of intensity w. The distance $l_1/2$ of the vertex o of this latter curve from the vertical through A will be found from the condition that the total load along the portion CO of the curve ACO is the same as the total load along the curve CD. Hence

$$\frac{l_1}{2} = \frac{l}{2} + \xi\frac{p}{w}. \qquad (c)$$

We denote by f and H the sag of the cable and the tensile force in the cable at D after application of the live load. One relation between these two quantities is obtained by making the equation of moments with respect to point D which gives

$$f = \frac{1}{H}\left[\frac{wl^2}{8} + \frac{p\xi}{2}(l - \xi)\right]. \qquad (d)$$

The second equation is obtained from the condition that the length of the cable remains unchanged * during application of the live load. Using for the length of the curves AO, CO and CD the approximate equation (b), the condition of inextensibility of the cable is

$$\frac{l}{2}\left(1+\frac{8}{3}\frac{f_w^2}{l^2}\right)=\frac{l_1}{2}\left(1+\frac{1}{24}\frac{w^2l_1^2}{H^2}\right)$$
$$-\frac{\xi(w+p)}{w}\left[1+\frac{\xi^2(w+p)^2}{6H^2}\right]+\xi\left[1+\frac{1}{6}\frac{\xi^2(w+p)^2}{H^2}\right]. \quad (e)$$

Introducing notations

$$\frac{p}{w}=n, \qquad \frac{2\xi}{l}=z, \quad (f)$$

we obtain from equation (e)

$$H=H_w\sqrt{1+3nz+3n^2z^2-(2n^2+n)z^3}. \quad (10)$$

Substituting this value of H into equation (d), we obtain

$$f=f_w\frac{1+n(2z-z^2)}{\sqrt{1+3nz+3n^2z^2-(2n^2+n)z^3}}. \quad (11)$$

To find what portion of the span must be loaded to produce the maximum deflection at the middle of the bridge, we put equal to zero the derivative of expression (11) with respect to z which gives the equation

$$(2n^2+n)z^4-2n(n-1)z^3-3(n-1)z^2-4z+1=0.$$

Solving this equation for several numerical values of n, we obtain for z the values given in Table I. Substituting these values of z into equation (11), we find the values of the sag f of the cable after application of the live load. The calculated ratios of the change in sag to the initial sag are given in the third line of Table I. In the case of long span bridges, the ratio p/w is usually small,† say smaller than 1/4, and it

* The small influence on the deflection of an elastic elongation of the cable will be discussed later.

† In the case of the Washington bridge over Hudson River this ratio is about 1/6.

may be seen from Table I that the deflection at the middle is of the order of one hundredth of the sag f_w or of one thousandth of the span l of the bridge. Such deflections can be considered as sufficiently small to make the use of any stiffening truss unnecessary.

TABLE I.

$n =$	0	0.10	0.25	0.50	1.00
$z =$	0.333	0.322	0.306	0.289	0.253
$\frac{f - f_w}{f_w} =$	0	0.0069	0.0151	0.0281	0.0456
$\frac{H}{H_w} =$	1	1.047	1.112	1.213	1.379

To calculate the deflection at the middle due to elastic deformation of the cable produced by live load, we use the approximate formula (9) in which $H - H_w$, instead of H, must be substituted. Then the deflection due to the elongation of the cable is

$$\Delta f = \frac{3}{16} \cdot \frac{H_w l}{A_c E_c} \cdot \frac{l}{f}\left(\frac{H}{H_w} - 1\right)\left(1 + \frac{16}{3}\frac{f^2}{l^2}\right). \qquad (g)$$

The values of the ratio H/H_w for various values of n calculated from equation (10) are given in the last line of Table I. Taking for a numerical example $n = 1/4$, $H_w/A_cE_c = 0.002$,* $f/l = 0.1$, we find $H/H_w = 1.112$ and equation (g) gives $\Delta f = 0.00044l$. This deflection must be added to the deflection $0.00151l$, calculated from equation (11), to obtain the total deflection produced by live load.

Let us consider now the deflection of the cable produced by a concentrated force applied at the middle of the span. This force can be considered as a load distributed along a very short distance, and equation (11) can be used also in this case. From notation (f) it follows that

$$nz = \frac{2p\xi}{wl} = \frac{P}{Q} = \psi \qquad (h)$$

* This value depends evidently on the allowable stresses produced by dead load.

where ψ denotes the ratio of the live load P to the dead load Q of the bridge. Substituting ψ for nz and zero for z into equation (11), we obtain

$$f = f_w \frac{1 + 2\psi}{\sqrt{1 + 3\psi + 3\psi^2}} . \tag{12}$$

In the case of long span bridges, the concentrated load P is small in comparison with the dead load Q of the bridge and ψ is a small quantity. Developing then the radical in the denominator of expression (12) into a series and taking only the first three terms of that series, we obtain

$$\sqrt{1 + 3\psi + 3\psi^2} \approx 1 + \frac{3}{2}\psi + \frac{3}{8}\psi^2$$

and equation (12) gives

$$f = f_w \left(1 + \frac{1}{2}\psi - \frac{9}{8}\psi^2 \right) .$$

Hence the deflection produced in the cable by a concentrated force applied at the middle is

$$\Delta f = f - f_w = f_w \frac{\psi}{2} \left(1 - \frac{9}{4}\psi \right) . \tag{13}$$

Assuming, for example, $\psi = 0.01$ * and $f_w/l = 0.1$, we obtain

$$\Delta f = 0.000489l$$

which is a very small deflection. To find the deflection due to elastic elongation of the cable produced by a concentrated force, we calculate first the change $H - H_w$ in the horizontal tensile force. Equation (10) in this case gives

$$H = H_w \sqrt{1 + 3\psi + 3\psi^2} \approx H_w \left(1 + \frac{3}{2}\psi + \frac{3}{8}\psi^2 \right)$$

and we obtain

$$H - H_w = \frac{3}{2} H_w \psi \left(1 + \frac{1}{4}\psi \right) .$$

* In the case of the Washington Bridge, this value of ψ corresponds to a concentrated load of 570 tons.

Substituting this for H in equation (9), we find

$$\Delta f = \frac{9}{32} \cdot \frac{H_w}{A_c E_c} \frac{l}{f} \psi \left(1 + \frac{1}{4} \psi \right) \left(1 + \frac{16}{3} \frac{f_w^2}{l^2} \right) l.$$

For small ψ which we have in the case of large spans, this deflection is a very small one.

We discussed up to now the symmetrical case of loading, Fig. 2. The case of a non-symmetrical distribution of uniform live load can be treated in a similar manner. Let us consider now a general case of vertical live load acting on a cable with both ends on the same level. The initial ordinates of the funicular curve are obtained from equation of moments which gives

$$y = \frac{\mathfrak{M}_w}{H_w} \cdot \qquad (i)$$

In this equation $\mathfrak{M}_w$ is bending moment due to dead load calculated as for a simply supported beam and H_w the horizontal component of the tensile force produced in the cable by dead load. If live load is now applied, the bending moment calculated as for a simple beam becomes $\mathfrak{M}_w + \mathfrak{M}_p$ and the horizontal component of cable tension becomes $H_w + H_p$. Denoting by η the vertical deflections of the cable, we obtain, from equation of moments,

$$y + \eta = \frac{\mathfrak{M}_w + \mathfrak{M}_p}{H_w + H_p} \qquad (j)$$

Subtracting equation (i) from this equation, we obtain

$$\eta = \frac{\mathfrak{M}_p - H_p y}{H_w + H_p} \cdot \qquad (14)$$

It is seen that the vertical deflections η can be readily calculated provided we know the horizontal component H_p of cable tension produced by live load. This later quantity can be found from geometrical considerations.

Let us consider an infinitely small element ab of the cable, Fig. 3. Under the action of live load this element elongates somewhat and takes a new position $a_1 b_1$. We denote by ξ and η the horizontal and the vertical components of the

small displacement of point a. The initial length of the element is obtained from the equation

$$ds^2 = dx^2 + dy^2. \qquad (k)$$

The length of the same element after application of live load is found from the equation

$$(ds + \Delta ds)^2 = (dx + d\xi)^2 + (dy + d\eta)^2, \qquad (l)$$

in which Δds is the elongation of the element produced by

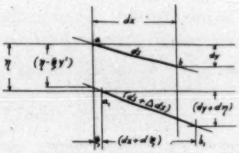

FIG. 3.

live load. Neglecting the small change in slope of the cable produced by live load,* we put

$$\Delta ds = \frac{ds H_p}{A_c E_c} \frac{ds}{dx}. \qquad (m)$$

Since $H_p ds/dx$ is that part of the tensile force in the cable which is produced by live load and which is usually much smaller than the part produced by dead load, the unit elongation $\Delta ds/ds$ is usually much smaller than one thousandth. In such a case $(\Delta ds)^2$ in equation (l) can be neglected. From the same reason, and from the observation that the curve of the cable is a flat curve, we neglect also $d\xi^2$. Then we obtain, from equations (k) and (l),

$$ds \Delta ds = dx d\xi + dy d\eta + \tfrac{1}{2} d\eta^2,$$

which gives

$$d\xi = \frac{ds}{dx} \Delta ds - \frac{dy}{dx} d\eta - \frac{1}{2} \frac{d\eta}{dx} d\eta.$$

Substituting expression (m) for Δds in this equation and

* The error introduced by this omission will be discussed later, see p. 227.

integrating, we obtain

$$\xi = \frac{H_p}{A_c E_c}\int_0^x \left(\frac{ds}{dx}\right)^3 dx - \int_0^x y'\eta' dx - \frac{1}{2}\int_0^x \eta'^2 dx. \quad (15)$$

With the values of y' and η' which are encountered in long span bridges, the value of ξ usually does not surpass one thousandth of x.* At the ends of the cable ξ vanishes and we obtain from equation (15)

$$\frac{H_p}{A_c E_c}\int_0^l \left(\frac{ds}{dx}\right)^3 dx = \int_0^l y'\eta' dx + \frac{1}{2}\int_0^l \eta'^2 dx. \quad (n)$$

The integral on the left side of this equation for the assumed parabolic shape of the cable can be readily evaluated and we obtain

$$\int_0^l \left(\frac{ds}{dx}\right)^3 dx = \int_0^l (1 + y'^2)^{3/2} dx = l\left\{\frac{1}{4}\left(\frac{5}{2} + \frac{16f^2}{l^2}\right)\left(1 + \frac{16f^2}{l^2}\right)^{1/2} + \frac{3l}{32f}\log_e\left[\frac{4f}{l} + \left(1 + \frac{16f^2}{l^2}\right)^{1/2}\right]\right\}. \quad (o)$$

On the right side of equation (n) we make integration by parts. Observing that η vanishes at the ends of the cable, and using equation (2) we obtain

$$\left.\begin{aligned} \int_0^l y'\eta' dx &= \left| y'\eta \right|_0^l - \int_0^l y''\eta dx = \frac{w}{H_w}\int_0^l \eta dx. \\ \frac{1}{2}\int_0^l \eta'^2 dx &= \frac{1}{2}\left| \eta'\eta \right|_0^l - \frac{1}{2}\int_0^l \eta''\eta dx = -\frac{1}{2}\int_0^l \eta''\eta dx. \end{aligned}\right\} \quad (p)$$

Substituting expressions (o) and (p) into equation (n) and denoting the integral (o) by L, we obtain

$$\frac{H_p}{A_c E_c} L = \frac{w}{H_w}\int_0^l \eta dx - \frac{1}{2}\int_0^l \eta''\eta dx. \quad (16)$$

This equation, together with equation (14), give the system of equations sufficient for calculation of vertical deflections of the cable.

* The maximum value of ξ/x occurs near the supports where η' and y' usually have their largest numerical values.

Let us apply these equations to the above discussed case shown in Fig. 2. In this case

$$\mathfrak{M}_p = p\xi x, \quad \text{for} \quad x < \frac{l}{2} - \xi;$$

$$\mathfrak{M}_p = p\xi x - \frac{1}{2}p\left(x - \frac{l}{2} + \xi\right)^2, \quad \text{for} \quad \frac{l}{2} + \xi > x > \frac{l}{2} - \xi;$$

$$\eta = \frac{1}{H_w + H_p}\left[p\xi x - \frac{w}{2H_w}x(l-x)H_p\right], \quad \text{for} \quad x < \frac{l}{2} - \xi;$$

$$\eta = \frac{1}{H_w + H_p}\left[p\xi x - \frac{1}{2}p\left(x - \frac{l}{2} + \xi\right)^2 - \frac{w}{2H_w}x(l-x)H_p\right], \quad \text{for} \quad \frac{l}{2} + \xi > x > \frac{l}{2} - \xi;$$

$$\eta'' = \frac{wH_p}{H_w(H_w + H_p)}, \quad \text{for} \quad x < \frac{l}{2} - \xi;$$

$$\eta'' = \frac{-pH_w + wH_p}{H_w(H_w + H_p)}, \quad \text{for} \quad \frac{l}{2} + \xi > x > \frac{l}{2} - \xi.$$

Substituting these expressions into equation (16), assuming that the cable is inextensible, and introducing our previous notations (f), we obtain, for calculation of H_p, the following quadratic equation

$$\left(\frac{H_p}{H_w}\right)^2 + 2\left(\frac{H_p}{H_w}\right) - 3nz - 3n^2z^2 + nz^3 + 2n^2z^3 = 0,$$

which gives for $H_p + H_w$ the same value as obtained from our previous equation (10).

Sometimes equation (16) is simplified by omitting the second term on the right side and taking

$$\frac{H_p}{A_cE_c}L = \frac{w}{H_w}\int_0^l \eta dx. \tag{17}$$

Considering an inextensible cable and substituting for η its

expression (14) we obtain, from equation (17),

$$H_p = \frac{\int_0^l \mathfrak{M}_p dx}{\int_0^l y dx} = \frac{3}{2fl}\int_0^l \mathfrak{M}_p dx. \qquad (18)$$

In the case shown in Fig. 2 equation (18) gives

$$H_p = \frac{nH_w}{2}(3z - z^3).$$

Applying this approximate formula to the numerical examples given in Table I, p. 219, we find that the results obtained are in good agreement with those given in the last line of Table I.

3. FUNDAMENTAL EQUATIONS FOR STIFFENED SUSPENSION BRIDGES.

It is seen from the preceding discussion that the deflection of the cable produced by live load is small only in the case of heavy long span bridges. Otherwise the deflections may be

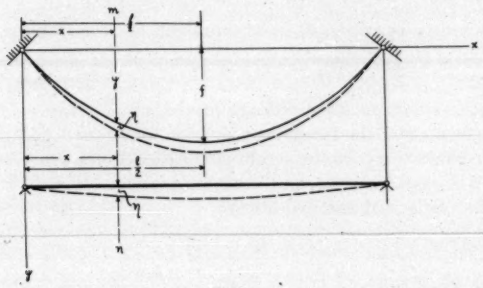

FIG. 4.

considerable. In order to reduce them, stiffening trusses are usually introduced. A simplest structure of this kind, shown in Fig. 4, consists of a single-span cable stiffened by a simply supported truss of constant cross section. It is assumed that by a proper assembly the dead load of the structure, uniformly distributed along the span, is entirely transmitted to the cable

which takes the parabolic form shown in the figure by full line. A live load produces deflection of the cable and of the truss as indicated in the figure by dotted lines. We assume that both these deflections are equal.* The spacing of hangers is assumed small as compared with the length of span so that the action of the hangers on the cable and on the truss can be considered as continuously distributed along the span.

Let us consider first the case when the structure is carrying only dead load. The truss does not suffer bending in this case, and the equation of moments for the forces to the left of a cross section *mn*, Fig. 4, then gives

$$\mathfrak{M}_w - H_w y = 0. \qquad (a)$$

When live load is applied and deflections η are produced, there will be bending moment M acting in a cross section *mn* of the truss and the equation of moments for the forces to the left of this cross section is

$$\mathfrak{M}_w + \mathfrak{M}_p - (H_w + H_p)(y + \eta) - M = 0. \qquad (b)$$

Subtracting equation (*a*) from equation (*b*), we obtain

$$M = \mathfrak{M}_p - (H_w + H_p)\eta - H_p y. \qquad (19)$$

From this equation, the bending moment at any cross section of the truss can be calculated provided the horizontal component of the tensile force in the cable and deflection η are known.

In the case of very rigid stiffening trusses, the deflections η can be neglected and we obtain

$$M = \mathfrak{M}_p - H_p y. \qquad (20)$$

This bending moment is independent of deflections and can be evaluated by the methods used in the analysis of rigid statically indeterminate structures. Investigations show that the stiffening trusses in large-span bridges are usually very flexible, and in calculation of bending moments recourse must be made to the more complete equation (19) which

* That is, the elongation of the hangers and their small inclination during deformation are neglected in this discussion.

requires the calculation of deflections η * of the truss. Using for the truss the differential equation of the deflection curve of a beam

$$EI\frac{d^2\eta}{dx^2} = -M,$$

we obtain, by using expression (19), the following equation for calculation η

$$EI\frac{d^2\eta}{dx^2} - (H_w + H_p)\eta = H_p y - \mathfrak{M}_p. \qquad (21)$$

The quantity $\mathfrak{M}_p$ in this equation can be readily calculated for any distribution of live load over the span. The quantities y and H_w are given by equations (2) and (3), and only the quantity H_p is unknown. It depends on the deflections η, and for its determination equation (16) of the preceding article is used. Equation (21) together with equation (16) completely defined the deflections of the stiffening truss. In solution of these equations the trial and error method is used. We assume a certain value for H_p, for instance the value obtained for the unstiffened cable, and with this value solve equation (21). The obtained expression for η we substitute in the integrals on the right side of equation (16). Since H_p was taken arbitrarily, the result of this substitution usually will not equal the left side of equation (16), and it will be necessary to repeat the calculation with a new assumed value of H_p. These trial calculations are continued so far as to obtain H_p with a sufficient accuracy. The procedure of this calculation with all details will be discussed in the next two articles.

Now we will discuss how accurate equations (16) and (21) are and what is the magnitude of errors introduced in these equations by neglecting various small quantities during their derivation. We begin with the discussion of elongation of the cable. In the derivation of equation (m) of the preceding article, we neglected the change in the deflection of the cable

* J. Melan was the first who indicated the importance of considering deflections in analysis of suspension bridges, see his book, "Theorie der eisernen Bogenbrücken und der Hängebrücken," Leipzig 1906. English translation by D. B. Steinman, Chicago, 1913. Melan's theory has been widely used in analysis of large span suspension bridges in this country.

produced by live load. Taking into account this additional deflection we obtain

$$\Delta ds = \frac{ds H_p}{A_c E_c}\left[1 + (y' + \eta')^2\right]^{\frac{1}{2}} \approx \frac{ds H_p}{A_c E_c}\left(\frac{ds}{dx} + y'\eta' + \frac{1}{2}\eta'^2\right).$$

Using this more accurate expression for Δds we obtain, instead of equation (n) of the preceding article, the following equation

$$\frac{H_p}{A_c E_c}\int_0^l \left(\frac{ds}{dx}\right)^3 dx = \int_0^l y'\eta' dx + \frac{1}{2}\int_0^l \eta'^2 dx - \frac{H_p}{A_c E_c}\int_0^l \left(\frac{ds}{dx}\right)^2 \left(y'\eta' + \frac{1}{2}\eta'^2\right) dx.$$

The last term on the right side of this equation represents the required correction. Since $H_p/A_c E_c$ is usually smaller than one thousandth we conclude that the relative error in the magnitude of the right side of equation (n) due to the use of the approximate expression (m) is of the order of one thousandth, which can be disregarded in a practical analysis.

Let us consider now the effect on the bending moment in the truss of horizontal displacements ξ in the cable which were entirely disregarded in our previous derivation. To take these displacements into account, we observe that the vertical distances between the full line and dotted line curves, marked by η in Fig. 4, are more accurately equal to $\eta - \xi dy/dx$, as shown in Fig. 3. We note also that each element of the load transmitted to the cable, and approximately equal to $-dx(H_w + H_p)d^2y/dx^2$, has a horizontal displacement ξ, which produces the change in moment of this element equal to

$$-\xi dx(H_w + H_p)\frac{d^2y}{dx^2}.$$

With these two considerations we obtain, instead of expression (19), the following more accurate value of the bending moment:

$$M = \mathfrak{M}_p - (H_w + H_p)\eta - H_p y + (H_w + H_p)\xi\frac{dy}{dx} - (H_w + H_p)\int_0^x \frac{d^2y}{dx^2}\xi dx. \quad (22)$$

V.2
194

The required correction in the bending moment is represented by the last two terms in this expression. To get a clearer idea regarding the magnitude of this correction, let us calculate the intensity of the load acting on the truss. This intensity is obtained as the second derivative with respect to x of the bending moment (22), taken with opposite sign, which gives

$$-\frac{d^2M}{dx^2} = p + H_p\frac{d^2y}{dx^2} + (H_w + H_p)\frac{d^2\eta}{dx^2} - (H_w + H_p)\frac{d}{dx}\left(\frac{d\xi}{dx}\frac{dy}{dx}\right). \quad (23)$$

The last term in this expression represents the correction due to horizontal displacements of the cable.

The same expression for the intensity of the load on the truss is obtained also in another manner by subtracting the intensity of the upward pull of the hangers on the truss from the combined intensity $w + p$ of the downward loading. The intensity of the vertical loading on the cable at a distance x from the left support is

$$q = -(H_w + H_p)\frac{d^2}{dx^2}\left(y + \eta - \xi\frac{dy}{dx}\right). \quad (c)$$

The upward pull transmitted to a length dx of the truss at x is the downward pull on a horizontal length $dx[1 + (d\xi/dx)]$ at $x + \xi$ on the deflected cable. Hence the required intensity of the load on the truss is

$$w + p - \left(q + \xi\frac{dq}{dx}\right)\left(1 + \frac{d\xi}{dx}\right) = w + p - q - \frac{d}{dx}(q\xi). \quad (d)$$

Substituting for q its expression (c) and neglecting small terms of higher order, we obtain the previous expression (23).*

* The correction due to horizontal displacements ξ of the cable has been discussed in a recent paper by R. J. Atkinson and R. V. Southwell, Proc. of the Institution of Civil Engineers, session 1938–1939, p. 289. These authors overlooked the term $-\xi(dy/dx)$ in the above expression (c) and did not obtain a satisfactory expression for the correction.

produced by live load. Taking into account this additional deflection we obtain

$$\Delta ds = \frac{ds H_p}{A_c E_c}[1 + (y' + \eta')^2]^{\frac{1}{2}} \approx \frac{ds H_p}{A_c E_c}\left(\frac{ds}{dx} + y'\eta' + \frac{1}{2}\eta'^2\right).$$

Using this more accurate expression for Δds we obtain, instead of equation (n) of the preceding article, the following equation

$$\frac{H_p}{A_c E_c}\int_0^l \left(\frac{ds}{dx}\right)^3 dx = \int_0^l y'\eta' dx + \frac{1}{2}\int_0^l \eta'^2 dx - \frac{H_p}{A_c E_c}\int_0^l \left(\frac{ds}{dx}\right)^2 \left(y'\eta' + \frac{1}{2}\eta'^2\right) dx.$$

The last term on the right side of this equation represents the required correction. Since $H_p/A_c E_c$ is usually smaller than one thousandth we conclude that the relative error in the magnitude of the right side of equation (n) due to the use of the approximate expression (m) is of the order of one thousandth, which can be disregarded in a practical analysis.

Let us consider now the effect on the bending moment in the truss of horizontal displacements ξ in the cable which were entirely disregarded in our previous derivation. To take these displacements into account, we observe that the vertical distances between the full line and dotted line curves, marked by η in Fig. 4, are more accurately equal to $\eta - \xi dy/dx$, as shown in Fig. 3. We note also that each element of the load transmitted to the cable, and approximately equal to $-dx(H_w + H_p)d^2y/dx^2$, has a horizontal displacement ξ, which produces the change in moment of this element equal to

$$-\xi dx(H_w + H_p)\frac{d^2y}{dx^2}.$$

With these two considerations we obtain, instead of expression (19), the following more accurate value of the bending moment:

$$M = \mathfrak{M}_p - (H_w + H_p)\eta - H_p y + (H_w + H_p)\xi\frac{dy}{dx} - (H_w + H_p)\int_0^x \frac{d^2y}{dx^2}\xi dx. \quad (22)$$

The required correction in the bending moment is represented by the last two terms in this expression. To get a clearer idea regarding the magnitude of this correction, let us calculate the intensity of the load acting on the truss. This intensity is obtained as the second derivative with respect to x of the bending moment (22), taken with opposite sign, which gives

$$-\frac{d^2M}{dx^2} = p + H_p\frac{d^2y}{dx^2} + (H_w + H_p)\frac{d^2\eta}{dx^2} - (H_w + H_p)\frac{d}{dx}\left(\frac{d\xi}{dx}\frac{dy}{dx}\right). \quad (23)$$

The last term in this expression represents the correction due to horizontal displacements of the cable.

The same expression for the intensity of the load on the truss is obtained also in another manner by subtracting the intensity of the upward pull of the hangers on the truss from the combined intensity $w + p$ of the downward loading. The intensity of the vertical loading on the cable at a distance x from the left support is

$$q = -(H_w + H_p)\frac{d^2}{dx^2}\left(y + \eta - \xi\frac{dy}{dx}\right). \quad (c)$$

The upward pull transmitted to a length dx of the truss at x is the downward pull on a horizontal length $dx[1 + (d\xi/dx)]$ at $x + \xi$ on the deflected cable. Hence the required intensity of the load on the truss is

$$w + p - \left(q + \xi\frac{dq}{dx}\right)\left(1 + \frac{d\xi}{dx}\right) = w + p - q - \frac{d}{dx}(q\xi). \quad (d)$$

Substituting for q its expression (c) and neglecting small terms of higher order, we obtain the previous expression (23).*

* The correction due to horizontal displacements ξ of the cable has been discussed in a recent paper by R. J. Atkinson and R. V. Southwell, Proc. of the Institution of Civil Engineers, session 1938–1939, p. 289. These authors overlooked the term $-\xi(dy/dx)$ in the above expression (c) and did not obtain a satisfactory expression for the correction.

Substituting for ξ the first two terms in expression (15) into the last term of expression (23), we find that the correction in the intensity of the load on the truss, due to horizontal displacements ξ, is

$$-(H_w+H_p)\frac{d}{dx}(\xi' y') = -(H_w+H_p)\left\{-\frac{w}{H_w}\left[\frac{H_p}{A_cE_c}s'^3 - y'\eta'\right] + y'\left[\frac{3H_p}{A_cE_c}s'^2 s'' + \frac{w}{H_w}\eta' - y'\eta''\right]\right\},$$

where primes denote the first derivative with respect to x.

For flat curves we can take

$$s' \approx 1 + \frac{1}{2}y'^2, \qquad s'' \approx -\frac{w}{H_w}y',$$

which gives

$$-(H_w+H_p)\frac{d}{dx}(\xi' y') = \frac{(H_w+H_p)w}{H_w}\left[\frac{H_p}{A_cE_c}(s'^3 + 3s'^2y'^2) - 2y'\eta'\right] + (H_w+H_p)\eta''y'^2. \quad (e)$$

From our previous discussion we conclude that the first term on the right side of this equation is of the order of one thousandth of w and can be neglected in practical calculation. The second term, $(H_w+H_p)\eta''y'^2$, can also be considered as small in comparison with the term $(H_w+H_p)\eta''$ representing the effect on the intensity of the load of vertical deflections of the cable. Hence the total effect of horizontal displacements of the cable can be considered as small and usually can be neglected in practical calculation. If we would like to take that effect into consideration, we can begin with a solution of equations (16) and (21). Knowing η we calculate ξ from equation (15) and the more accurate value for bending moment from equation (22).

In a similar manner the effect of extension of hangers on the magnitude of bending moment can be evaluated. The

calculation shows that this effect is also very small and can be neglected.*

Let us consider now the effect of shearing force on deflection of a stiffening truss. For this purpose we take the differential equation of the deflection curve in the following form:

$$EI\frac{d^2\eta}{dx^2} = -M + mEI\frac{d^2M}{dx^2}, \qquad (f)$$

in which the second term on the right side represents the effect of shearing force on deflection. The magnitude of factor m in this term depends on the kind of structure used for the stiffening truss. In the case of an I-beam, we take

$$m = \frac{1}{A_w G} \qquad (g)$$

where A_w is the cross-sectional area of the web of the beam and G is the modulus of elasticity of the material in shear.

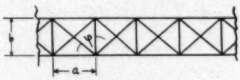

FIG. 5.

In the case of a truss, as shown in Fig. 5, we take †

$$m = \frac{1}{A_d E \sin\varphi \cos^2\varphi} \qquad (h)$$

where A_d is the sum of cross-sectional area of the two diagonals in a panel.

Substituting for M in equation (f) its expression (19), we obtain

$$EI[1 + m(H_w + H_p)]\frac{d^2\eta}{dx^2} - (H_w + H_p)\eta = -\mathfrak{M}_p + H_p y - mEI\left(p - \frac{H_p}{H_w}w\right). \qquad (24)$$

* Such calculations were made by F. E. Turneaure, see the book "Modern Framed Structures" by Johnson, Bryan and Turneaure, Vol. 2, 9th ed., p. 299, 1917.

† See writer's book, "Theory of Elastic Stability," 1936, p. 143.

This equation is of the same form as equation (21) and we see that the effect of shearing force can be readily taken into account provided the factor m is known.

In derivation of equation (16) the elastic elongation of the cable alone was considered. The equation can be readily generalized and extended to those cases in which an elongation of the cable depends also on a change in its temperature. Instead of equation (m) of the preceding article, we use in such a case the equation

$$\Delta ds = \frac{ds H_s}{A_c E_c} \frac{ds}{dx} + ds\epsilon t \qquad (i)$$

where ϵ is the coefficient of thermal expansion, and H_s is the horizontal component of the tensile force produced in the cable by the combined action of live load and temperature change. Using equation (i), instead of equation (m), and introducing the notation

$$\int_0^l \left(\frac{ds}{dx}\right)^2 dx = L_1$$

we obtain

$$\frac{H_s}{A_c E_c} L + \epsilon t L_1 = \frac{w}{H_w} \int_0^l \eta dx - \frac{1}{2} \int_0^l \eta'' \eta dx. \qquad (25)$$

This equation, instead of equation (16), must be used if we are considering a simultaneous action of live load and temperature change.

4. ANALYSIS OF STIFFENING TRUSSES.

Let us begin with the case in which a single concentrated load P is acting on the truss. Making the second derivative of equation (21), we find that deflections of the truss in this case are the same as those occurring in a simply supported beam subjected to the combined action of an axial tensile force $H_w + H_p$, of a uniformly distributed upward lateral load of intensity $H_p w/H_w$, and a concentrated load P as shown in Fig. 6. In such a case, with notation

$$\frac{H_w + H_p}{EI} = k^2 \qquad (26)$$

the deflections produced by the load P in the part of the beam to the left of this load, $(x < l - c)$, are *

$$\eta_1 = -\frac{P}{H_w + H_p} \cdot \frac{\sinh kc}{k \sinh kl} \sinh kx + \frac{Pcx}{(H_w + H_p)l} . \quad (27)$$

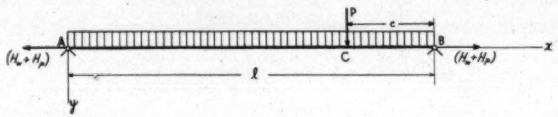

FIG. 6.

For the portion of the beam to the right of the load, $(x > l - c)$ the deflections are

$$\eta_1 = -\frac{P}{(H_w + H_p)} \frac{\sinh k(l - c)}{k \sinh kl} \sinh k(l - x) + \frac{P(l - c)(l - x)}{(H_w + H_p)l} . \quad (28)$$

The deflections produced by the upward pull are †

$$\eta_2 = -\frac{H_p}{H_w} \cdot \frac{wl^2}{H_w + H_p} \left\{ \frac{\cosh\left(\frac{kl}{2} - kx\right)}{k^2l^2 \cosh\frac{kl}{2}} - \frac{1}{k^2l^2} + \frac{x(l - x)}{2l^2} \right\} . \quad (29)$$

The total deflections η of the truss are obtained by superposing deflections η_1 on deflections η_2.

To determine the magnitude of tension H_p, entering into equations (27), (28), and (29), we use equation (17), which is obtained from equation (16) by omitting the second term on the right side.‡ Substituting expressions (27) to (29) into

* See "Strength of Materials," Vol. 2, p. 39.

† See "Strength of Materials," Vol. 2, p. 40.

‡ This term usually has only a small effect on the magnitude of H_p. This effect will be discussed in the next article.

equation (17) and performing the integration, we obtain, for calculating H_p, the equation

$$H_p\left[\frac{H_w + H_p}{A_c E_c}\cdot\frac{L}{l} + \frac{1}{12}\left(\frac{8f}{l}\right)^2 \times\left(1 - \frac{12}{k^2l^2} + \frac{24}{k^3l^3}\tanh\frac{kl}{2}\right)\right] = P\frac{8f}{l}\left\{\frac{1}{2}\frac{c}{l}\left(1 - \frac{c}{l}\right) - \frac{1}{k^2l^2\sinh kl}\times[\sinh kl - \sinh kc - \sinh k(l-c)]\right\}. \quad (30)$$

In the case of long span bridges the quantity kl is usually a number of considerable magnitude * and all terms in equation (30), containing k are small and in a first approximation can be neglected. The term $(H_w + H_p)/A_cE_c$ can also be neglected as very small, and we obtain

$$H_p = \frac{3}{4}P\frac{l}{f}\cdot\frac{c}{l}\left(1 - \frac{c}{l}\right).$$

For $c = l/2$ this gives

$$H_p = \frac{3}{2}P\frac{l}{8f}.$$

The same result we obtain, for small ψ, from equation (10), which indicates that by omitting all terms containing k we obtain, from equation (30), for H_p the same value as in the case of an unstiffened suspension bridge.

Equation (30) can be used for calculating the influence line for H_p. In such a case we assume that P is a small load moving along the truss. Then H_p can be neglected in comparison with H_w, $kl \approx l\sqrt{H_w/EI}$, and we obtain

$$H_p = P\frac{8f}{l}\frac{\frac{1}{2}\frac{c}{l}\left(1 - \frac{c}{l}\right) - \frac{1}{k^2l^2\sinh kl}\times[\sinh kl - \sinh kc - \sinh k(l-c)]}{\frac{H_w}{A_cE_c}\frac{L}{l} + \frac{1}{12}\left(\frac{8f}{l}\right)^2\left(1 - \frac{12}{k^2l^2} + \frac{24}{k^3l^3}\tanh\frac{kl}{2}\right)}.$$

* In the case of the Ambassadore Bridge (Detroit) $kl = 9.52$. In the case of the Washington Bridge, after placing the planned stiffening truss, $kl = 35$.

The magnitude of H_p depends not only on position of the load P but also on the quantities kl, H_w/A_cE_c, and f/l. In Fig. 7*a* is shown the influence line for H_p calculated on the assumption that $kl = 10$, $H_w/A_cE_c = 0.002$ and $f/l = 0.1$. For

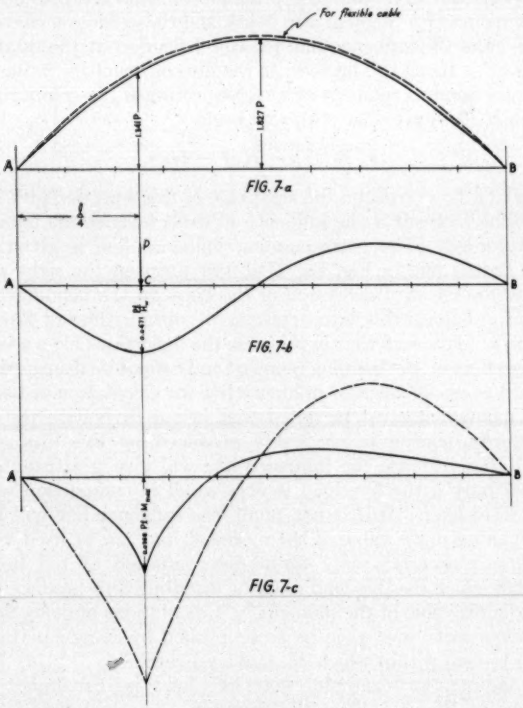

FIG. 7.

comparison there are shown in the same figure by dotted line the values of H_p for a non-stiffened cable. It is seen that for the assumed value of kl the stiffened truss has only a small effect on the magnitude of H_p.

Having H_p and using equations (27) to (29), we can calculate the deflections of the truss. In Fig. 7*b* the deflection curve is constructed for the case where $c = 0.75l$. Since H_p is neglected in comparison with H_w, the deflections become proportional to P and the principle of superposition holds. The reciprocity theorem also holds, and the deflection curve in Fig. 7*b* is the influence line for the deflection at the quarter point C. Using this line we can readily construct the influence line for bending moment at C. Neglecting H_p in comparison with H_w in expression (19), we obtain

$$M = \mathfrak{M}_p - H_p y - H_w \eta.$$

The first two terms on the right side of this equation give the bending moment if the influence of deflections of the truss is disregarded. The corresponding influence line is given by the dotted line in Fig. 7*c*. The last term on the right side gives the effect of deflection of the truss on the bending moment. Taking this into account, we obtain the full line in Fig. 7*c*. It is seen that in this case the deflections have a very large effect on the bending moment and cannot be disregarded.

In using the derived influence line for calculation of bending moment it must be noted that in our derivation the increase of tension in the cable produced by live load was neglected. Hence the influence line will give a satisfactory result only if the live load is very small in comparison with the dead load. If it is not small, the influence line will not give an accurate value of the moment, and can be used with sufficient accuracy only for a determination of the limits within which the live load must be distributed to produce the maximum value of the moment.* Calculations of deflections and moments must then be accomplished by using equations (27) to (30) within which H_p has been retained.

Assume, for example, that live load is distributed as shown in Fig. 8. Then the equation for calculating H_p is obtained from equation (30) by substituting pdc, instead of P, and integrating the right side of the equation from $c = a$

* The use of influence lines in analysis of suspension bridges was first proposed by T. Godard, "Annales des Ponts et Chaussées" 7e série, Vol. 8, 1894, p. 105.

to $c = b$, which gives

$$H_p\left[\frac{H_w + H_p}{A_c E_c} \cdot \frac{L}{l} + \frac{1}{12}\left(\frac{8f}{l}\right)^2\left(1 - \frac{12}{k^2l^2} + \frac{24}{k^3l^3}\tanh\frac{kl}{2}\right)\right]$$

$$= 8fp\left\{\frac{3l(b^2 - a^2) - 2(b^3 - a^3)}{12l^3} - \frac{1}{k^2l^2}\right.$$

$$\left.\times\left[\frac{b-a}{l} - \frac{\cosh kb - \cosh ka + \cosh k(l-a) - \cosh k(l-b)}{kl\sinh kl}\right]\right\}. \quad (31)$$

The value of H_p can now be calculated from this equation by successive approximations. We start by omitting all terms

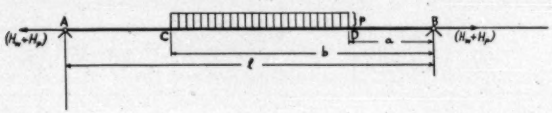

FIG. 8.

containing k and neglect also the term with $(H_w + H_p)/A_cE_c$. In this way we obtain the first approximation for H_p which will be close to the true value, if kl is of considerable magnitude,* say $kl = 10$. To get a better accuracy, we use the approximate value of H_p to calculate k from equation (26) and then substitute this value of k into equation (31), which gives then the second approximation for H_p which is usually accurate enough for practical application. If necessary, further approximations can be calculated in the same manner. When H_p has been calculated, the deflection curve will be found by using equations (27) to (29) together with the method of superposition. To find the deflections for the portion AC of the truss, Fig. 8, we substitute pdc, for P, into equation (27) and integrate from $c = a$ to $c = b$. This gives

* An example of such calculation is given in a paper by A. A. Jakkula, Publications of the International Association for Bridge and Structural Engineering, Vol. 4, p. 333, 1936.

(for $x < l - b$)

$$\eta_1 = \frac{pl}{H_w + H_p} \int_a^b \left[-\frac{\sinh kc}{kl \sinh kl} \sinh kx + \frac{cx}{l^2} \right] dc$$

$$= \frac{pl^2}{H_w + H_p} \left[\frac{\cosh ka - \cosh kb}{k^2 l^2 \sinh kl} \sinh kx + \frac{(b^2 - a^2)x}{2l^3} \right].$$

To obtain the complete deflection, we superpose on this deflection the deflection η_2 produced by the upward pull (eq. 29) which gives, for $x < l - b$,

$$\eta = \eta_1 + \eta_2 = \frac{pl^2}{H_w + H_p}$$

$$\times \left[\frac{\cosh ka - \cosh kb}{k^2 l^2 \sinh kl} \sinh kx + \frac{(b^2 - a^2)x}{2l^3} \right]$$

$$- \frac{H_p w l^2}{H_w (H_w + H_p)} \left[\frac{\cosh \left(\frac{kl}{2} - kx \right)}{k^2 l^2 \cosh \frac{kl}{2}} - \frac{1}{k^2 l^2} + \frac{x(l-x)}{2l^2} \right].$$

In a similar manner the deflections in the portions CD and DB of the truss can be obtained. A simpler method of calculation deflections is shown in the next article.

If a combined action of live load and temperature change is considered, the equation for calculation of the additional horizontal tension H_s is obtained by substitution into equation (31) H_s for H_p and $H_s L/A_c E_c + \epsilon t L_1$ for $H_p L/A_c E_c$ (see p. 232).

THE CALIBRATION OF THE ELECTROMAGNETIC MICROBAROGRAPH.

BY

EUGENE L. SULKOWSKI,

Assistant Seismologist, University of Pittsburgh.

INTRODUCTION.

For many years pressure oscillations of relatively short periods have been noticed on barograms recorded by instruments of low sensitivity and trace speed. These pressure fluctuations in the atmosphere attracted the attention of meteorologists, some of whom attempted to record and study the shorter periods. Difficulty in former years was encountered in the construction of barographs of high sensitivity and trace speed. Until recently, little experimental and no routine observation was attempted.

In 1874, de Rossi observed these variations in barometric pressure and directed attention to the possibility of a connection between microseismic motion and change in atmospheric pressure.[1] A definite and separate study of microbaroms was made by a Japanese scientist, Shida, who constructed a microbarograph of his own design and found that there were atmospheric oscillations in Tokyo with periods averaging six seconds.[2]

It has been observed that cyclonic storms generate pressure oscillations and that the amplitude of these oscillations varies with the intensity of the storm. On ships at sea a pumping motion of the barometer is noticeable while passing through hurricanes or typhoons. Gherzi describes such pumping in which the amplitudes amount to 5 mm. of Hg or more.[3] This type of pumping was recorded on a barograph with the passage of a hurricane over Washington, D. C. An enlargement of a

[1] M. S. de Rossi, *Bulletin del Vulcanismo Italiano*, 1 (1874).

[2] T. Shida, *Nature* (Review), 92: 45 (1909).

[3] E. Gherzi, "Etudes sur les Microseismes," Observatoire de Zi-Ka-Wei. *Notes de Seismologie*, No. 5 (1924).

portion of the barogram shows the "raggedness" of the trace due to the "pumping" effect.[4]

It has been found by meteorologists that there is a whole range of frequencies of pressure oscillations brought about by adiabatic changes in the atmosphere. Brunt [5] presented a

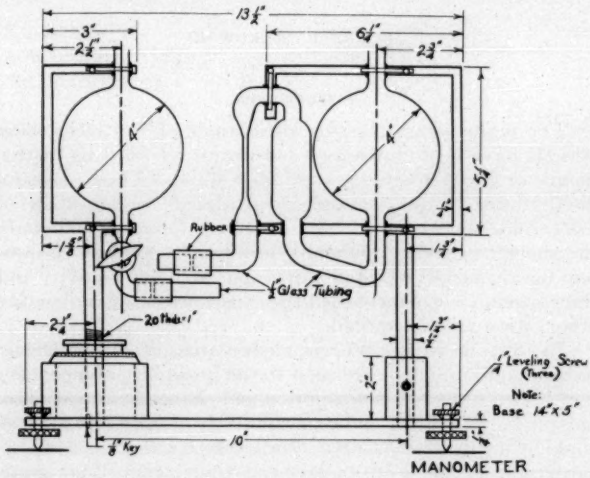

FIG. 1.

paper giving the equations for the periods of such oscillations. Johnson,[6] in his discussions of Brunt's paper, presented a table of periods that are expected from certain variations of the temperature gradient as compared with the dry adiabatic rate.

More recently, the study of microbaroms has attracted the attention of seismological laboratories, for the seismologist is

[4] D. C. Bradford, "On a Study of Microseisms Recorded at Sitka, Alaska," *Bulletin of the Seismological Society of America*, **25**: 323–342 (October, 1935).

[5] D. Brunt, "The Period of Simple Vertical Oscillations in the Atmosphere," *Quarterly Journal of the Royal Meteorological Society*, **53**: 30 (1927).

[6] N. K. Johnson, "Atmospheric Oscillations Shown by the Microbarograph," *Quarterly Journal of the Royal Meteorological Society*, **55**: 13 (1929).

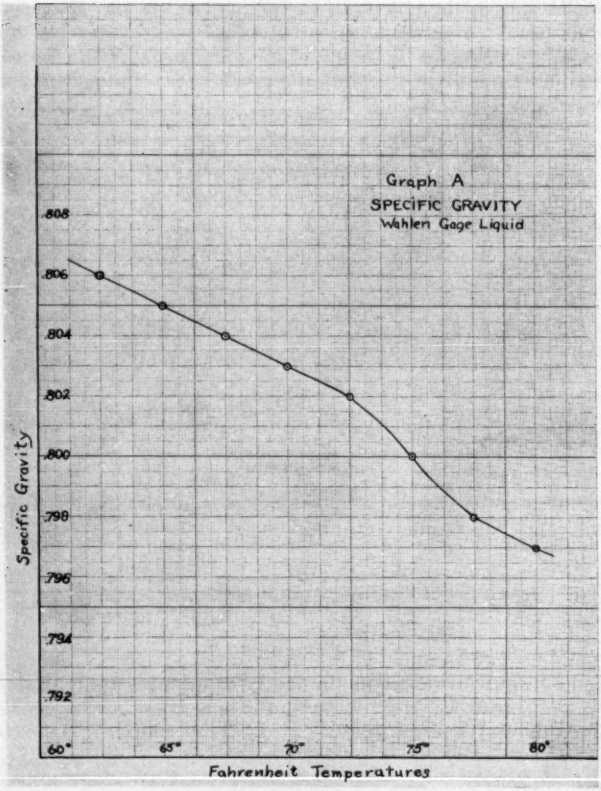
Graph A
SPECIFIC GRAVITY
Wahlen Gage Liquid
.808
.806
.804
.802
.800
.798
.796
.794
.792
Specific Gravity
60°
65°
70°
75°
80°
Fahrenheit Temperatures

FIG. 2.

interested in the theory of microseisms as caused by pressure oscillations in the atmosphere. At the seismological station of St. Louis University, a microbarograph was constructed and set in operation for the study of microseisms.[7] At Pasadena, H. Benioff and B. Gutenberg designed a microbarograph and

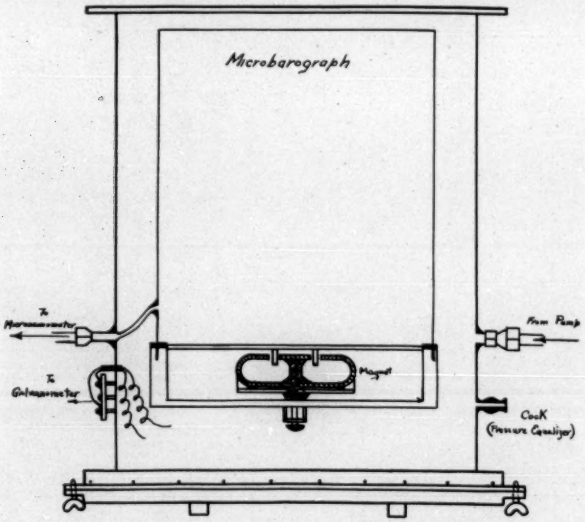

FIG. 3.

applied the instrument to the study of microseisms.[8] Later the instrument was used to study the velocity of sound waves caused by battleship gunfire.[9] H. F. Baird and C. J. Banwell

[7] J. B. Macelwane and J. E. Ramirez, "The Electromagnetic Microbarograph and Its Performance," *Transactions of the American Geophysical Union*, 1: 125–128 (1938). The original microbarograph at Saint Louis University was constructed in 1934 at the shops of the Columbia Can Company by Mr. Carl Methudy and D. C. Bradford. It was placed in test operation in the spring of 1935.

[8] H. Benioff and B. Gutenberg, "An Electromagnetic Microbarograph," Paper presented at the meeting of the Seismological Society of America, April 1, 1938.

[9] B. Gutenberg, "The Velocity of Sound Waves in the Stratosphere in Southern California," *Bulletin of American Meteorological Society*, p. 192 ff. (May, 1939).

at Christchurch, New Zealand, have constructed a microbarograph using a condenser microphone and vacuum tubes. The apparatus was used to record air pressure oscillations and the results were applied to recorded microseisms.[10] From the meteorologist's view point, the microbarograph should find application in the study of the effects of microbaroms on

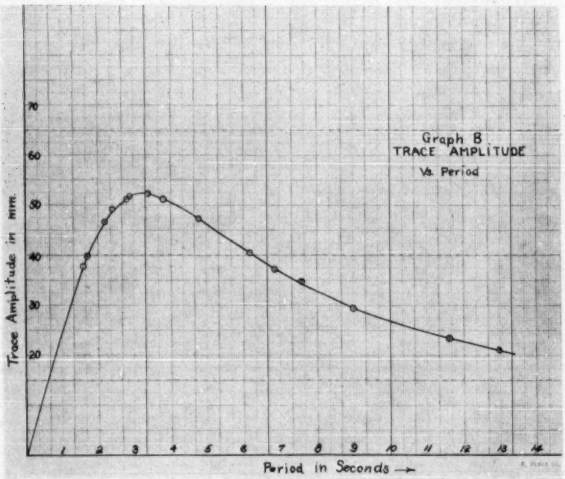

FIG. 4.

weather conditions. To arrive at definite conclusions in the observation of weather, the instrument must be calibrated in order to interpret the results to a high degree of accuracy.

THE MICROBAROGRAPH AT THE UNIVERSITY OF PITTSBURGH.

To investigate the propagation of short period atmospheric oscillations, an electromagnetic microbarograph was designed, constructed, and calibrated at the University of Pittsburgh

[10] H. J. Baird and C. J. Banwell, "Recording of Air Pressure Oscillations Associated with Microseisms at Christchurch," *New Zealand Journal of Science and Technology*, 21: No. 6B, 315B–392B (1940).

Seismological Laboratory. This paper describes the apparatus and method used in calibrating the microbarograph.

Fundamentally, the Pittsburgh instrument resembles those used by St. Louis [11] and California Institute of Technology at Pasadena.[12] This microbarograph, constructed by James Shear, a former graduate assistant, with collaboration of D. C. Bradford and the author, differs in type of magnet and

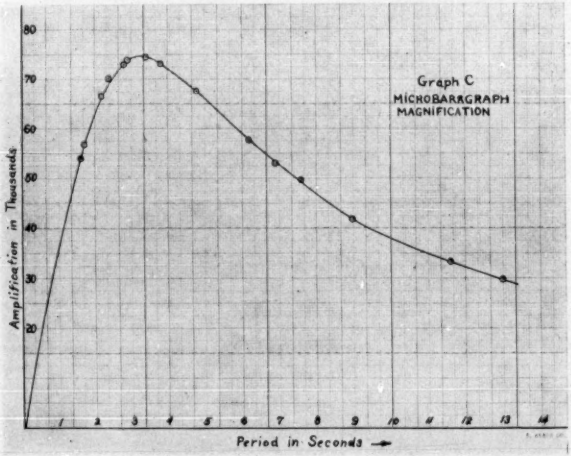

FIG. 5.

mounting used. An alnico steel magnet of a high flux density was loaned to the observatory by a local research organization.

As seen in the drawings, the magnet and coil are easily accessible for adjustments. The coil is centered in the magnetic field by the use of a sensitive amplifier and earphones. The output of the coil is coupled to the input of the amplifier and the earphones are coupled to the output of the amplifier. A sound heard in the phones during the movement of the microbarograph diaphragm, denotes the contact of the coil with the magnet. If no sound is detected, the coil is centered.

[11] J. B. Macelwane and J. E. Ramirez, op. cit., p. 126.
[12] B. Gutenberg, op. cit., p. 194.

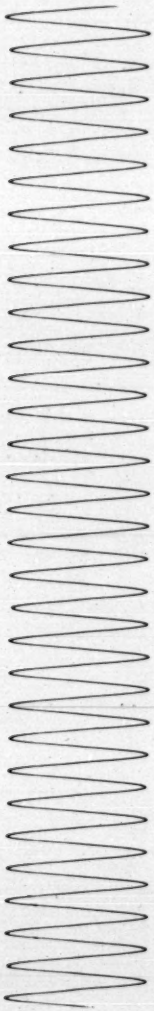

FIG. 6.

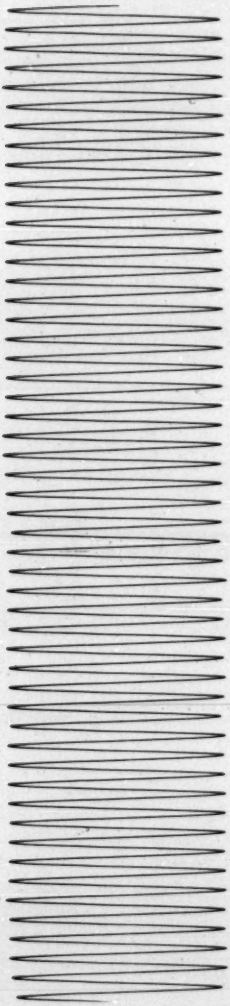

FIG. 7.

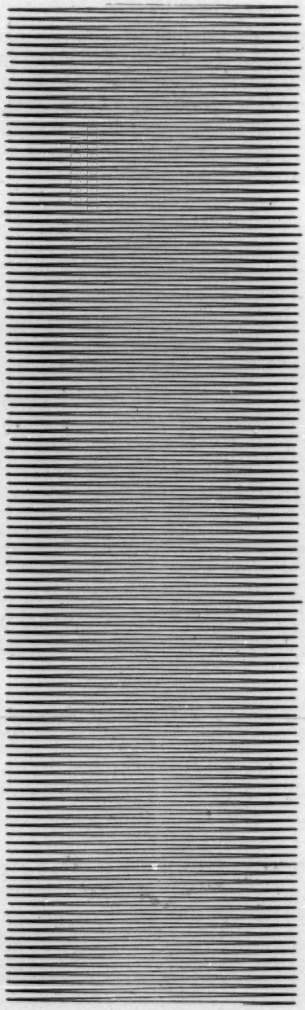

FIG. 8.

To date there has been no paper on the calibration of the microbarograph presenting the amplification as a function of the period. At St. Louis, the instrument was calibrated by the contact [13] of an off-center flywheel with the diaphragm. The flywheel, set into rotation and allowed to die down, gave a constant amplitude with a varying period. Sufficiently accurate results were unobtainable because the motion was unidirectional, the vibrations died down in two or three

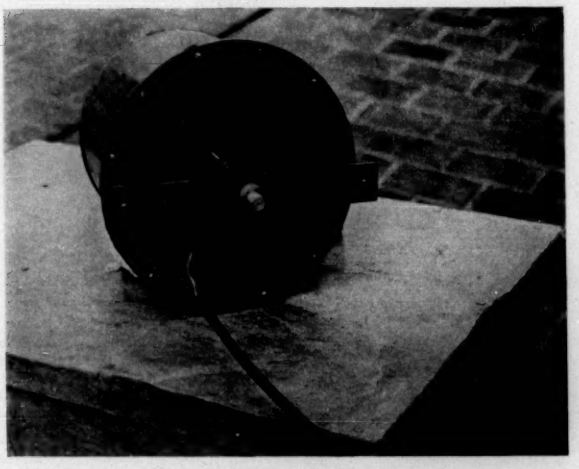

FIG. 9. Electromagnetic microbarograph.

minutes, and the flywheel caused the membrane to move off-center with each impulse. This method did not approximate the true motion due to atmospheric oscillations. The statement of magnification was indefinite as it was reached by the comparison of mechanical-optical magnification to galvanometric magnification.

The equipment used in the calibration of the Pittsburgh microbarograph consists of a chamber, pump, motor and speed reducer, micromanometer, galvanometer, and recording

[13] J. B. Macelwane and J. E. Ramirez, op. cit., p. 127.

V.2
194

drum. Each unit is presented in the order named and all details of dimensions and structure are given in the drawings.

The chamber is constructed of 18 gauge galvanized sheet iron and the lid of 10 gauge iron. The lid, entirely covered by a gasket, is attached to the chamber by wing bolts which pierce the rim. By applying a heavy grease to the rim the lid is made completely air tight. To the chamber, near the rim, are soldered a connector for the pump, pressure equalizer, connector for the micromanometer, and a copper tube for the lead-through of the wires. The pressure equalizer is used to

FIG. 10. Reservoir.

equalize periodically the atmospheric pressure between the room and chamber. The copper tubing, filled with an insulating compound, permits the electrical wires to the galvanometer to be led from the chamber in an air tight conduit. The chamber rests in a wooden cradle. The pump can be attached to the pump connector or micromanometer connector without changing the final results.

The brass pump is used to vary the pressure in a positive and negative direction in the chamber; that is, on the "in" stroke the piston slightly compresses the chamber air and on the "out" stroke the chamber air is slightly rarefied. The

displacement of the pump during compression is equal to the pump displacement during rarefaction. The piston end is fitted with a thin leather gasket and leakage is prevented by greasing the piston and gasket. The pump and piston guide are mounted on a brass plate which is firmly attached to a wooden base. This allows the outlet of the pump to be attached horizontally to the chamber.

Since the microbarograph was to be calibrated within a range of periods from approximately *15* seconds to *1* second, some method of driving the pump with a variable frequency

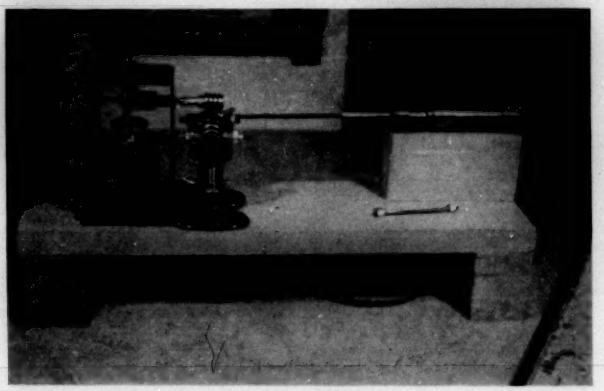

FIG. 11. Speed reducer and pump.

was to be desired. At the beginning of the project, an electric motor with a rheostat in the field circuit was tried. This method was not entirely satisfactory as the motor brushes burned and caused the motion of the rotor to be erratic. Finally an electrical unit manufactured by the Sundt Engineering Co. of Chicago, Ill., and called the Sunco Vari-Speed (Model A150–0) was used. This unit is readily adaptable for calibration as the dial can be set for any frequency between 138.6 cycles and 1028 cycles per minute. As this frequency is too high to operate the pump directly, a worm and gear with a ratio of thirty to one are coupled to the vari-speed, thus

giving the pump a periodicity from 1 to 13 seconds. The worm gear is attached to the vari-speed drive shaft and the gear wheel is placed on the shaft which drives the pump piston. The gear wheel shaft rotates in two rings of ball bearings to eliminate friction and erratic rotation. This unit is supported by stands, the height of which can be varied. The total stroke of the pump is 7/8 of an inch, that is the compressional stroke is 7/16 of an inch and the rarefactional stroke is 7/16 of an inch. Details of the mounting and placement of the drive can be secured from the drawing.

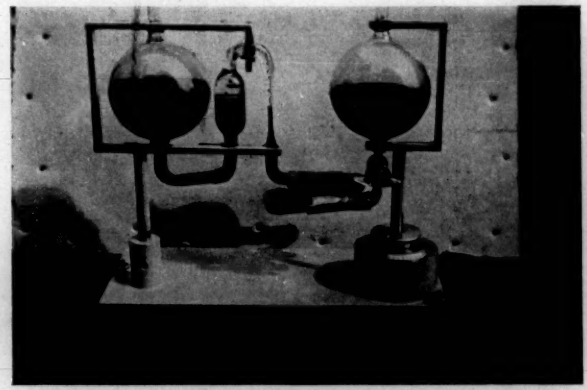

FIG. 12. Micromanometer.

To measure the pressure and rarefaction applied by the pump to the chamber, a micromanometer was constructed. This instrument, known as the Wahlen Gauge, is similar in design to that presented in the paper by Louis W. Huber.[14] The micromanometer at the University of Pittsburgh differs from that used by L. W. Huber in the type of measuring device employed in holding the movable bulb. Huber's instrument measures the liquid displacement by raising or lowering

[14] Louis W. Huber, "Wahlen Micromanometer Accurately Measures Static and Velocity Heads in Mine Ventilation," *Coal Age*, 23: No. 17, 669–674 (April 26, 1923).

the movable bulb with a rebuilt micrometer. Difficulty would be encountered in constructing this instrument with its multiplicity of accurately machined parts. With the weight of a brass guide bar and a bulb half-filled with liquid, the micrometer would be subject to excessive wear and loss of accuracy. The drawing shows the type of micrometer and mounting employed in the micromanometer used by the author (Fig. 1). The micrometer was calibrated in thousandths of an inch and can be interpolated to 0.0001 inches. A solution of methyl alcohol saturated with kerosene and

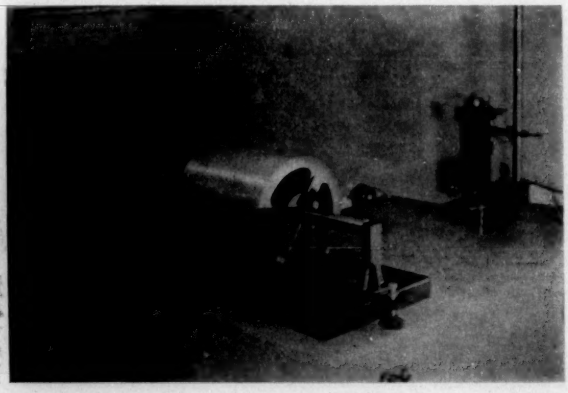

FIG. 13. Drum and galvonometer.

V.2
194

dyed with chrysiodine is the liquid used in the instrument. An accompanying graph shows the variation in specific gravity with change in the temperature of this solution (Graph *A*) (Fig. 2). As kerosene is the clear liquid in the inverted U-tube, a definite line of demarcation is obtained at the junction of the colored solution and the kerosene. A thin line is etched on the constricted tube and it serves as the zero setting of the demarcation line. A displacement of the liquid can be directly measured by raising or lowering the movable bulb with the micrometer until the liquid line coincides with the etched line.

A Henson drum set at a trace speed of 60 mm. per min. and a Rubicon galvanometer with a period of 3.3 seconds are used for photographic recording. The length of the optical lever is 763 mm. The galvanometer is critically damped by a 132 ohm resistor in series with the 137.3 ohm microbarograph coil.

PROCEDURE IN CALIBRATION.

The vari-speed drive was set at a predetermined period for each run of a record. The exact period of the pump was then read from the photographic trace. Fifteen records were made to find the magnitude of light beam displacement as a function of the period. Each pump period was recorded for approximately twelve minutes. Before and after each run the air pressure in the laboratory and chamber were balanced by the pressure equalizer. The micromanometer was not in operation during the period of recording. For measuring the applied pressure the pump was operated manually and the maximum movement of the micromanometer indicating line was noted.

To measure the volume change in the interior of the microbarograph the micromanometer was attached to it by a short piece of hard rubber tubing placed through the wall of the reservoir (Fig. 3). Precautions were taken to prevent the communication of air between the microbarograph interior and chamber and each with the air in the laboratory. As the pump pressure was applied to the reservoir, the pressure change in the interior of the microbarograph was noted. The volume change was then obtained by the application of Boyle's Law.

CALCULATIONS.

All volumes are calculated.

Total interior volume of chamber	2461.25 in.^{3}
Total volume occupied by microbarograph (Approximate)	957.66 in.^{3}
Approximate volume of air in chamber after placement of microbarograph	1503.5 in.^{3}
Volume of pump displacement	0.037336 in.^{3}
Ratio of air volume in chamber to pump displacement	$\frac{1503.5 \text{ in.}^3}{0.037336 \text{ in.}^3} = 40{,}269$

Knowing the volume ratio of reservoir to pump and knowing that this ratio was recorded, we can state that the magnification of the instrument is approximately 40,000 at an as yet unknown point on the magnification curve. Since the magnification of the microbarograph system depends upon the period of the galvanometer, it can be assumed that the curve will present points higher and lower than 40,000 depending on the period at which the galvanometer is excited. The photographic records also show that the displacement of the light spot varies with the period of the pump (Table I). A graph presents this displacement as a function of the period (Graph *B*) (Fig. 4).

By the application of Boyle's Law, it is possible to calculate the pressure which the pump applied to the air in the chamber.

TABLE I.

Recorded Data.

The double amplitude was measured at ten points on each record. The double amplitudes were noted and finally averaged, thus obtaining the amplitude for each period.

Period ..... 13.0 s		Period ..... 11.6 s	
Double Amplitude (mm.).		Double Amplitude (mm.).	
42.2		46.5	
43.0		47.0	
43.0		47.0	
41.7		47.5	
41.5		47.0	
42.0		47.5	
40.5		46.5	
41.7		46.5	
41.5		46.5	
42.5		46.5	
Average	41.9 mm.	Average	46.8 mm.
Amplitude	20.9 mm.	Amplitude	23.4 mm.
Period ..... 9.0 s		Period ..... 7.6 s	
Double Amplitude (mm.).		Double Amplitude (mm.).	
58.0		68.5	
58.5		68.5	
59.5		69.5	
58.5		70.0	
58.5		68.5	
58.5		69.0	
58.5		69.0	
59.0		68.0	
58.7		68.5	
58.5		68.0	
Average	58.6 mm.	Average	68.7 mm.
Amplitude	29.3 mm.	Amplitude	34.8 mm.

TABLE I.—*Continued*

Period ..... 6.9 s	Period ..... 6.2 s
Double Amplitude (mm.).	Double Amplitude (mm.).
74.0	81.0
74.0	81.0
74.0	81.0
74.2	81.0
74.5	80.0
75.0	81.0
74.0	81.0
74.5	80.7
74.0	81.2
74.0	81.2
Average ..... 74.1 mm.	Average ..... 80.9 mm.
Amplitude ..... 37.1 mm.	Amplitude ..... 40.4 mm.
Period ..... 4.8 s	Period ..... 3.8 s
Double Amplitude (mm.).	Double Amplitude (mm.).
95.0	102.0
95.0	102.0
95.0	103.0
95.0	102.5
94.2	103.0
94.5	102.5
95.0	102.0
94.5	102.0
95.0	102.0
95.0	102.5
Average ..... 94.8 mm.	Average ..... 102.3 mm.
Amplitude ..... 47.4 mm.	Amplitude ..... 51.1 mm.
Period ..... 3.4 s	Period ..... 2.9 s
Double Amplitude (mm.).	Double Amplitude (mm.).
104.2	104.0
104.5	103.7
104.5	104.0
104.0	104.0
104.5	103.5
104.5	103.5
104.5	104.0
104.5	104.0
104.0	103.7
104.5	103.5
Average ..... 104.1 mm.	Average ..... 103.7 mm.
Amplitude ..... 52.1 mm.	Amplitude ..... 51.8 mm.
Period ..... 2.8 s	Period ..... 2.4 s
Double Amplitude (mm.).	Double Amplitude (mm.).
102.0	98.0
102.0	98.5
102.5	98.4
102.0	98.0
102.4	98.2
102.5	98.0
102.4	98.0
102.0	98.0
102.5	98.0
102.5	98.0
Average ..... 102.2 mm.	Average ..... 98.1 mm.
Amplitude ..... 51.1 mm.	Amplitude ..... 49.1 mm.

TABLE I.—*Continued*

Period ..... 2.2 s	Period ..... 1.7 s
Double Amplitude (mm.).	Double Amplitude (mm.).
94.0	80.0
93.5	80.5
93.5	80.2
93.0	79.6
93.5	79.7
93.0	79.5
93.5	79.5
93.5	79.7
93.5	79.7
94.0	80.0
Average ..... 93.5 mm.	Average ..... 79.8 mm.
Amplitude ..... 46.7 mm.	Amplitude ..... 39.9 mm.

Period ..... 1.6 s

Double Amplitude (mm.).

75.5
75.5
76.0
75.5
76.0
76.0
75.6
76.0
75.2
75.1

Average ..... 75.6 mm.
Amplitude ..... 37.8 mm.

Let V_0 = (1,503.5 + 0.037336) in.^{3}, air vol. in chamber + pump volume

P_0 = 739.9 mm. Hg, atmospheric pressure

P_f = final pressure in chamber

V_f = 1,503.5 in.^{3}, final volume of air in chamber

$P_0V_0 = P_fV_f$

$(1{,}503.5 + 0.037336)739.9 = (1{,}503.5)Pf$

P_f = 739.91536 mm. Mercury, atmospheric pressure + pump pressure

739.91536 mm. − 739.9 mm. = 0.01536 mm. Mercury, pump pressure.

Since the air volume in the chamber was calculated approximately, the pump pressure of 0.01536 mm. of Mercury

is also approximate, but it can serve as a check on the reading obtained by the micromanometer.

$$\begin{aligned} 0.00945 \text{ in.} &= \text{micromanometer reading} \\ 0.803 &= \text{specific gravity of micromanometer fluid at } 70^\circ \text{ Fahrenheit} \\ \frac{0.00945 \times 0.803}{13.6} &= 0.005579 \text{ in. or } 0.0141 \text{ mm. Hg. pump pressure as read by micromanometer.} \end{aligned}$$

We can assume that the pressure as read by the micromanometer is reasonably correct as it checks very closely with the calculation obtained by Boyle's Law. The maximum sensitivity is,

$$\frac{0.0141 \text{ mm.}}{52.1 \text{ mm.}} = 0.00027 \text{ mm. Hg, mm. of displacement of the light spot.}$$

Data and calculations for obtaining the volume change in the interior of the microbarograph are as follows,

$$\begin{aligned} 0.007071 \text{ mm. Mercury} &= \text{applied pressure in microbarograph as read on micromanometer.} \\ \text{Let } V_m &= 1{,}516{,}460.64 \text{ mm.}^3 = \text{interior volume of microbarograph} \\ P_m &= 739.9 \text{ mm. Hg, atmospheric pressure} \\ V_x &= \text{final interior volume} \\ P_x &= 739.9 \text{ mm.} + 0.007071 \text{ mm., final pressure} \\ V_m P_m &= V_x P_x \\ 1{,}516{,}460.64 \times 739.9 &= V_x \times 739.907071 \\ V_x &= 1{,}516{,}446.15 \text{ mm.}^3 \\ 1{,}516{,}460.64 \text{ mm.}^3 - 1{,}516{,}446.15 \text{ mm.}^3 &= 14.49 \text{ mm.}^3, \text{ difference in volume} \\ 1{,}516{,}460.64 \text{ mm.}^3 &= \text{volume of microbarograph} \\ 20{,}645.06 \text{ mm.}^3 &= \text{area of microbarograph diaphragm} \\ \frac{14.49 \text{ mm.}^3}{20{,}645{,}06 \text{ mm.}^2} &= 0.0007 \text{ mm., depression of diaphragm due to applied pump pressure.} \end{aligned}$$

Since the diaphragm movement is of such a small magnitude, it may be assumed that the entire surface area moves

this distance. As the pump displacement is the same during the pressure application and rarefaction, it is therefore equal to the applied pressure. This statement may apply to the test of pressure in the reservoir and in the microbarograph.

Since we know the displacement of the light spot at different periods and the displacement of the microbarograph diaphragm, the magnification of the instrument is therefore the ratio of the spot displacement to the diaphragm displacement (Table II). For example,

TABLE II.

Table of Amplifications.

Diaphragm displacement = 0.0007 mm.

Period.	Spot Displacement. Amplitude (mm.).	Amplification.
13.0	20.9	29,857
11.6	23.4	33,428
9.0	29.3	41,857
7.6	34.8	49,714
6.9	37.1	53,000
6.2	40.4	57,714
4.8	47.4	67,714
3.8	51.1	73,000
3.4	52.1	74,428
2.9	51.8	74,000
2.8	51.1	73,000
2.4	49.1	70,142
2.2	46.7	66,714
1.7	39.9	57,000
1.6	37.8	54,000

Diaphragm movement = 0.0007 mm. (constant at periods applied during calibration)

Light spot displacement = 51.8 mm. at period of 2.9 seconds

$$\text{Magnification} = \frac{51.8 \text{ mm.}}{0.0007 \text{ mm.}} = 74{,}000.$$

The magnification for each period is obtained by the above method and a curve is plotted with the magnification as a function of the period (Graph *C*) (Fig. 5).

In conclusion, the author wishes to express his appreciation to D. C. Bradford, Director of the Seismological Observatory, for suggestions and criticisms during the course of equipment construction and calibration of the microbarograph and to F. E. Williams for data on the micromanometer liquid.

SEISMOLOGICAL OBSERVATORY,
UNIVERSITY OF PITTSBURGH,
PITTSBURGH, PENNSYLVANIA.

BREAKDOWN AND TIME-LAG OF DIELECTRIC MATERIALS.

BREAKDOWN OF LIQUID CARBON TETRACHLORIDE.

BY

S. S. ATTWOOD,
Professor of Electrical Engineering, University of Michigan,

AND

W. H. BIXBY,
Assistant Professor of Electrical Engineering, Wayne University.

The breakdown of solid and liquid dielectric materials subjected to strong electric fields is a problem of great practical importance which has received considerable theoretical attention. Only recently, however, has theory been developed to the point where the breakdown field can be predicted even approximately from fundamental physical constants. Experimental data on the breakdown and time-lag of liquid carbon tetrachloride is given here and the applicability of various theories discussed.

ELECTRIC VS. THERMAL TYPES OF BREAKDOWN

Above a certain temperature breakdown is caused by thermal instability. An electric field of constant strength established in a dielectric leads to dielectric losses which, after some time, raise the temperature and produce a temperature gradient extending from the "hot-spot" through the dielectric and electrodes to the surrounding ambient. The system is stable thermally so long as the rate of heat dissipation is greater than the rate of generation. A sufficient increase in the field strength leads to instability and the hot-spot temperature continues to rise until the dielectric is punctured, whereupon the electrode voltage drops to zero almost instantaneously. Still higher fields simply accelerate the process. The breakdown field strength is the maximum value which can be applied continuously without producing instability and breakdown, and, as indicated in Fig. 1, must fall off rapidly with an increase in the ambient temperature.

The thermal breakdown process is an essentially slow one since a field exceeding the breakdown value by a small amount may require hours to produce puncture. Finally it may be noted that this type of breakdown does not yield a

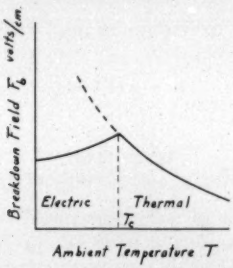

FIG. 1. Temperature dependence for fields of constant strength.

true measure of dielectric strength since the electrodes and the ambient play an important part in the process.

Electric type breakdown, with which this article is particularly concerned, is found in the lower temperature ranges below T_c in Fig. 1. (T_c for glass and NaCl crystal approxi-

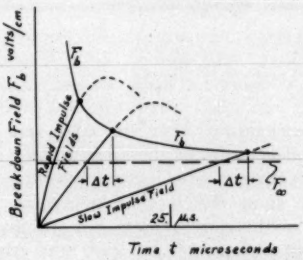

FIG. 2. Time dependence for impulse fields.

mates 200° C.) Here the conductivity and dielectric losses are small, thermal instability is not involved and the breakdown field is limited quite obviously by other than thermal factors. Increasing temperature tends to increase the break-

down field unless the adverse influence of increasing molecular spacing produces an even greater decrease.

The time factor in electric breakdown is revealed clearly if impulse fields from an impulse or lightning generator are applied suddenly to the electrodes. The effect is illustrated in Fig. 2. Slowly applied fields, say those requiring more than 25 microseconds, give breakdown values F_b which vary but little and approach asymptotically the critical value F_∞ which is the breakdown strength for a steadily applied field and represents the intrinsic electric strength of the dielectric. If we assume that breakdown is a time consuming process which begins only when the impulse field has reached the value F_∞ there must be an over-field $F_b - F_\infty$ and a time-lag Δt in order to complete the process. Immediately thereafter the electrode voltage drops almost instantaneously to zero. As the impulse field is applied more and more rapidly the over-field increases markedly while the time-lag declines but slightly. The time-lag appears to have a value of approximately two microseconds.

The importance of time-lag is illustrated in the technical application of dielectric materials as electrical insulation. Not infrequently insulation is subjected to rapidly applied fields, similar to those of Fig. 3, which originate in surges caused by lightning discharges or transients arising from switching changes in connected electrical circuits.

BREAKDOWN OF LIQUID CARBON TETRACHLORIDE.

Carbon tetrachloride was chosen for study for a number of reasons. It was felt that the breakdown values of a liquid would be less erratic than is usually true for solid materials. Furthermore the simple molecular structure, consisting of four chlorine atoms tetrahedrally disposed about the center carbon core, was in its favor, as well as the fact that its Debye dipole moment is zero. It was thought that the absence of the latter might prevent the introduction of a complicating effect.

The CCl_4 was placed in a test-cup containing two brass spheres of one inch diameter set to a spacing of .0635 cm. The impulse generator consisted of a .125 uf. condenser charged through a rectifier to 77.7 kilovolts. At this poten-

tial the condenser was discharged through a spark gap in series with a 1020 ohm non-inductive resistance and a variable inductance. Variation of the latter gave a wide control of the rate of rise of potential over the resistance whose terminals

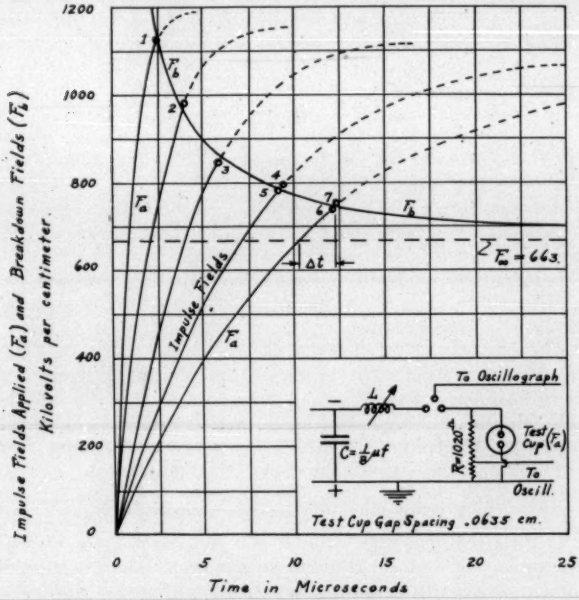

FIG. 3. Applied impulses and breakdown fields for CCl_4 in test cup.
Slowly applied impulses and breakdowns not illustrated:
No. 8—740 kv./cm. at 33 microseconds.
No. 9—755 kv./cm. at 56 microseconds.
No. 10—755 kv./cm. at 640 microseconds.

were connected across the test-cup. Seven of the ten impulses used are shown in Fig. 3. The breakdown values are indicated by circles. A cold-cathode ray oscillograph with the film placed in the vacuum was used to observe the growth of the impulses and the breakdown values F_b. A very slow

impulse (No. 10) required a different circuit in which the 77.7 K.V. condenser discharged through a spark-gap into a parallel arrangement of a condenser, resistance and test-gap. All breakdowns occurred on the front of the impulse waves so that the rate of rise of voltage was not far from linear.

The test-cup spheres were polished and cleaned with fresh CCl_4 before each test sample was poured in. After oscillographic records of the full test wave and timing wave were obtained the sample in the test-cup was connected and oscillographic records of approximately forty breakdowns at one minute intervals with the same impulse were recorded on one film. For each of the impulse waves the maximum breakdown value was obtained and is plotted as a circle in Fig. 3. That repeatable values of the breakdown could be obtained is indicated by impulses No. 4 and No. 5, which were identical, and again by No. 6 and No. 7. There was no discernible difference between tests using either chemically or commercially pure CCl_4.

Study of the breakdown values together with consideration of time-lag indicates that the asymptotic or long time breakdown field occurred at 42 K.V. With a gap length of .0635 cm. this gives $F_\infty = 663{,}000$ volts per cm. for the critical field strength of CCl_4. The theoretical curve through the breakdown points is discussed later under time-lag after theories of breakdown have first been considered.

OLDER THEORIES OF BREAKDOWN.

Older theories of electrical breakdown have been summarized by S. Whitehead.[1] Most of these theories are notable chiefly for their failure to predict even the correct order of magnitude, several in fact predict values of about 10^8 volts per cm. instead of the observed value of approximately 10^6 volts per cm. Certain of the older theories assumed that breakdown is due to the ionization of molecules by moving ions carrying the current. Modern views of ionic conduction would make it highly doubtful if ions could acquire the necessary energy or complete the process of breakdown in the

[1] S. Whitehead," Dielectric Phenomena, III, Breakdown of Solid Dielectrics." (Benn.)

time that is observed. The evidence would seem to indicate that breakdown surely is electronic in character.

Nor can it be expected, as von Hippel [2] has pointed out, that an extension of the theory of breakdown of gases would provide a solution for the condensed states of liquids and solids. In gases electrons are prevented from accelerating above a certain velocity by inelastic impacts with the atoms in which the electron kinetic energy is transformed into excitation energy of the electronic system of the atom. At atmospheric pressure, with a mean-free-path of 10^{-4} cm., about 30,000 volts per cm., or 3 volts per mean-free-path, is needed to create cumulative ionization. Only beyond this value can we expect breakdown to become possible. Extension of this type of reasoning to the closely packed atmospheres of liquids and solids would call for a breakdown field of 60 million volts per cm., a value some 60 times too large.

MODERN THEORIES OF BREAKDOWN.

Modern theories of breakdown, that is of the critical field strength or the intrinsic electric strength F_∞, have been stimulated in part by the careful breakdown experiments on the alkali-halide crystals reported by von Hippel [2] and in part by his proposal of a mechanism not previously considered which could restrain the motion of the electrons through the crystal and prevent their acceleration. One of these theories has been developed by Seeger and Teller [3] (and later modified slightly [4]) and the other by Fröhlich.[5]

Both theories are restricted to materials like the alkali-halides which are ionic type crystals. In NaCl, for instance, the ionic constituents are Na^+ and Cl^- arranged alternately throughout the crystal. CCl_4, it may be assumed, is ionic in character also with the central carbon core charged to four

[2] von Hippel, "Electric Breakdown of Solid and Liquid Insulators," *J. of Applied Phys.*, 8, Dec. 1937, p. 815. "The Electric Breakdown in Gases and Solid Insulators," *Ergeb. d. Exakt. Naturwiss*, 14, 1935, p. 79.

[3] Seeger and Teller, "On the Electrical Breakdown of the Alkali Halides," *Phys. Rev.*, 54, Oct. 1, 1938, p. 515.

[4] Seeger and Teller, *Phys. Rev.*, 58, Aug. 1, 1940, p. 279. (The formula in Reference 3 is modified slightly.)

[5] Fröhlich, "Dielectric Breakdown in Solids," *Reports on Progress in Physics*, VI, 1939, p. 411, of the Physical Society (London).

positive units, having yielded one electron to each of the four chlorine atoms or ions. The breakdown formulas developed by Seeger and Teller and by Fröhlich, with minor modifications, may at once be applied to the evaluation of F_∞ for CCl_4.

The mechanism proposed by von Hippel [2] assumes that the dielectric contains a certain number of electrons, at least partially free from molecular binding, which move under the influence of an electric field and excite vibrations of the positive and negative ionic constituents of the dielectric. For field strengths below the breakdown value an energy balance is reached by which the energy abstracted from the field by the electrons is completely absorbed by the ionic oscillators and the electron velocity is held to a relatively low value. The ionic oscillators therefore present a "resistance" to the free motion of the electrons and prevent their acceleration. The critical field strength F_∞ is reached when the "resistance" is a maximum and the ionic oscillators are absorbing energy at the maximum possible rate and the electrons achieve their maximum steady value of velocity. Stronger fields, it is assumed, can drive the electrons across the maximum resistance point and accelerate them until they acquire energy sufficient for ionization. Ionization in this case implies the release of an electron from the negative ion. The onset of ionization, it may be supposed, is merely the beginning of breakdown and that the period of time-lag is yet required before the voltage across the electrodes collapses and breakdown is complete.

THE SEEGER-TELLER FORMULA AND CCl_4.

The Seeger-Teller [3,4] theory calculates the energy absorption of the ionic oscillators per centimeter of electron motion in the direction of the field in terms of the ratio of the electron's kinetic energy to the energy quantum of the oscillator. This yields

$$eF = \frac{dW}{ds} = \frac{2\pi^2 e^2 m\nu}{h}\left(\frac{1}{k'} - \frac{1}{k}\right)\left(\frac{k}{k'}\right)^{1/2} \cdot \frac{1}{2x}\log\frac{2x - 1 + 2(x^2 - x)^{1/2}}{2x - 1 - 2(x^2 - x)^{1/2}}, \quad (1)$$

in which $x = \frac{1}{2}mv^2/h\nu$. The variable part of this equation is plotted in Fig. 4 and has a maximum value of .91 at $x = 1.7$. The critical field value then is

$$F_\infty = \frac{1.82\pi^2 emv}{h}\left(\frac{1}{k'} - \frac{1}{k}\right)\left(\frac{k}{k'}\right)^{1/2} \quad \text{(e.s.u.)}. \qquad (2)$$

In this equation the electronic charge is $e = 4.8 \times 10^{-10}$ e.s.u., the electronic mass is $m = 9.03 \times 10^{-28}$ g. and Planck's constant is $h = 6.55 \times 10^{-27}$ erg-seconds. Aside from these

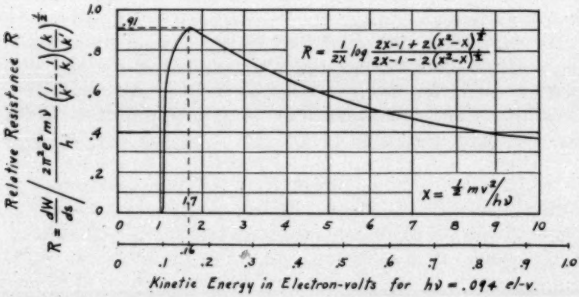
Relative Resistance R
R = dW/ds / 2π²e²mν/h (1/k' - 1/k)(k/k')^½
R = 1/2X log 2X-1 + 2(X²-X)^½ / 2X-1 - 2(X²-X)^½
X = ½ mv²/hν
1.0
.8
.6
.4
.2
0
.91
1.7
0 1 2 3 4 5 6 7 8 9 10 X
0 .1 .2 .3 .4 .5 .6 .7 .8 .9 1.0
Kinetic Energy in Electron-volts for hν = .094 e/-v.

FIG. 4. Resistance of oscillating ions as a function of electron velocity.

values it is necessary to know ν, the frequency of the absorptive oscillators, k, the dielectric constant for long wave-lengths (the static value) and k', the dielectric constant or square of the index of refraction for short wave-lengths between the infrared and ultraviolet regions.

For CCl_4 we may take $\nu = 22.85 \times 10^{12}$, corresponding to a wave-length of $13.13\mu = 13.13 \times 10^{-4}$ cm., and a quantum $h\nu = .1496 \times 10^{-12}$ ergs, equivalent to .094 electron-volts. The maximum steady velocity that an electron could acquire would then be given by 1.7 times this value, equivalent to .16 electron-volts. At this frequency the four chlorine negative ions vibrate as a unit in opposition to the vibration of the quadruply charged carbon positive ion. According to Marvin [6] infrared light of this frequency is almost completely

[6] Marvin, "Transmission and Dispersion of Liquid Chlorides," *Phys. Rev.* (1), **34**, 1912, p. 161.

absorbed, and from his evaluation of the index of refraction in the near infrared the value of $k' = 2.086$ is obtained. k, at 24° C., is given by Morgan and Lowry [7] as 2.23. Substituting these values and multiplying by 300 the calculated critical value is $F_\infty = 262{,}000$ volts per cm., which may be compared with the test value of 663,000 volts per cm.

In applying Equation 2 the "effective mass" m^* of the electron instead of the ordinary mass m should be used. A conduction electron in a solid or liquid dielectric is not "free" but is subject to a potential energy field varying periodically with the molecular spacing. In such an atmosphere the effective mass may be several times as large as the ordinary mass. Unfortunately calculations of this ratio are very difficult and so far are not convincing. If the discrepancy between test and calculated values of F_∞ is ascribed to this cause we obtain the ratio

$$\frac{m^*}{m} = \frac{663{,}000}{262{,}000} = 2.54,$$

which compares favorably with the similar values for the alkali-halide crystals for which the theory was originally developed.

The theory as outlined assumes that the electron moves in the field direction. If however the electron is forced on the average to move at some angle with the field (say 45°) the calculated value of F_∞ could be raised by the secant of the angle (say $\sqrt{2}$) and the burden placed on the mass ratio m^*/m reduced accordingly. Eventually this theory will have to be modified to provide an estimate of the temperature dependence of breakdown.

THE FRÖHLICH FORMULA AND CCl$_4$

The Fröhlich theory,[5] though similar in many respects to the Seeger-Teller theory, differs in one underlying point of great importance and far reaching consequences. In the Seeger-Teller theory the electrons are restricted to velocities corresponding to about .16 electron-volt but in the Fröhlich theory it is assumed that their velocities and kinetic energies

[7] Morgan and Lowry, *J. Phys. Chem.*, 34, 1930, p. 2385.

are much larger and correspond to several electron-volts. If the kinetic energies E of this group lie below a certain critical value E_c the energy received in falling through the field F is entirely absorbed by the ionic oscillations and they are precluded thereby from gaining further energy. However $E_c \sim 1/F$ so that E_c declines as the field strength is increased. The criterion for breakdown then takes the form that the field must be increased to the point where E_c has fallen to the value I, the potential energy required to ionize the negative ion by removal of its extra electron.

The formula for the critical field strength then takes the form

$$F_\infty = \frac{\pi^2 e(mh)^{1/2}}{2^{1/3}} \frac{(k - k')\nu^{3/2}}{a_M I} \times \left[\log \frac{4\sqrt{IE_0}}{h\nu}\right]^{1/2} \left[1 + \frac{2}{\epsilon^{h\nu/k_1 T} - 1}\right]^{1/2} \text{(e.s.u.).} \quad (3)$$

In addition to the values previously assigned,

$a_M = 5.45 \times 10^{-8}$ cm. (Average spacing between CCl_4 molecules)

$$I = \frac{hc}{\lambda_0} = \frac{(6.55 \times 10^{-27}) \times (3 \times 10^{10})}{2280 \times 10^{-8}} = 8.62 \times 10^{-12} \text{ ergs} \equiv 5.42 \text{ electron-volts.}$$

(Ionization potential energy)

λ_0 is the limit of absorption occurring for $\lambda < \lambda_0$.

$$E_0 = \frac{2^{4/3}h^2}{32ma_M^2} = 1.262 \times 10^{-12} \text{ ergs} \equiv .794 \text{ electron-volts.}$$

$$\left[\log \frac{4\sqrt{IE_0}}{h\nu}\right]^{1/2} = 2.12$$

$k_1 = 1.37 \times 10^{-16}$ erg-seconds per degree (Boltzmann constant)

$\left[1 + \frac{2}{\epsilon^{h\nu/k_1 T} - 1}\right]^{1/2} = 1.025$ (Temperature dependence for $T = 300°$ abs.).

Substitution of these values and multiplication by 300 gives $F_\infty = 198{,}600$ volts per cm. compared with the test value of

663,000 volts per cm. Consideration of the directional field effect might raise this value by $\sqrt{2}$.

Two changes have been made in Fröhlich's formula. In his form "a" is the distance from the plus to the minus ion in the alkali-halide crystals. $1/2a^3$ then equals the number of pairs of ions per cubic centimeter. For CCl_4 this value is equal to $1/a_M^3$ whence "a" is replaced by $a_M/2^{1/3}$. λ_0 should be the wave length corresponding to the first absorption maximum in the ultra-violet but this value does not seem to appear in the literature and the limit of absorption,[8] a somewhat higher value, has been used instead and yields a correspondingly higher value of F_∞.

It is beyond the scope of this paper to criticize either theory critically. Both, it will be noted, predict the correct order of magnitude without the use of arbitrary constants, relying instead on values which are determinable experimentally without too much difficulty. An interesting critical defense of each theory is given in a pair of papers by Fröhlich [9] and by Seeger and Teller.[10]

TIME-LAG.

Breakdown occurs in a finite time only when the applied field exceeds the critical breakdown value F_∞. The excess value required for slowly applied fields is small, and the breakdown value F_b appears to be constant from about 25 to 1000 microseconds or more. But when the rate of voltage application is high the applied field F_a can rise well above the critical value during the time in which the overall breakdown is being developed. The true time-lag, measured from the time point where the slowly applied field crosses the critical breakdown value F_∞ proves to be 2.3 microseconds. As the field of the impulse wave is applied to the electrodes more and more rapidly the time-lag decreases at a slow rate. See Δt in Figs. 2, 3, 5 and 6.

For $F_a > F_\infty$ the electrons pass over the top of the "resistance" curve, encounter a rapidly declining resistance,

[8] Henrici, *Zeit. f. Phys.*, **77**, 1932, p. 35.

[9] Fröhlich, "Dielectric Breakdown in Ionic Crystals," *Phys. Rev.*, **56**, Aug. 15, 1939, p. 349.

[10] Seeger and Teller, "Remarks on the Dielectric Breakdown," *Phys. Rev.*, **56**, Aug. 15, 1939, p. 352.

accelerate and in a period of about 10^{-13} seconds acquire the (approximate) 5 electron-volts of energy necessary for ionization of the Cl^- ion and move through a distance of approximately 130 molecular spacings.

Presumably the time-lag period of approximately 10^{-6} seconds is a measure of the time required to complete the breakdown process, and in view of the shortness of the ionization time we may assume that the phenomenon is highly

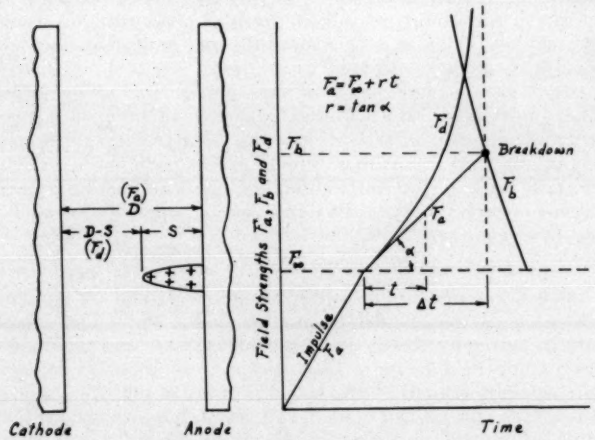

FIG. 5. Relation of field strengths and growth of streamer.

complex. Lacking detailed knowledge it is not unreasonable to suppose that the time-lag is the period required for the growth of a positive space-charge streamer which is built up in a tremendously large number of steps, each built in a very short period of time.

This process of streamer construction should begin at the anode, at least in the case of a uniform field, because of the ability of the anode readily to remove the products of ionization in the form of the ionizing electrons as well as the electrons removed from the Cl ions. The positive ion streamer becomes in effect a needle-like extension of the anode

into the dielectric. The convergence of the field around the pointed head of the streamer increases the probability of further ionization in this region and the streamer grows rapidly but in a series of steps in the general direction of the cathode until the dielectric is punctured. Conceivably the streamer may grow in a zig-zag path with the direction taken by each step being determined by local conditions. Some of the photographs of the breakdown process obtained by von Hippel [2] tend to support this view of the mechanism.

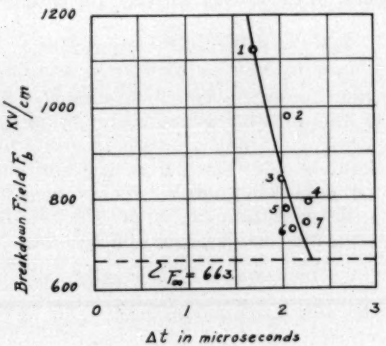

FIG. 6. Relation of time-lag to breakdown field.

Let us assume that the time required to build each step is proportional to the time required for an electron passing over the top of the resistance curve to acquire its ionization energy. The steps are then built progressively more rapidly, partly because the applied field F_a is increasing and partly because the actual field F_d from cathode to streamer head is increasing even more rapidly as the distance $D - S$ in Fig. 5 decreases.

Here $F_d(D - S) = F_aD$ and $F_a = F_\infty + rt$ with r equal to the rate of growth of applied field F_a. The rate of growth of the streamer is proportional to F_d. Then, if C is a constant,

$$\frac{dS}{dt} = CF_d = C\frac{D}{D-S}F_a = C\frac{D}{D-S}(F_\infty + rt)$$

and

$$\int_{S=0}^{D} (D - S)dS = CD \int_{t=0}^{\Delta t} (F_\infty + rt)dt,$$

giving

$$\frac{D^2}{2} = CD\left(F_\infty + \frac{r}{2}\Delta t\right)\Delta t$$
$$= CD\tfrac{1}{2}(F_\infty + F_b)\Delta t.$$

The breakdown value of the applied field F_b and the time are then dependent on each other through the simple relation

$$\tfrac{1}{2}(F_\infty + F_b)\Delta t = \frac{D}{2C} = \text{constant}, \qquad (4)$$

which is constant for any given gap spacing D. According to Equation (4) the time-lag is inversely proportional to the mean of the critical and breakdown field strengths.

The constant is determined from the limiting condition, for slowly applied fields, that $F_b = F_\infty = 663{,}000$ volts per cm. and the observed time-lag is $\Delta t = 2.3 \times 10^{-6}$ seconds. Finally, for CCl_4 the time-lag equation becomes

$$(663{,}000 + F_b)\Delta t = 3.05, \qquad (5)$$

which is plotted in Figs. 3 and 6.

SUMMARY.

Experimental data on the electrical breakdown of liquid carbon tetrachloride indicate, first, that modern theories of breakdown may be applicable to a wide range of dielectric materials provided their molecular constitution is ionic, and second, that the technically important time-lag follows a simple rule in its dependence on over-voltage.

The opportunity is taken to express appreciation of helpful comments received from Professors A. von Hippel, E. Teller and R. J. Seeger.

THE PATH EQUATION FOR MOTION ON THE SURFACE OF THE ROTATING EARTH IN A UNIFORM PARALLEL FIELD OF FORCE WITH INITIAL VELOCITY ALONG THE FIELD.

BY

W. S. KIMBALL,

Lt. Comdr., U.S.N.R., U. S. Naval Academy, Annapolis, Maryland.

INTRODUCTION.

The special case of motion in a uniform parallel force field on the earth's surface where the initial velocity equals the gradient speed but is in the direction of the field, is here investigated, using the special form of Coriolis' force that occurs under tangential accelerations on the constantly rotating earth. The gradient line across the field is shown to pass through the starting point or origin and the distance along the field which it will go before turning back towards the gradient line, $y = 0$, is found to be $c = 2.2b$ where b is the characteristic distance of the acceleration field, a, i.e., the distance along the field starting from rest that would be covered before gradient velocity will be attained across and normal to the field, as treated in the previous article.

The path equation from the origin to this maximum $y = c$ is not the same as the equation for the return path back to $y = 0$, because in the one case the acceleration term $K = 3\omega_L v_r$ of Coriolis' force supports the velocity term $C = 2\omega_L v$ whereas on the return trip the acceleration term K has experienced sign reversal and opposes C and the motion back towards $y = 0$.

Both path equations involve elliptic integrals and the approximate solution of these transcendental equations that gives the maximum $y = xb = c = 2.2b$ is also the solution of the quartic algebraic equation:

$$x^4 + 2x^3 - 3x^2 - 12x - 4 = 0.$$

The return trip back against the field from $y = c$ to $y = 0$ is made very gradually under an effective constant field equal to b^2/c^2 times the impressed field, a, or about one fifth of it.

1. THE CHARACTERISTIC DISTANCE $b = a/8\omega_L 2$ FOR A UNIFORM FORCE FIELD a ON THE SURFACE OF THE ROTATING EARTH AND THE GRADIENT LINES ACROSS THE PARALLEL FIELD FOR VARIOUS INITIAL VELOCITIES.

As previously,* we here consider motion in a uniform parallel field of acceleration, a, taken in the y direction as in Fig. 1 but specialized in this article to the case of an initial

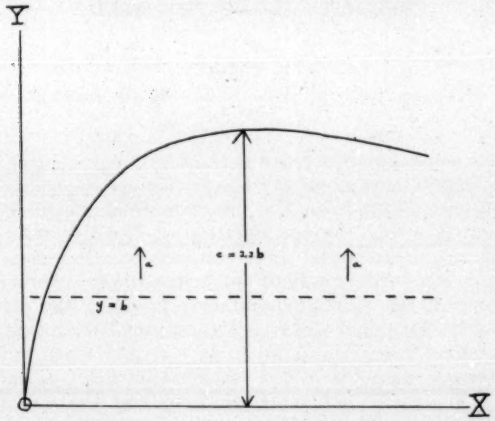

FIG. 1. The path in a uniform force field, a, with initial velocity equal to the gradient speed, but parallel to the force field and showing $c = 2.2b$ for the maximum distance along the field.

velocity at the origin in the y direction and of magnitude equal to the gradient velocity $v_0 = \sqrt{2ab}$, such as would balance the field in a steady state if directed across the field in the x direction according to the Coriolis' force equation:

$$a = 2\omega_L v_0; \quad v_0 = \sqrt{2ab}; \quad b = a/8\omega_L{}^2. \tag{1}$$

Eq. (1) give the gradient velocity and the distance b characteristic of the field strength in terms of the field, a, and the component of the earth's rotation at latitude ϕ: $\omega_L = \omega \sin \phi$.

As to the significance of the distance, b, we have seen* that unit mass starting from rest at the origin will attain

* Special Form of Coriolis' Compound Centripetal Acceleration due to the Rotating Earth. JOURNAL OF THE FRANKLIN INSTITUTE, 234, p. 453 (1942).

gradient velocity across the uniform field along $y = b$ approached asymptotically after traversing this distance b in the field direction along a curved path. And for every initial velocity not zero there will be a gradient line ultimately approached asymptotically and at a less distance in the plus y direction given by

$$y_0 = b - \frac{v_0^2}{2a} \tag{2}$$

determined by requirement (1) for all gradient velocities in the uniform field, a, regardless of initial speed v_0, this formula (2) being a consequence of the energy* equation:

$$v^2 = v_0^2 + 2ay = 2ab + 2ay. \tag{3}$$

And for the case in hand we note that $y_0 = 0$ because we are taking $v_0^2 = 2ab$, so that the x axis is our gradient line approached asymptotically by the curve of Fig. 1.

2. THE POTENTIAL ENERGY CIRCLE IS OF RADIUS c, THE MAXIMUM DISTANCE TRAVERSED IN THE FIELD DIRECTION.

Since unit mass starting from the origin will be accelerated until it reaches its maximum y according to (3), the acceleration field involved in Coriolis' force will be included between the limits of y given by $y = 0$ and $y = c$, using this letter for the maximum y shown in Fig. 1. Furthermore it will be a linear acceleration field because, as noted before, it is a combination of the constant field "a" with the harmonic field representing energy stored on the potential energy circle, and being linear with the above boundary conditions it is uniquely determined, and its kinetic energy is:

$$E_r = \frac{v_r^2}{2} = ay - \frac{ay^2}{c} = \frac{u^2}{2} - H. \tag{4}$$

Note that this is the energy, $ay = u^2/2$, acquired from the field minus that part of it stored on the potential energy circle of radius c and constant kinetic energy $v_c^2/2 = ac$ for which the y or x component of centripetal force does work:

$$H = \frac{ay^2}{c} = \int \frac{v_c^2}{c} \cos\theta dy = \int \frac{2ac}{c} \frac{(y)}{(c)} dy \tag{5}$$

* The integral of the tangential force along the path: $\int a \sin \theta ds = \int a dy$.

being harmonic motion or projection on a straight line of motion in a circle at constant speed. And the circle in question is the potential energy circle of radius c and center on the x axis whose circumference (one quadrant) approximates the path from the origin to M where $y = c$, as shown in Fig. 1. And this harmonic energy H of (5) makes no contribution to tangential acceleration since it represents energy stored as constant motion on a circle and balanced by the effect of the earth's rotation. Hence it has to be subtracted from, ay, the impressed field energy, to give (4) the energy of the tangential acceleration field.

Using this value of v_r, we have for Coriolis' force:

$$C+K=2\omega_L v+3\omega_L v_r=2\omega_L\sqrt{2a(b+y)}+3\omega_L\sqrt{\frac{2ay(c-y)}{c}} \quad (6)$$

showing the term due to tangential path acceleration as well as that due to velocity.

3. THE PATH EQUATION IN A UNIFORM FIELD FOR AN INITIAL VELOCITY EQUAL TO THE GRADIENT VELOCITY BUT DIRECTED ALONG THE FIELD.

The normal force equation that determines the path is given by balancing the Coriolis' force against the centrifugal force plus the normal component of the field:

$$\frac{v^2}{r}+a\cos\alpha=C+K, \quad (7)$$

where $\alpha = \text{arc tan } y'$, is the inclination of the path. And the curvature will be

$$\frac{1}{r}=\frac{-y''}{(1+y'^2)3/2}=\frac{d}{dy}\cos\alpha.$$

Making this substitution and using (3) and (6) gives:

$$2a(y+b)\frac{d}{dy}\cos\alpha+a\cos\alpha = 2\omega_L\sqrt{2a(y+b)}+3\omega_L\sqrt{\frac{2ay(c-y)}{c}}. \quad (8)$$

This is a linear differential equation in $\cos\alpha$ and its derivative, with integrating factor $1/\sqrt{y+b}$. We may factor out

$8\omega_L{}^2\sqrt{b} = a/\sqrt{b}$ and write it:

$$2\sqrt{b}\sqrt{y+b}\,\frac{d}{dy}\cos\alpha + \left(\frac{\sqrt{b}}{\sqrt{y+b}}\right)\cos\alpha = 1 + \frac{3}{2\sqrt{c}}\,\frac{cy-y^2}{\sqrt{(b+y)(cy-y^2)}}, \quad (9)$$

which integrates to

$$2\sqrt{b(b+y)}\cos\alpha = y + \frac{3}{2\sqrt{c}}\int_0^y \frac{(cy-y^2)dy}{\sqrt{(b+y)(cy-y^2)}}, \quad (10)$$

where the constant of integration is zero since $\cos\alpha = 0$ when $y = 0$ at the origin with initial velocity and direction along the y axis.

Under the transformation $y = c(1 - z^2)$, the integral on the right of (10) becomes:

$$\int_0^y \frac{(cy-y^2)dy}{\sqrt{(b+y)(cy-y^2)}} = \frac{-2c^2}{\sqrt{b+c}}\int_1^z \frac{(z^2-z^4)dz}{\sqrt{(1-z^2)(1-k^2z^2)}}$$

$$= \tfrac{2}{3}(\sqrt{b+c})\left[cz\sqrt{(1-z^2)(1-k^2z^2)} + 2b\int_1^z \frac{dz}{\sqrt{(1-z^2)(1-k^2z^2)}}\right.$$

$$\left. -(2b+c)\int_1^z \sqrt{\frac{1-k^2z^2}{1-z^2}}\,dz\right], \text{ using } k^2 = \frac{c}{b+c}. \quad (11)$$

When this is introduced into (10) we have:

$$2\sqrt{b(b+y)}\cos\alpha = y + \sqrt{\frac{b+c}{c}}\left[cz\sqrt{(1-z^2)(1-k^2z^2)}\right.$$

$$\left. + 2b(u-K) - (2b+c)(E(u)-E)\right] \quad (12)$$

where

$$u = \int_0^z \frac{dz}{\sqrt{(1-z^2)(1-k^2z^2)}} \text{ and } E(u) = \int_0^z \sqrt{\frac{1-k^2z^2}{1-z^2}}\,dz$$

and K and E are the complete elliptic integrals of the first and second kind given by taking the upper limits equal to unity.

We have used c for the maximum of y, where the slope and

inclination, α, of the curve are zero:

$$y = c, \quad z = 0 \quad \text{at} \quad \cos\alpha = 1, \quad \text{and} \quad u = E(u) = 0. \tag{13}$$

Hence, using (13) in (12), we have:

$$2\sqrt{b(b+c)} = c + \sqrt{\frac{b+c}{c}}\,[(2b+c)E - 2bK]. \tag{14}$$

We may solve this equation graphically for c as in terms of b, remembering that by (11) for E and K, $k^2 = c/(b+c)$.

Its approximate solution is found to be:

$$c = (2.2)b, \text{ and hence } k^2 = \frac{11}{16} = \sin^2 56°, \quad \begin{matrix} K = 2.05706, \\ E = 1.24918. \end{matrix} \tag{15}$$

If this value of c is introduced into (12), we have the equation of the path in the form:

$$2\sqrt{b(b+y)}\cos\alpha = y + \frac{4}{\sqrt{11}}\left[\frac{1}{\sqrt{3.2b}}\sqrt{(b+y)(2.2b-y)y} + 2b(u-2.057) - 4.2b(E(u)-1.249)\right]. \tag{16}$$

This formula gives $\cos\alpha$ and hence the graph to any desired degree of accuracy. Thus for five values of y we have:

$y = c(1-z^2)$	$z = \sin\phi$	ϕ	u	E	$\cos\alpha$	α
0	1	$\pi/2$	2.05706	1.24918	0	90°
$.22b = .1c$	.94868	71° 34′	1.49977	1.06213	.1388	82° 1′
$1.1b = c/2$	$1/\sqrt{2}$	45°	.84449	.73336	.642	50° 4′
$1.65b = \frac{3}{4}c$	.5	30°	.54052	.50761	.86	30° 41′
$2.2b = c$	0	0	0	0	1	0°

These values of α, the inclination of the curve for various y's from the origin to its maximum at M are shown on the graph of Fig. 1. Note that with an initial velocity $v_0 = \sqrt{2ab}$, the curve swings to the right less quickly (as is to be expected) than for the case of zero initial velocity previously treated.

Thus for y = half its maximum, the path direction here is about 50°, whereas, with no initial velocities it is about 36°, and with y = three-quarters of its maximum, we now have about 30° for path inclination, whereas formerly it was 20°.

4. THE PATH EQUATION WITH THE SAME INITIAL CONDITION $V_0 = \sqrt{2ab}$ IN THE DIRECTION OF THE FIELD, BUT FROM ITS MAXIMUM AT $y = c$ BACK TO THE GRADIENT LINE $y = 0$.

The path equations (12) and (16) apply to the curve of Fig. 1 and 2 only between the origin and M the maximum of y,

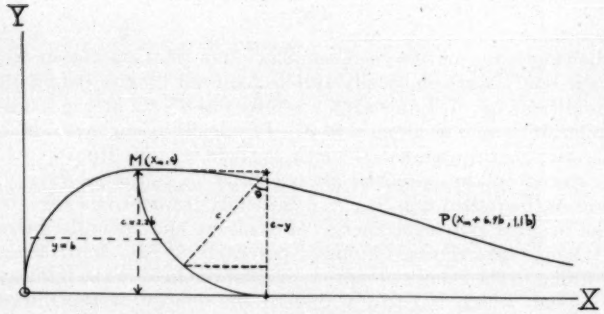

FIG. 2. The path in the uniform field showing the slow return after maximum at M to the gradient line $y = 0$, with the potential energy circle, and the point of inflection P, distant about $7b$ along the path from the maximum M.

because the differential equations (7) to (9) which yield (12) and (16) show normal force terms C and K of the *same* sign and supporting each other and causing the sharp deflection shown between 0 and M of Fig. 2. At the maximum point M, K and the tangential acceleration are zero and beyond M, K and the tangential acceleration experience a reversal in sign and become negative so that during the return trip from M to the x axis, K is working against C to reduce rather than increase the Coriolis' normal force, and instead of (7), we have

$$\frac{v^2}{r} + a \cos \alpha = 2\omega_L v - 3\omega_L v_r. \qquad (17)$$

The velocity v will still be given by (3) but the tangential acceleration field energy $v_r^2/2$ and associated normal force K are now only

$$\left.\begin{aligned} E_r &= \frac{v_r^2}{2} = \frac{ab^2}{c^2}\left(y - \frac{y^2}{c}\right) = a_r\left(y - \frac{y^2}{c}\right), \\ v_r &= \frac{b}{c}\sqrt{\frac{2ay(c-y)}{c}}, \\ K &= 3\omega_L v_r = 3\omega_L \frac{b}{c}\sqrt{\frac{2ay(c-y)}{c}}, \end{aligned}\right\} \quad (18)$$

showing a normal force K smaller than that of (6) in the ratio b/c. Mathematically this is required by the boundary conditions on (17) and (25) whereby $\cos\alpha = 1$ at the maximum M as well as along $y = 0$. Physically it corresponds to the fact that the work ac done by the field in going from 0 to M is stored on the potential energy circle as potential energy, and in the return trip to $y = 0$ is merely transformed back to the original potential energy of position and, being a mere exchange between two kinds of potential energy, contributes nothing to the energy of motion against the field in the minus y direction which is entirely due to the energy of the initial velocity ab, without which stock of supplied energy no back trip would be made towards $y = 0$, but the path would swing along $y = b$ as for the case of zero initial velocity.

It is also to be noted from (18) that not even all of the initial energy $E_0 = ab$ is available for accelerated motion back to $y = 0$, but only the fraction b/c of it: ab^2/c being the amount stored on the potential energy circle shown in Fig. 2 on the return trip from $y = c$ at M to $y = 0$. Thus, for this return trip, we have energy linear in y and independent of the path and hence due to a constant reacting force, given by:

$$-a_r = -\frac{ab^2}{c^2}, \quad \text{and} \quad E = \frac{ab^2}{c^2}(c - y), \qquad (19)$$

and for the harmonic energy stored on the potential energy

circle, we have

$$H = E\cos\theta = \frac{ab^2}{c^3}(c - y)^2, \tag{20}$$

which is the integral of the component of centripetal force where the constant energy of motion is ab^2/c in the circle of radius c shown in Fig. 2. The difference between (19) and (20) gives (18): $E_r = E - H$, applicable to the return trip instead of (4).

Use (3) and (18) to replace v and v_r of (17) and $1/r = d/dy \cos\alpha$, then:

$$2a(y + b)\frac{d}{dy}\cos\alpha + a\cos\alpha = 2\omega_L\sqrt{2a(y + b)} - 3\omega_L\frac{b}{c}\sqrt{\frac{2ay(c - y)}{c}}. \tag{21}$$

Use (1) to remove a and ω_L by division and multiply by the integrating factor $1/\sqrt{y + b}$. Then (21) becomes:

$$2\sqrt{b(b+y)}\frac{d}{dy}\cos\alpha + \frac{\sqrt{b}}{\sqrt{b+y}}\cos\alpha = 1 - \frac{3}{2}\frac{b}{c\sqrt{c}}\sqrt{\frac{cy-y^2}{b+y}}, \tag{22}$$

which integrates to:

$$2\sqrt{b(b+y)}\cos\alpha = y + 2b - \frac{3}{2}\frac{b}{c\sqrt{c}}\int_0^y \frac{(cy-y^2)dy}{\sqrt{(b+y)(cy-y^2)}}. \tag{23}$$

Here the constant of integration is $2b$, because $\cos\alpha = 1$ at the position $y = 0$, the gradient line approached asymptotically. Under the transformation $y = c(1 - z^2)$ the integral on the right becomes (11) and hence:

$$2\sqrt{b(b+y)}\cos\alpha = y + 2b - \frac{b}{c}\sqrt{\frac{b+c}{c}}\left[cz\sqrt{(1-z^2)(1-k^2z^2)} + 2b(u-K) - (2b+c)(E(u)-E)\right], \tag{24}$$

where K, and E are complete elliptic integrals of the first and second kind and u, and $E(u)$ are given by (12).

Or, introducing (15) and $y = c(1 - z^2)$, we have:

$$\left.\begin{aligned} &2\sqrt{b(b+y)}\cos\alpha \\ &\quad = y+2b-\frac{b}{c}\sqrt{\frac{b+c}{c}}\left[\frac{1}{\sqrt{b+c}}\sqrt{(b+y)(cy-y^2)}\right. \\ &\qquad \left.+2b(u-K)-(2b+c)(E(u)-E)\right], \\ &2\sqrt{b(b+y)}\cos\alpha \\ &\quad = y+2b-\frac{20}{11\sqrt{11}}\left[\frac{1}{\sqrt{3.2b}}\sqrt{(b+y)(2.2by-y^2)}\right. \\ &\qquad \left.+2b(u-2.057)-4.2b(E(u)-1.249)\right]. \end{aligned}\right\} \quad (25)$$

The path is in the x direction at its maximum $y = c$, as well as at $y = 0$ (where the bracket vanishes). Thus at $y = c$ and $z = 0$ where $u = E(u) = 0$, we also have $\cos\alpha = 1$, and hence:

$$2\sqrt{b(b+c)} = 2b+c+\frac{b}{c}\sqrt{\frac{b+c}{c}}\,[2bK-(2b+c)E]. \quad (26)$$

The bracket in (26) is the same as the bracket in (14), and when this is eliminated between (26) and (14) we have the algebraic equation giving c in terms of b:

$$c^4 + 2c^3b - 3c^2b^2 - 12cb^3 - 4b^4 = 0, \quad (27)$$

whose solution accurate to 2 decimal places is found to be $c = 2.20b$, being also the solution of (26) and (14). The fact that (14) and (26) must have this same solution is the mathematical reason that requires v_r of (18) to be smaller than v_r of (4) in the ratio b/c, because unless this factor appears in (26) it will not give this same value of c given by (14).

Eq. (25) is sufficient to graph the path as accurately as desired using the angle of inclination α and y for coordinates. The minimum of $\cos\alpha$ occurs where the curvature $d/dy\ \cos\alpha = 0$, so that (22) reduces to

$$\frac{\sqrt{b}\cos\alpha}{\sqrt{b+y}} = 1 - \frac{3}{2}\frac{b}{c\sqrt{c}}\sqrt{\frac{cy-y^2}{b+y}}. \quad (28)$$

Multiply (28) by $2(b + y)$:

$$2\sqrt{b(b+y)}\cos\alpha = 2b + 2y - 3\frac{b}{c\sqrt{c}}\sqrt{(b+y)(cy-y^2)}. \quad (29)$$

Subtract (25) from (29) so as to eliminate $\cos\alpha$. Then:

$$0 = y - 2\frac{b}{c\sqrt{c}}\sqrt{(b+y)(cy-y^2)} + \frac{b\sqrt{b+c}}{c\sqrt{c}}[2b(u-K) - (2b+c)(E(u)-E)]. \quad (30)$$

Eq. (30) is the condition on y which gives minimum $\cos\alpha$ at the point of inflection. We may solve this equation graphically, remembering that $c = 2.2b$ and using the values of u, $E(u)$, K and E given by (12) and (15) with $y = c(1 - z^2)$. Its approximate solution is $y = c/2 = 1.1b$. Using this critical value of y, the minimum $\cos\alpha$ at the point of inflection is given by (25) or (29) as $\cos\alpha = .9499$, or $\alpha = 18° 12'$ showing that in going from its maximum point M back to the gradient line $y = 0$, the path is only deflected very gradually, having about 1/5 of a right angle as the maximum deflection. If we take half this deflection as the approximate average from M to the point of inflection, then the distance along the x axis of the point of inflection from M would be:

$$c/2 \cot 9° = 1.1b(6.3138) = 6.9b \quad (31)$$

and its coordinates $(x_m + 6.9b,\ 1.1b)$ as shown in Fig. 2, whose $(x_m,\ 2.2b)$ are the coordinates of M the position of maximum y.

Surface Finish of Journals.—This subject was treated on by R. W. DAYTON, H. R. NELSON, and L. H. MILLIGAN in *Mechanical Engineering*, Vol. 64, No. 10. Their paper deals only with the effect of shaft finish on the seizure of plain bearings. Such seizure, which occurs when hydrodynamic lubrication is not maintained, is a serious problem in heavily loaded high speed bearings, such as those in the master rod of radial aircraft engines. It is known that surface finish has an important effect on the seizure of such bearings. Tests were made on an Amsler machine. Fine finishes were studied, the roughest having a profilometer reading of only 10 microinches. It was found that there was rather good correlation between the seizure results and the product of profilometer readings taken in the axial and circumferential directions. Those surfaces having higher roughness-product readings had greater seizure tendency. This was approximately true irrespective of the finishing methods employed, which included grinding, sandpapering, loose-abrasive lapping and lapping with bonded abrasive wheels, but sand-papered surfaces gave rather better than average seizure resistance and loose-abrasive-lapped surfaces rather poorer than average seizure resistance. However, a loose-abrasive-lapped surface finished by ring lapping, and therefore exceptionally free from chatters and other defects, gave exceptionally good results when extremely fine abrasive paper was used lightly to finish its surface before testing. The seizure results of all specimens also correlated well with the appearance of taper sections of the surfaces. A study by means of taper sections and photomicrographs of the mechanism of wearing-in showed that the surfaces which wore-in most readily had a very fine-scale roughness sometimes referred to as "fuzz." This fuzz is not indicated to be harmful on a journal which has sufficiently fine surface finish as to have a reasonably high initial seizure resistance. One effect that takes place during wearing-in was shown to be an extremely minute smoothing of the topmost part of the surface roughnesses, and this produced a large change in the frictional characteristics. The actual area of contact is thus indicated to be only a small percentage of the conventionally calculated area even for the finely-finished and accurate surfaces being dealt with in this investigation. Trueness and large-scale roughnesses such as waviness, flat spots, and grinding chatter are also probably very important.

R. H. O.

NOTES FROM THE NATIONAL BUREAU OF STANDARDS.*

NEW ALLOY FOR FIVE-CENT COINS.

Observant people may have noticed recently a slight change in the color of new 5-cent coins. The fact is that the familiar "nickel" no longer contains nickel. As in many other cases, the use of nickel in coinage has had to give way to more urgent military needs.

The request of the War Production Board not to use nickel in "nickels" met with a sympathetic response from Hon. Nellie Tayloe Ross, Director of the Mint. But the proposed change was far from easy to carry out. Many requirements had to be met. The new 5-cent coin had to resemble closely the old one in color and appearance and freedom from tarnish. The new alloy had to be hard enough to resist wear and at the same time take clean-cut impressions from the Mint dies. The bullion value of the new alloy had to be less than the actual value of the coins, otherwise the new coins might be melted up and used for other purposes. Finally, the new coins had to work properly in coin vending machines.

This last requirement proved to be troublesome and the Bureau of the Mint and the War Production Board requested the cooperation of the National Bureau of Standards in finding a solution. Vending machines are protected by various devices so that they cannot be operated with slugs. Consequently, it was necessary in the new alloy to match within limits the electrical conductivity, the magnetic permeability, the resilience and the weight of the old "nickel."

The Bureau at once proceeded with the preparation of samples of an alloy of equal weights of silver and copper, as well as of similar alloys containing small percentages of silicon, manganese, etc. Each alloy was prepared as an ingot or slab, portions of which were converted into specimens for chemical analysis, determination of electrical resistance, and other properties. Sample coin-selector mechanisms were obtained

* Communicated by the Director.

from eight manufacturers and their normal performance was determined by repeated use of 200 bona fide "nickels" until each mechanism had been subjected to 2,000 tests. Two mechanisms were chosen for tests on "slugs" made of new alloys—one because of its superior selectivity, the other because it was typical of units in actual use.

Although the Bureau of the Mint would have preferred a simple, binary alloy, such as copper-silver, the tests immediately showed that such coins would invariably be rejected by vending machines because of low electrical resistance. Experiments were then made with small percentages of alloying elements such as phosphorus, silicon, and aluminum, which are known to raise the resistivity of copper. While the first two increased the resistivity of the silver-copper alloy slightly, they made the alloy hard, brittle, and unworkable. Small additions of aluminum did not have much effect on resistivity, but they lowered the density and improved the working qualities, besides making the coins somewhat more resistant to tarnish.

Electrolytic manganese in various amounts was then tried, and it was found that when the percentage of manganese reached a little over 6, the alloy first showed definite signs of being acceptable in the machines. Further increases in manganese, up to 10.5 per cent., progressively increased the resistivity and improved the acceptance. The alloy containing 45 per cent. of silver, 45 per cent. of copper, and 10 per cent. of electrolytic manganese, therefore, appeared promising. Although the cold-rolled sheet was slightly harder than a similar sheet of copper-nickel (91 as compared to 85 on the Rockwell B scale), this did not appreciably affect the workability in laboratory experiments, a fact confirmed at the Bureau of the Mint, where the 10-per cent. manganese alloy was rolled, stamped, and minted in an experimental run. Except that somewhat higher pressure was required in rolling and minting, the making of these coins followed conventional procedure. Tests of the minted coins in the vending machines confirmed the evidence obtained from smooth slugs, i.e., that the 10-per cent. alloy is about as acceptable as the present nickel.

Manganese lowered the density of the silver-copper alloy

from 9.52 to 8.97 grams per cubic centimeter, but the latter figure is near enough to the value of the copper-nickel (8.77) to have permitted coins made of the new alloy to be kept to the customary weight of 5 grams per coin by a slight reduction in thickness of the planchet, and without changing the diameter. Moreover, the addition of manganese alters the golden or brassy color of the silver-copper alloy to something approaching the appearance of the copper-nickel alloy, though a slightly yellow tinge remains. A surface film of silver, produced by pickling in nitric or sulfuric acid after hot-work or annealing treatments, was believed to be too soft to result in any permanent improvement in appearance or in resistance to tarnish.

The silver-copper-manganese alloys were all inferior to copper-nickel in the matter of tarnish. When the slugs were handled repeatedly in making the machine tests, they became discolored with a dark greenish film which came off on the fingers. This might not be serious on coins in active use or where the cloth lining of pockets or receptacles would tend to remove the tarnish, but apparently it can not be eliminated.

A few four-component alloys were prepared to study the effect on the silver-copper-manganese alloy of the presence of another alloying element or metallic impurity. It was found that the addition of 2.6 percent of aluminum raised the resistivity from about 25 to 32 and produced an alloy that had a perfect record of acceptance in the machines. The density is closer to the regular nickel alloy and the workability seemed to be improved. The quaternary alloy is somewhat harder than the ternary alloy, but it is tougher and stood up better under rolling. For all these reasons, an alloy containing about 7.5 per cent. of manganese and 2.5 per cent. of aluminum appeared to be preferable to the 10-per cent. manganese alloy. Virgin aluminum would not have been necessary; aluminum-copper and certain grades of scrap could have been used.

When the Bureau started the investigation it was understood that electrolytic manganese in amounts sufficient to meet the needs of the coinage would be available. Later, the War Production Board advised that it might be necessary to substitute non-electrolytic manganese in whole or in part for the electrolytic product. Alloys were consequently prepared

by adding ferro-manganese to 8 and 9 per cent. manganese alloys to observe the effect of increasing the iron content above the usual 0.04 per cent. which is present in the alloys made from electrolytic manganese. The presence of 0.35 per cent. or more of iron renders the silver-copper-manganese alloys ferromagnetic and these were, therefore, rejected by the machines. However, 0.15 per cent. of iron was found to be permissible, but to obtain this low value would require a low-iron manganese.

Finally, a change in the silver situation made it necessary to lower the silver content of the alloy because, otherwise, the 5-cent coin might actually have been worth more than this as metal. An alloy of 56 per cent. copper, 35 per cent. silver, and 9 per cent. manganese was selected by the Bureau of the Mint as a reasonable compromise, and this is now being used in coining 5-cent pieces. As a result, it is estimated that an additional 300 tons of nickel will be available annually for the production of war materials.

THERMAL EXPANSION OF TITANIUM.

In the Journal of Research for February (RP1520), Peter Hidnert gives the linear thermal expansion of titanium (97.2 per cent.) at various temperatures between $-190°$ and $+700°$ C. The coefficient or rate of expansion of titanium increases from about $5 \times 10^{-6}/°$ C. at $-150°$ C. to about $12 \times 10^{-6}/°$ C. at 650° C. The data on thermal expansion do not confirm the conclusion by Koenigsberger and Schilling concerning polymorphic transformations of titanium at about 310° and 590° C., based on determinations of electric resistance. The results of the present investigation are in agreement with Schulze's conclusion in regard to the absence of these transformations, which is also based on resistance measurements.

EFFECT OF ALTITUDE ON KNOCK RATING.

Following the work described in Technical News Bulletin 302 (June 1942), altitude chamber tests were made at air pressures from sea level to 8,000 feet and higher on two vari-

able compression engines. These were adjusted in each case to give standard knock on fuels of from 40 to 100 octane number. The results were analyzed to determine the effect of altitude on octane number requirement. According to a paper by Donald B. Brooks before the winter meeting of the Society of Automotive Engineers in Detroit on January 14, the resulting relations are nearly identical for the two engines and are in good agreement with road tests, indicating that the effect of altitude may be expected to be about the same for all engines.

REVISED REQUIREMENTS FOR WEIGHING AND MEASURING DEVICES.

Revised specifications, tolerances, and regulations for commercial weighing and measuring devices are set forth in the Bureau's Handbook H29, which has just been released.

This revised edition incorporates all changes adopted by the National Conference on Weights and Measures and recommended for promulgation by the States, since the publication of H22 in February 1938; in other words, H29 is the same as a completely annotated copy of H22.

In providing for subsequent revisions, the new Handbook is arranged on a different plan from the old one. Instead of attaching all correction sheets to stubs at the back of the book, two or three blank pages are inserted after each of the several codes of specifications, and on these pages any corrections can be pasted, thus grouping related material and making the book handier to use.

The publication of H29 is of particular interest at this time because certain of the recommendations of the National Conference on containers, scales, etc., are being incorporated in various Limitation Orders of the War Production Board. The price is 60 cents a copy; orders should be sent to the Superintendent of Documents, Government Printing Office, Washington, D. C.

---

pH VALUES OF PHOSPHATE SOLUTIONS

A paper (RP1524) by Roger G. Bates and S. F. Acree in the February number of the Journal of Research, reports a

series of acidity values for a number of solutions of phosphates which may be used to improve the measurement of acidity and to facilitate its control. The measurement and control of acidity and alkalinity, as explained in TNB305 (September, 1942), is of almost universal importance in industrial processes which are carried out in solutions.

This control is dependent upon accurate methods of determining acidity, or "pH." The Bureau has in progress the selection and purification of substances suitable as "pH standards" and is determining their values at a number of temperatures. These compounds can be used for the calibration of measuring equipment and for the regulation of acidity in the research laboratory, factory, or wherever the problem of pH control arises.

It has long been recognized that one of the most useful standards for determining pH in the region of acidity close to that of water is a mixture of primary and secondary phosphate salts. A study of 42 phosphate mixtures at 13 temperatures between 0° and 60° C. by electromotive force methods has now been completed. The second dissociation constant of phosphoric acid and related thermodynamic quantities have been evaluated, and pH values have been assigned to each of the phosphate solutions for any temperature between 0° and 60° C.

COMBINATION OF WOOL WITH WEAK ACIDS.

Wool is often exposed during processing to solutions containing weak acids, certain of which have long been known to have profound effects on the swelling and the elastic properties of the fibers. Nevertheless, practically all studies of the chemistry of the reaction of wool with acids have been made with strong acids, i.e., those which are totally dissociated into their constituent ions. RP1523 (February *Journal of Research*) by research associates of the Textile Foundation supplies some of the missing information.

It is shown that wool combines with undissociated molecules of weak acids as well as with their ions. Because of the high concentrations of weak acids which are present in solutions of low pH values, more weak acid may be combined

by wool in the undissociated form than in the ionic form. The total amount of some of these weak acids which may be removed from solution by wool may far exceed the amounts of common strong acids which may be combined. The relative tendencies of the 13 weak acids investigated to combine with wool in the undissociated form vary over a 300-fold range. The effect of a variation of temperature on this kind of combination with wool is shown to be very small; because of this it is suggested that the combination is a solvation of the wool molecules, the weak acids displacing water which is always found combined with wool when moisture is present. If this is true, the combination of undissociated acids with wool is a result of their hydroxylic properties rather than their acidic characteristics.

WATER PERMEABILITY OF WALLS.

Building Materials and Structures Report BMS94, recently released, gives the results of water-permeability measurements made by Cyrus C. Fishburn on small stucco- and gunite-faced walls and on walls built of "Knap concrete units," before and after outdoor weathering. Six kinds of stucco facings, two thicknesses of gunite facings, and seven kinds of units were represented in a group of 26 walls.

All of the stucco- and gunite-faced walls were highly resistant to water penetration. Periods of outdoor exposure at Washington, D. C., varying from 16 to 49 months, had no important effect on permeability. The resistance to penetration of walls built of "Knap concrete units" was excellent after the walls were painted. Photographs showing the appearance of eight typical specimens add to the value of the presentation.

Copies of BMS94 are obtainable from the Superintendent of Documents, Government Printing Office, Washington, D. C., at 10¢ each.

High Speed Water Softening Process Makes Its Municipal Debut.—ALEX VAN PRAAG, JR. (*Engineering News-Record*, Vol. 129, No. 13). New to the municipal water softening field is the "Spiractor" process installed by The Permutit Co. at Teutopolis, Ill. It is a type of cold lime process water softening plant. It is the invention of Dr. E. T. ZENTNER of Czechoslovakia and has been in use for about five years in Europe where a number of plants, including some very large ones, have been installed. It is also used in England but is relatively new here and the Teutopolis is the first municipal installation. The Spiractor is a conical-shaped tank, the top diameter of which is 4.5 ft., the conical sides are 11 ft. high. The top consists of a rounded or "bumped" head fitted with a manhole and also a charging hole for catalyst. This tank is slightly more than half filled with fine granules of calcium carbonate catalyst (about 0.1 to 0.2 mm. in size). Raw water enters the bottom through a special fitting containing a tangentially disposed nozzle. Through another opening in this fitting, the proportioned dosage of lime suspension is pumped. This mixes with the upward swirling water, the flow rate of which is high enough to maintain the granular bed in a suspended condition and low enough to avoid carrying any of the granules over the top of the tank. The immediate contact of the chemically treated water and the suspended catalyst granules greatly accelerates softening reactions between the added lime and the hardness content of the water. The resulting relatively insoluble reaction products are thus formed while the water is still in contact with the granules and consequently deposit on the surface of the granules in the form of successive firmly adherent layers, i.e., accretions. Agglomeration of the granules into compact masses does not occur because the catalyst bed is maintained in a suspended condition. As water continues to pass through the Spiractor, the accretions on these granules cause them to grow in size resulting in an increase in the total catalyst bed volume until it is necessary to remove a portion of the coarsest of the enlarged granules through a drawoff valve at the bottom of the unit. Fresh catalyst is then discharged into the top of the unit.

R. H. O.

THE FRANKLIN INSTITUTE.

STATED MONTHLY MEETING, FEBRUARY 17, 1943.

The stated monthly meeting of The Franklin Institute was called to order at 8:20 by Mr. Charles S. Redding, President. The National Anthem was played.

The President announced that the minutes for the January meeting were published in full in the JOURNAL OF THE FRANKLIN INSTITUTE for February and that if no objection were raised, they would be declared approved as printed. They were so approved.

The Chairman called upon the Assistant Secretary, Dr. John Frazer, for a report. Dr. Frazer stated that since the last meeting the following additions have been made to membership:

Honorary	1
Sustaining	1
Active	100
Associate	39
Student	24
Total	165

In accordance with our usual custom Dr. Frazer then moved that the two Franklin Medalists for the year 1943 be elected to honorary membership in The Franklin Institute and proposed:

Dr. George Washington Pierce
7 Berkeley Place
Cambridge, Massachusetts

Dr. Harold Clayton Urey
355 Highwood Avenue
Leonia, New Jersey

The motion having been seconded and carried unanimously, the Chair declared these gentlemen duly elected.

Mr. Redding then introduced the speaker of the evening, Dr. Charles F. Brooks, Director, Blue Hill Meteorological Observatory, Harvard University, who spoke to a large and interested audience on the subject of "Snowstorms."

By means of slides and motion pictures, Dr. Brooks illustrated that snowstorms were caused by the interaction of cold and warm air masses and ended his talk by explaining methods of forecasting snowstorms.

His paper in full will be published in a subsequent number of the Journal. At the end of his talk Dr. Brooks kindly answered questions from the floor.

The meeting was dismissed with a rising vote of thanks at 9:55 p.m.

COMMITTEE ON SCIENCE AND THE ARTS.

(Abstract of Proceedings of Stated Meeting held Wednesday, February 10, 1943.)

HALL OF THE COMMITTEE,
PHILADELPHIA, FEBRUARY 10, 1942.

DR. JOSEPH S. HEPBURN *in the Chair.*

The following reports were presented for final action:

No. 3084: Work of Francisco Ballén.

This report recommended the award of a Howard N. Potts Medal to DON FRANCISCO BALLÉN, of Lima, Peru, "In consideration of his leadership in the scientific restoration of a valuable natural resource of high value to his country."

No. 3121: Levy Medal.

This report recommended the award of a Louis E. Levy Medal to ANDERS HENRIK BULL, of Forest Hills, New York, for his paper entitled "Soil Pressure Distribution along Flexible Foundations," which appeared in the June issue of the JOURNAL OF THE FRANKLIN INSTITUTE for 1942.

At the January 13, 1943, Stated Meeting, the following report was presented for final action:

No. 3109: Low Temperature Silver Brazing Alloys.

This report recommended the award of a John Price Wetherill Medal to ROBERT HOWLAND LEACH, of Fairfield, Connecticut, "In consideration of his development and perfection of silver alloys applicable for the brazing of similar and dissimilar metals, and exhibiting in the molten state marked properties of fluidity and wetting qualities and in the solid state producing a joint exhibiting, in light of the low melting point, outstanding ductility and strength."

This recommendation was advertised in the February issue of the JOURNAL OF THE FRANKLIN INSTITUTE.

JOHN FRAZER,
Secretary to Committee

LIBRARY NOTES.

The Committee on Library desires to add to the collections any technical works that members would wish to contribute. Contributions will be gratefully acknowledged and placed in the library. Duplicates received will be transferred to other libraries as gifts of the donor.

Photostat prints of any material in the collections can be supplied on request. The average cost for a print 9 × 14 inches is thirty-five cents.

The library and reading room are open on Mondays, Tuesdays, Fridays and Saturdays from nine o'clock A.M. until five o'clock P.M., Wednesdays and Thursdays from two until ten o'clock P.M.

RECENT ADDITIONS.

AERONAUTICS.

Aerosphere. 1942.

FREY, CARROLL. The Fist Air Voyage in America. 1943.

V.2
194

JORDANOFF, ASSEN. Jordanoff's Illustrated Aviation Dictionary. 1942.
LEE, JOHN G. Fighter Facts and Fallacies. 1942.
MANLY, G. B. Aircraft Electrical and Ignition Systems. 1942.
WELLS, T. A. Wells' Manual of Aircraft Materials and Manufacturing Processes. 1942.
MULLIGAN, JOHN A. Handbook of Brick Masonry Construction. First Edition. 1942.

CHEMISTRY AND CHEMICAL TECHNOLOGY.

BOWEN, E. J. The Chemical Aspects of Light. 1942.
BUERGER, M. J. X-Ray Crystallography. 1942.
Chemical Engineering Catalog 1942–43. 1942.
DEGERING, ED. F., AND OTHERS. An Outline of Organic Nitrogen Compounds. 1942.
ENGELDER, CARL J. Calculations of Qualitative Analysis. Second Edition. 1942.
GAETZ, HALLEY TANSLEY. Water-White Hydrocarbons from Trinidad Asphalt. 1935.
GAETZ, HALLEY TANSLEY. Water-White Hydrocarbons from Trinidad Asphalt. 1937.
GILMAN, HENRY, Editor-in-Chief. Organic Chemistry. Two Volumes. Second Edition. 1943.
HINSHELWOOD, C. N. The Kinetics of Chemical Change. 1940.
Printing Ink Makers' Association of Philadelphia. Raw Materials Used in Printing Inks. 1942.
REMINGTON, JOHN STEWART. The Paint Laboratory Note Book. 1942.
SAND, HENRY J. S. Electrochemistry and Electrochemical Analysis. Volume 3. 1942.
STOKLEY, JAMES. Science Remakes Our World. 1942.
TRESSLER, DONALD K., AND CLIFFORD E. EVERS. The Freezing Preservation of Foods. 1943.

ELECTRICITY AND ELECTRIC ENGINEERING.

FINK, DONALD G., Editor. Television Standards and Practice. First Edition. 1943.
MÜLLER, RALPH H., R. L. GARMAN AND M. E. DROZ. Experimental Electronics. 1942.
PERRY, EDGAR C., AND HARRY V. SCHAFEBOOK. Fundamental Jobs in Electricity. 1943.
PUCHSTEIN, A. F., AND T. C. LLOYD. Alternating-Current Machines. Second Edition. 1942.
SANDRETTO, P. C. Principles of Aeronautical Radio Engineering. First Edition. 1942.

ENGINEERING.

American Association of State Highway Officials. Standard Specifications for Highway Materials. Fourth Edition. Two Volumes. 1942.
HOOL, GEORGE A., AND W. S. KINNE, Editors-in-Chief. Stresses in Framed Structures. Second Edition. 1942.

GEOLOGY.

BAGNOLD, R. A. The Physics of Blown Sand and Desert Dunes. No date.
TRASK, PARKER D., AND H. WHITMAN PATNODE. Source Beds of Petroleum. 1942.

GRAPHIC ARTS.

BIEGELEISEN, J. I., AND MAX ARTHUR COHN. Silk Screen Stenciling as a Fine Art. 1942.
HOWER, RALPH M. The History of an Advertising Agency. 1939.
Photograms of the Year 1943.

HISTORY.

WILDES, HARRY EMERSON. The Delaware. 1940.

MANUFACTURES.

BERGEN, WERNER VON, AND WALTER KRAUSS. Textile Fiber Atlas. 1942.
BICHOWSKY, F. RUSSELL. Industrial Research. 1942.

MATHEMATICS.

KELLS, LYMAN M., WILLIS F. KERN, AND JAMES R. BLAND. Spherical Trigonometry with Naval and Military Applications. First Edition. 1942.
MILLER, DENNING. Popular Mathematics. 1942.
PETERS, J. Seven-Place Values of Trigonometric Functions. 1942.

MECHANICAL ENGINEERING.

HEYWOOD, JOHNSON. Grinding Wheels and their Uses. Second Edition. 1942.
NORTON, ARTHUR EDWIN. Lubrication. First Edition. 1942.
PAGE, RAY M. 14,000 Gear Ratios. First Edition. 1942.

METEOROLOGY.

STARR, VICTOR P. Basic Principles of Weather Forecasting. 1942.

MILITARY SCIENCE.

BEBIE, JULES. Manual of Explosives, Military Pyrotechnics and Chemical Warfare Agents. 1943.
HAVEN, CHARLES T. A Comprehensive Small Arms Manual. 1943.
SLOANE, ERIC. Camouflage Simplified. 1942.

MINING AND METALLURGY.

American Institute of Mining and Metallurgical Engineers Transactions. Iron and Steel Division. 1942.
BIRINGUCCIO, VANNOCCIO. The Pirotechnia. Translated from the Italian with an Introduction and Notes by Cyril Stanley Smith and Martha Teach Gnudi. 1942.

NAVAL ARCHITECTURE AND NAVIGATION.

GRIMWOOD, V. R. American Ship Models. 1942.
LANE, CARL D. The Boatman's Manual. 1942.

MANNING, GEORGE C. Manual of Ship Construction. 1942.
ROBISON, REAR ADMIRAL S.S., AND MARY L. ROBISON. A History of Naval Tactics from 1530 to 1930. 1942.

PHARMACY.

U. S. Pharmacopœial Convention. The Pharmacopœia of the United States. Twelfth Revision. 1942.

PHYSICS.

DINGLE, HERBERT. Mechanical Physics. 1942.
LUCKIESH, MATTHEW, AND FRANK K. MOSS. Reading as a Visual Task. 1942.
MACH, ERNST. The Science of Mechanics. Fifth Edition. 1942.

NOTES FROM THE BIOCHEMICAL RESEARCH FOUNDATION.

An Ultracentrifugal and Electrophoretic Investigation of an Ascitic Fluid from a Cancer Patient.—EDWARD B. SANIGAR, LAURA E. KREJCI AND ELMER O. KRAEMER. The many studies of the composition of ascitic fluid which have been made have shown that the total protein content of the fluid can vary over a wide range. The protein constituents have as a rule been determined by precipitation with the usual protein precipitants (ammonium sulfate, alcohol, etc.) and have been expressed as content of albumin and globulin. The electrophoresis apparatus of Tiselius (*Transactions of the Faraday Society*, **33**: 524, 1937) permits a more accurate determination of the albumin and globulin content, and the further differentiation of the globulin into the alpha, beta and gamma globulin fractions. Electrophoretic analyses by Hesselvik (*Acta Medica Scandinavica*, **51**: 461, 1939) and Luetscher (*Journal of Clinical Investigation*, **20**: 99, 1941) have shown that ascitic fluids contain the same protein constituents as normal human plasma, but that the percentage composition, like the total protein content, may vary between wide limits.

No previous studies have been made to determine whether the proteins of ascitic fluid resemble those of normal serum in sedimentation behavior. It seemed desirable, therefore, to carry out such an investigation by means of the Svedberg ultracentrifuge (Svedberg and Pedersen, *The Ultracentrifuge*, Oxford University Press, 1940). Parallel mobility experiments were made in the Tiselius electrophoresis apparatus, and the effects of drying the fluid by evaporation from the frozen state were also investigated.

SOURCE OF MATERIALS.

The ascitic fluid was obtained from a patient suffering from advanced carcinoma of the appendix with widespread abdominal metastases resulting in ascites. About two and one-half liters were obtained in this, the fourth, drainage.

V.2
194

The fluid contained cancer cells and was of a dark straw color with a slight pinkish tinge due to bleeding. The cancer and blood cells, together with a small amount of fibrinous precipitate, separated on ordinary centrifuging or settled spontaneously on standing. The blood serum used for comparison was obtained from a healthy fasting subject.

EXPERIMENTAL METHODS.

The ultracentrifuge runs were made in a Svedberg oil turbine ultracentrifuge using a cell of 3 mm. thickness at cell temperatures of 23.0 to 23.5° C. and speeds of 56,000 to 57,000 r.p.m., the temperature and speed being substantially constant during any one run. The sedimenting boundaries were followed by the refractive index method of Lamm, using an adjustable scale projection apparatus to obtain suitable scale displacements on the photographs. The sedimentation diagrams, such as those shown in Figs. 1 and 2, were obtained in the usual manner, and from them the sedimentation constants (s_{20}), corrected for the viscosity and density of the medium, were calculated using the accepted expression:[1]

$$s_{20} = \frac{\Delta x}{\Delta t} \cdot \frac{1}{\omega^2 x_m} \cdot \frac{\eta_t}{\eta_{20}} \cdot \frac{1 - v_{20}\rho_{20}}{1 - v_t\rho_t}$$

Electrophoresis experiments were made using standard Tiselius equipment at 0–2° C. Before electrophoresis the fluid was dialyzed against large volumes of the buffer solution used as medium for the experiment. Migration of the boundaries was followed by the Longsworth method (Longsworth, *Journal of the American Chemical Society*, **61**: 529, 1939).

EXAMINATION OF THE WHOLE ASCITIC FLUID.

The sedimentation diagrams for the untreated ascitic fluid (Fig. 1) and for the ascitic fluid after dialysis against a buffer of pH 8 containing 0.15 M NaCl and 0.02 M phosphate (Fig. 2) showed two sedimentation boundaries. The values

[1] For exact details and theory of the procedure see *The Ultracentrifuge* by Svedberg and Pedersen, Oxford University Press, 1940. The required values of v_{20} for human serum albumin (0.748) and globulin (0.745) were taken from Table 48, page 406 in Svedberg and Pedersen and adjusted to conform with Appendix II of the same treatise for values of v_t. Values of ρ_t were computed from the figures given in Appendix III of the treatise.

of the sedimentation constants for the boundaries observed are shown in Table 1. This table also shows the percentage of the two protein fractions observed in the ultracentrifuge, calculated from the areas under the sedimentation curves. In computing the concentrations of these fractions, the curves

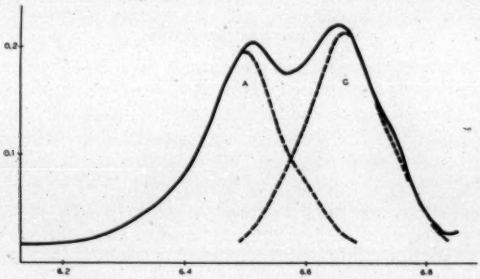

FIG. 1. Sedimentation curve for untreated ascitic fluid after ultracentrifugation for 160 minutes. A = albumin. G = globulin. Abscissas: Distance in cm. from center of rotation. Ordinates: Scale—line displacement in mm.

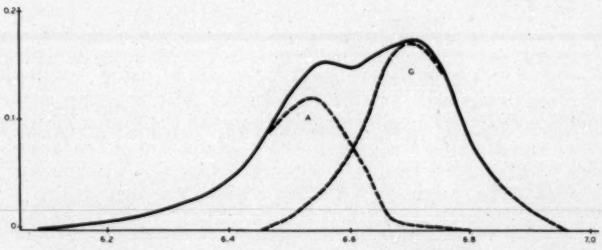

FIG. 2. Sedimentation curve for dialyzed ascitic fluid after ultracentrifugation for 160 minutes. A = albumin. G = globulin. Abscissas: Distance in cm. from center of rotation. Ordinates: Scale—line displacement in mm.

on the original sedimentation diagrams were resolved into their two components. The areas under the separate components were measured by a planimeter and were converted first into refractive increments by means of a factor involving apparatus constants, and then into protein concentrations,

using the specific refractive increments for serum albumin and serum globulin. To obtain the latter values, the specific refractive values given by Schretter (*Biochemische Zeitschrift*, **177**: 349, 1926) for sodium light ($\lambda = 589m\mu$) were adjusted to the values for light of $\lambda = 436m\mu$ (as used in the ultracentrifuge) by factors computed from results quoted by McFarlane (*Biochemical Journal*, **29**: 407, 1935; Table I, p. 412). The percentages of the protein fractions present as revealed by the electrophoretic study (Table 2) were com-

TABLE I.

Ultracentrifugal Analysis of Ascitic Fluid and of Normal Human Serum.

Fluid	Buffer	pH	Albumin		Globulin		Total Protein g./100 cc.	Dilution for Sedimentation	No. of Specimens	Total Protein, Micro-Kjeldahl g./100 cc.
			$s_{20} \times 10^{13}$	%	$s_{20} \times 10^{13}$	%				
Ascitic Fluid	—[1]	—	2.88	49	3.46	51	2.18	Undiluted	1	3.38
Ascitic Fluid	0.15 M NaCl 0.02 M phosphate	8.0	3.1	44	3.7	56	2.25	Undiluted	1	3.18
Human Serum[2]	1% NaCl used as diluent	—	2.63–3.92	—	4.47–5.95	—	5.09–8.43	2.5–6.3 g./100 cc.	11	—
Human Serum[3]	Phosphate buffer, $\mu = 0.1$	8.0	3.8	78	6.0	22	6.43	$\Delta n = .00300$	6	—

[1] Undialyzed; 0.9% NaCl used for reference run.
[2] Taken from McFarlane (*Biochemical Journal*, **29**: 660, 1935; Table 17, p. 682) for comparison.
[3] Taken from Kekwick (*Biochemical Journal*, **34**: 1248, 1940; Tables 1 and 2, p. 1250) for comparison. These figures and those quoted from Reference 2 in Table 2 refer to the same group of sera.

puted in a similar manner from the areas shown on the electrophoresis curves, using Schretter's figures for sodium light, since yellow light was used to obtain the photographs; the values are shown in Table 2. Nitrogen analyses were carried out by the Micro-analytical Department using a micro-Kjeldahl technique. The total computed concentrations, assuming a nitrogen content of 16 per cent., are shown in Table 1. The undialyzed ascitic fluid was found to have a non-protein nitrogen content of 0.03 grams per 100 cc.

The sedimentation constant for the more slowly sedimenting constituent of ascitic fluid lay in both instances within

the limits observed by McFarlane (*Biochemical Journal*, **29**: 660, 1935) for the sedimentation constant of the albumin fraction of undiluted or slightly diluted normal human serum. The sedimentation constant for the more rapidly sedimenting boundary, on the other hand, was lower than those of the globulin (G) fractions in any of the normal or pathological

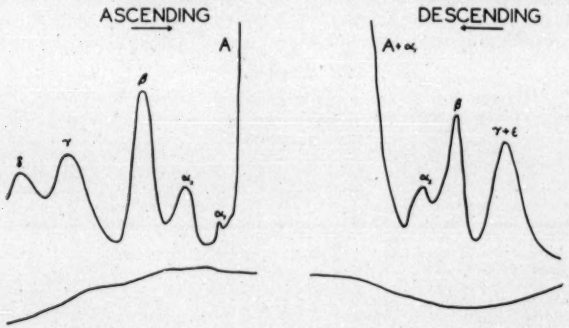

FIG. 3. Electrophoretic diagrams for normal human blood serum diluted 5 : 7 after migration for five hours at a potential gradient of about 3.5 V./cm. pH 8, 0.15 M NaCl, 0.02 M phosphate.

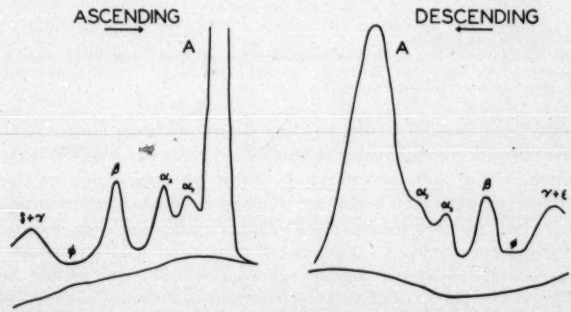

FIG. 4. Electrophoretic diagrams for undiluted ascitic fluid after migration for five hours at a potential gradient of about 3.5 V./cm. pH 8, 0.15 M NaCl, 0.02 M phosphate.

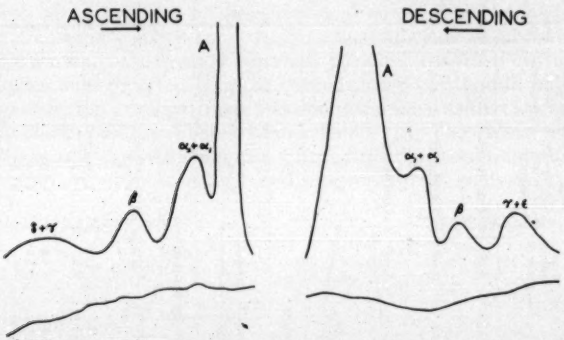

FIG. 5. Electrophoretic diagrams for dried ascitic fluid after migration for five hours at a potential gradient of about 3.5 V./cm. pH 8, 0.15 M NaCl, 0.02 M phosphate.

human sera examined by McFarlane (*Biochemical Journal*, **29**: 660 and 1175, 1935).

The electrophoretic pattern of undiluted ascitic fluid after dialysis against a buffer of pH 8 containing 0.15 M NaCl and 0.02 M phosphate (Fig. 4) resembled that of slightly diluted normal human serum after dialysis against the same buffer solution (Fig. 3) and the percentage composition was very similar. The alpha$_1$ globulin boundary was more prominent in the ascitic fluid than in the serum, and the delta boundary was fused with the gamma globulin boundary. The plateau between the beta and gamma globulin boundaries, probably due to fibrinogen, was more clearly defined in the electrophoretic pattern obtained with phosphate buffer of pH 8, ionic strength 0.1 (Fig. 6); but in this buffer the alpha$_1$ boundary was fused with the albumin boundary. The differences between the alpha globulin fractions of ascitic fluid and normal human serum are more clearly shown in Fig. 7 and Fig. 8.

In undiluted or slightly diluted normal blood serum the concentration of albumin indicated by the ultracentrifuge is greater than that given by electrophoresis (compare the data of the last line of Table 1 and the data quoted in reference 2 in Table 2; both refer to the same group of sera). This has

TABLE 2.

Electrophoretic Analysis of Ascitic Fluid and of Normal Human Serum.

Fluid	Buffer	pH	Percentage Composition						Total Protein g./100 cc.	Serum Dilution for Electrophoresis[1]	No. of Specimens	Reference
			Albumin %	α_1 %	α_2 %	β %	ϕ %	γ %				
Ascitic Fluid	0.15 M NaCl 0.02 M phosphate	8.0	52	7	9	12	3	17	3.06	Undiluted	1	—
Ascitic Fluid	Phosphate buffer, $\mu = 0.1$	8.0	62		7	14	4	13	3.08	Undiluted	1	—
Ascitic Fluid, Dried	0.15 M NaCl 0.02 M phosphate	8.0	52	15	7	10		16	3.45	Undiluted	1	—
Human Serum	0.15 M NaCl 0.02 M phosphate	8.0	60	2	5	14	—	19	6.30	5 : 7	1	—
For comparison, the observed ranges for the composition of ascitic fluid are listed below:												
Ascitic Fluid	Phosphate buffer, $\mu = 0.2$	7.7	37.5–76.3		3.4–7.7	8.5–20.0	0–7.6	7.0–39.3	0.3–3.5	1 : 3	7	1
Electrophoretic analyses of normal human serum from the literature are listed below for comparison:												
Human Serum	Phosphate buffer, $\mu = 0.1$	8.0	62.5		5.0	11.5	—	21.0	6.40	$\Delta n = .00300$	6	2
		7.7	66.3		4.5	12.2	—	17.0	6.5	1 : 4	5	3
Human Serum	Phosphate buffer, $\mu = 0.2$	7.7	64.2		8.5	16.8	—	10.5	—	1 : 4	1	4
		7.7	66.3		7.5	14.0	—	12.2	6.5	1 : 3	—	1
Human Serum	0.025 N LiCl[2]	7.8	64.4		7.9	14.1	—	13.6	6.83	1 : 4	6	5
	0.025 N LiV	7.8	69.0		6.9	12.6	—	11.4	6.51	1 : 4	6	6
	0.025 N HV	7.8	65.1		8.2	14.3	—	12.4	—	1 : 4	12	7
Human Serum	0.1 N NaV[2] 0.02 N HV	8.6	46.7	7.8	10.2	24.7	—	10.5	—	1 : 2	1	8

[1] Volume of serum : volume of serum plus buffer.

[2] V = diethylbarbiturate.

been accounted for by dissociation of some of the globulin molecules in the presence of high concentrations of albumin (McFarlane, *Biochemical Journal*, **29**: 407, 1935). For the ascitic fluid reported here the concentration of albumin indicated by the ultracentrifuge was about the same as that shown by electrophoresis (Table 1 and Table 2). The reason for this is not at present known. Equality of albumin concentration by ultracentrifugal and electrophoretic analysis has

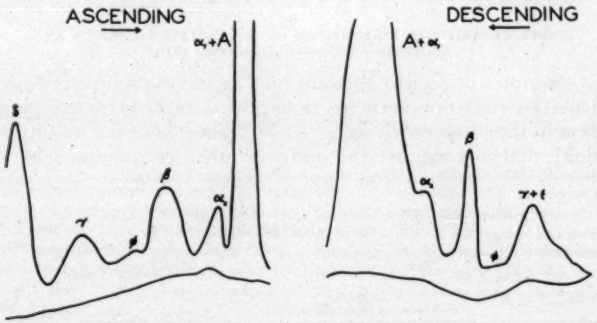

FIG. 6. Electrophoretic diagrams for undiluted ascitic fluid after migration for two hours at a potential gradient of about 8.6 V./cm. Phosphate buffer pH 8, ionic strength 0.1.

been shown to hold for serum only at low protein concentrations. The total protein content of this ascitic fluid as determined by electrophoretic and micro-Kjeldahl analyses, was high as compared with most of the values reported by Luetscher (*op. cit.*) (see Table 2), being about half the usual

REFERENCES TO TABLE 2.

1. Luetscher, *Journal of Clinical Investigation*, **20**: 99, 1941.
2. Kekwick, *Biochemical Journal*, **34**: 1248, 1940. These figures and those of the last line of Table 1 refer to the same group of sera.
3. Seibert and Nelson, *Journal of Biological Chemistry*, **143**: 29, 1942.
4. Svensson, *Kolloid-Zeitschrift*, **87**: 181, 1939.
5. Longsworth, Shedlovsky and MacInnes, *Journal of Experimental Medicine*, **70**: 399, 1939.
6. Scudder, *Annals of Surgery*, **112**: 502, 1940.
7. Moore and Lynn, *Journal of Biological Chemistry*, **141**: 819, 1941.
8. Longsworth, *Chemical Reviews*, **30**: 323, 1942.

value for normal human serum (see Table 2). The protein content estimated from the sedimentation diagrams was about 30 per cent. lower than that indicated by electrophoresis and micro-Kjeldahl analysis; the reason for this discrepancy is not clear. The ascitic fluid may have contained rapidly sedimenting material, which reached the bottom of the cell before the first photograph was taken, or, more probably, slowly sedimenting material, which experienced no measurable sedimentation during the course of the experiment.

ULTRACENTRIFUGAL EXAMINATION OF THE ISOLATED ALBUMIN AND GLOBULIN FRACTIONS OF ASCITIC FLUID.

Samples of ascitic albumin and ascitic globulin were prepared by electrophoretic fractionation of the fluid for examination in the ultracentrifuge. Electrophoresis of the undiluted fluid, dialyzed against the buffer of pH 8 containing 0.15 M

TABLE 3.

Ultracentrifugal Examination of Electrophoretically Separated Ascitic Albumin and Globulin.

Fraction	Composition (from electrophoretic analysis)	Total Concentration		$s_{20} \times 10^{13}$
		Electrophoresis g./100 cc.	Ultracentrifuge g./100 cc.	
Globulin	77% gamma globulin 5% fibrinogen 18% beta globulin	0.6	—	7.04
Albumin	90% albumin 10% alpha$_1$ globulin	0.6	0.6	4.7
Albumin	90% albumin 10% alpha$_1$ globulin	1.2	1.0	4.5
Albumin (from dried ascitic fluid)	88% albumin 12% alpha$_1$ globulin	2.0	—	3.9

NaCl and 0.02 M phosphate, was allowed to continue until the albumin and globulin boundaries were separated by the entire height of the cell.

The material isolated in the upper cathode compartment was largely gamma globulin but contained small amounts of fibrinogen and beta globulin (Table 3). The sedimentation diagram, shown in Fig. 10, disclosed the presence of a small

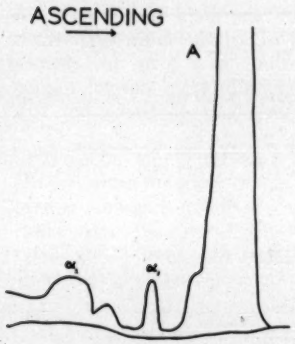

FIG. 7. Electrophoretic diagram for normal human blood serum diluted 5 : 7 after migration for five hours at a potential gradient of about 3.5 V./cm. and sixteen hours at a potential gradient of about 1.3 V./cm. pH 8, 0.15 M NaCl, 0.02 M phosphate. Ascending boundaries.

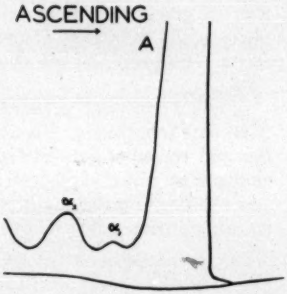

FIG. 8. Electrophoretic diagram for undiluted ascitic fluid after migration for seven hours at a potential gradient of about 3.4 V./cm. and fourteen and one-third hours at a potential gradient of about 0.4 V./cm. pH 8, 0.15 M NaCl, 0.02 phosphate. Ascending boundaries.

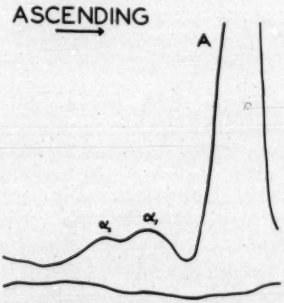

FIG. 9. Electrophoretic diagram for dried ascitic fluid after migration for five hours at a potential gradient of about 3.5 V./cm. and sixteen hours at a potential gradient of about 1.6 V./cm. pH 8, 0.15 M NaCl, 0.02 M phosphate. Ascending boundaries.

boundary both above and below the main boundary. The sedimentation constant, $s_{20} = 7.04$, of the main constituent was in good agreement with that, $s_{20} = 7.10$, for electrophoretically prepared gamma globulin from normal human serum (Kabat, *Journal of Experimental Medicine*, **69**: 103, 1939).

Pooled material withdrawn from the upper anode compartment (containing albumin, alpha$_1$ globulin, alpha$_2$ globulin, and traces of beta globulin) was dialyzed against several changes of phosphate buffer of pH 8, ionic strength 0.067. After discarding the slight precipitate deposited during dialysis, the solution was fractionated electrophoretically to remove

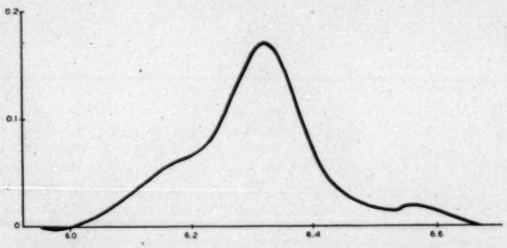

FIG. 10. Sedimentation curve for electrophoretically separated γ globulin from ascitic fluid after ultracentrifugation for 41 minutes. Abscissas: Distance in cm. from center of rotation. Ordinates: Scale-line displacement in mm.

the alpha$_2$ globulin; the alpha$_1$ globulin did not appear as a separate constituent and was not further removed. The resulting solution was dialyzed against several changes of phosphate buffer of pH 8, ionic strength 0.02; the small amount of precipitate which was formed was discarded.

This material was examined in the ultracentrifuge, both undiluted and diluted with an equal volume of buffer solution; one per cent. of sodium chloride was added to both solutions. The sedimentation diagrams are shown in Fig. 11 and Fig. 12. The sedimentation constants, 4.5 and 4.7, were in good agreement with the constant for purified human serum albumin, $s_{20} = 4.5$–4.6 (Sanigar, Krejci and Kraemer, *Biochemical Journal*, **33**: 1, 1939). The electrophoretic diagram after dialysis

against a buffer of pH 8 containing 0.15 M NaCl and 0.02 M phosphate showed the presence of alpha$_1$ globulin in the sample.

THE EFFECT OF DRYING BY EVAPORATION FROM THE FROZEN STATE ON THE PHYSICO-CHEMICAL PROPERTIES OF THE ASCITIC FLUID.

A portion of the ascitic fluid was dried by evaporation from thin frozen layers and stored at atmospheric pressure

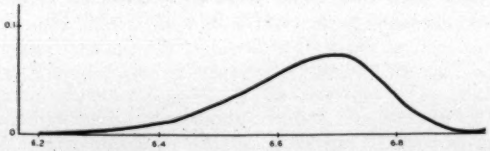

FIG. 11. Sedimentation curve for electrophoretically separated albumin from ascitic fluid after ultracentrifugation for 140 minutes. Protein concentration 1/2 of that shown in Fig. 12. Abscissas: Distance in cm. from center of rotation. Ordinates: Scale—line displacement in mm.

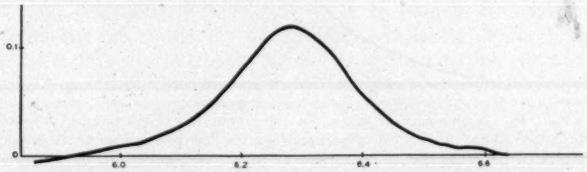

FIG. 12. Sedimentation curve for electrophoretically separated albumin from ascitic fluid after ultracentrifugation for 120 minutes. Protein concentration twice that shown in Fig. 11. Abscissas: Distance in cm. from center of rotation. Ordinates: Scale–line displacement in mm.

at 3° C. The dry residue constituted 5.2 per cent. of the weight of the fluid. The pH of the fluid reconstituted by addition of the required weight of water to the residue was 9.37; this was similar to that (pH 9.25) of human plasma after the same treatment (Krejci, *Journal of the Franklin Institute*, **234**: 596, 1942). Solution of the residue, like that of dried plasma, was accompanied by a perceptible rise of temperature.

The reconstituted fluid, like reconstituted plasma, was turbid. Prolonged centrifuging in a multispeed head, with

dry ice placed in the casing to prevent rise of temperature, removed most of the suspended matter. As with redissolved plasma, part was deposited as a sediment and part was thrown to the surface; the latter probably consisted of protein and fat. The electrophoretic pattern (Fig. 5) differed from that of the fresh fluid in that the concentration of the alpha$_1$ globulin fraction was increased at the expense of the other globulin fractions, and the alpha$_1$ globulin boundary was partially fused with the alpha$_2$ globulin boundary. The differences can be seen more clearly in Fig. 8 and Fig. 9. The

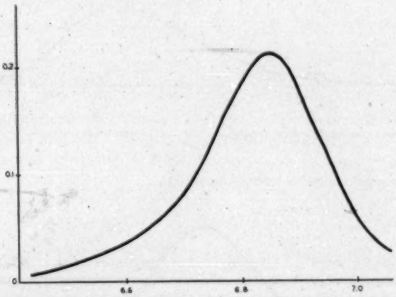

FIG. 13. Sedimentation curve for electrophoretically separated albumin from dried ascitic fluid after ultracentrifugation for 160 minutes. Abscissas: Distance in cm. from center of rotation. Ordinates: Scale—line displacement in mm.

residual turbidity migrated with the alpha$_1$ boundary. The drying of normal human plasma, on the other hand, causes little change in the electrophoretic pattern, and the residual turbidity migrates with the beta globulin boundary.

A sample of albumin was prepared from the dried ascitic fluid by the same procedure used for the separation of albumin from the fresh fluid. The sedimentation diagram is shown in Fig. 13. The sedimentation constant, $s_{20} = 3.9$, was lower than that for the albumin separated from the fresh fluid, $s_{20} = 4.5$ and 4.7. The lowering may in part have been the result of the increased concentration (McFarlane, *Biochemical Journal*, **29**: 407, 1935; Table III, p. 419). The symmetry

of the curves was good, and from the boundary spreading it appears that the homogeneity with respect to particle size was similar to that of the albumin from the fresh fluid. Brosteaux and Eriksson-Quensel (*Archives de physique biologique*, **12**: 1, 1935) found that horse serum albumin which had been dried in the presence of certain protective substances was apparently homogeneous, but had a higher sedimentation constant than before drying; while the soluble portion of serum globulin which had been dried with urea was apparently homogeneous but had a lower sedimentation constant than before drying. It is possible that the ascitic fluid may have contained some substances which, when the fluid was dried and redissolved, reduced the sedimentation constant of the albumin fraction without altering the degree of homogeneity. The same or similar substances may have been responsible also for the increase in the concentration of alpha$_1$ globulin at the expense of the other globulin fractions.

DISCUSSION OF RESULTS.

The resemblance of ascitic fluid to serum or plasma is shown by the similarity of the electrophoretic patterns and of the sedimentation behavior. The sedimentation constants for the purified albumin and globulin fractions of ascitic fluid are in good agreement with those for the corresponding fractions of normal human serum. This supports the evidence provided by the agreement of the mobilities of the electrophoretic fractions (Luetscher, *op. cit.*) that the proteins of ascitic fluid originate in the blood plasma.

The relative composition of the ascitic fluid reported here was nearly the same as that of normal human serum. This is not always so, however. In general (Luetscher, *op. cit.*) the relative composition of ascitic fluid resembles that of the parent plasma, with a higher proportion of albumin (the constituent of smaller size and greater penetrability). Since ascitic fluid is the result of a pathological condition, its physico-chemical behavior would be expected to show the same lack of uniformity and the same types of abnormalities as sera or plasma from similar pathological conditions.

The physico-chemical behavior of the ascitic fluid which we examined presented three abnormalities: an increase of

concentration and a change of boundary contour for the alpha globulin fraction; an unusually low sedimentation constant for the globulin fraction in the ultracentrifugation of whole ascitic fluid; and the absence of the dissociation phenomenon which is observed in the ultracentrifugation of undiluted or slightly diluted serum.

Many pathological conditions have been shown to alter the relative composition of serum or plasma, and febrile infections and extensive tissue destruction have been found to cause an increase of the alpha globulin fraction (Blix, *Zeitschrift für die gesamte experimentelle Medizin*, **105**: 595, 1939; Longsworth, Shedlovsky and MacInnes, *op. cit.;* Shedlovsky and Scudder, *Journal of Experimental Medicine*, **75**: 119, 1942). The variability of the sedimentation constants for the albumin and globulin fractions in serum is greater for pathological sera than for normal sera and has led McFarlane to suggest that "in pathological sera, and to a lesser degree in normal sera, a variable factor of which we have no precise knowledge influences the sedimentation of the proteins. This factor does not affect the sedimentation of purified proteins in solutions of defined inorganic composition." Few parallel ultracentrifuge and electrophoresis studies have been made on pathological sera. No pathological condition has yet been encountered in which partial dissociation of the globulin does not occur in the undiluted or slightly diluted serum.

The electrophoretic analyses of normal human sera which are listed for comparison in Table 2 show a definite consistency in the composition of sera which have been examined in any one buffer solution, and a regularity in the type of change produced by variation of buffer. The phosphate buffer of ionic strength 0.1 and the phosphate saline buffer give a low concentration of alpha$_2$ globulin and a high concentration of gamma globulin. The phosphate buffer of ionic strength 0.2 and the lithium barbiturate buffer cause a more even distribution of the globulin among the alpha$_2$, beta and gamma fractions with concentrations increasing in the order alpha$_2$, gamma and beta. A still different distribution appears (from the single analysis reported) to be produced by sodium barbiturate buffer. These variations emphasize the fact that each electrophoretic constituent represents not a

single protein but a population of proteins (Cohn, *Chemical Reviews*, **28**: 395, 1941), and that the mobilities of many are sensitive to changes in ionic environment.

The authors are greatly indebted to E. I. du Pont de Nemours and Co. for permission to use the Svedberg oil-turbine ultracentrifuge.

SUMMARY.

A physico-chemical study has been made of an ascitic fluid from a patient with advanced carcinoma of the appendix. The fundamental resemblance of ascitic fluid to human serum, already demonstrated by the similar mobilities of the electrophoretic fractions of the two fluids, is further shown by the agreement of the sedimentation constants for the purified albumin and globulin fractions. Drying by evaporation from the frozen state produced greater changes in the ascitic fluid than in normal human plasma. The influence of buffer composition on the electrophoretic pattern of human serum is discussed.

BOOK REVIEWS.

ALTERNATING CURRENT MACHINES, by A. F. Puchstein and T. C. Lloyd. 655 pages, illustrations and diagrams, 16 × 24 cms. New York, John Wiley & Sons, Inc., 1942. Price $5.50.

Practical electric power engineering requires continual consolidation of its position by crystallization of methods into standards, new and better concepts of properties and characteristics, as well as new applications of machinery based on advances in the art generally. Current literature provides definite evidence of progress in these lines. When the trial period is past the position of electric power engineering is enhanced and the methods and thought adapted to standard practice. It is at this point that a revision is necessary in texts on the subject.

The book at hand is in its second edition, the first having been published in 1936. The authors believe that sufficient progress has been made to require the revision of many parts of the text to bring it into line with present practice. The treatment starts out with synchronous generators. At this very beginning is an illustration of the changes due to the use of new standards. Here there are incorporated the recent methods of calculating alternator regulation and the new concepts of direct and quadrature axis synchronous reactance. This, of course, is reflected later under the heading of synchronous motors also. The other subjects, in order, are transformers which includes parallel operation, polyphase induction motors, single phase induction motors, synchronous motors, alternators in parallel, synchronous converters, mercury vapor rectifiers, series motors, and repulsion motors. Each of these subjects is treated in somewhat of the order of (1) construction of the machine, (2) discussion of operating characteristics, (3) calculation of operating characteristics from tests, (4) discussions and analyses of various related phenomena. Undoubtedly this rather standard method has its merits, one of which is the ordered knowledge resulting from following it.

Of necessity there are a great many drawings, illustrations, and curves throughout the work. The treatment may be classed as semi-rigorous—not brief enough or mathematically detailed to be rigorous, yet avoiding waste of time and space.

The method of working out examples is used to a great extent and, it is believed, without tiresome pursuit. The back of the book contains problems for exercise on the material in each chapter. They are carefully drawn to bring out the most pertinent knowledge. There are answers given in many cases, sufficient to give assurance that the correct procedure has been learned.

This is a good text for practical application. It fits into the classroom well. It can be used to advantage for home study for those who have had groundwork in alternating currents. It is especially valuable to practicing engineers for refresher work and reference purposes.

R. H. OPPERMANN.

THE PIROTECHNIA OF VANNOCCIO BIRINGUCCIO, by Cyril Stanley Smith and Martha Teach Gnudi. 476 pages, illustrations, 20 × 27 cms. New York, The American Institute of Mining and Metallurgical Engineers, 1942.

This translation from Italian is published by the American Institute of Mining and Metallurgical Engineers. It has been made possible by a grant from the Seely W. Mudd Memorial Fund, administered by a committee composed of Harvey S. Mudd, H. DeWitt Smith, and George Otis Smith.

Vannoccio Biringuccio was born in Siena in 1480. He was a master craftsman in the practices of smelting and of metal working. Contrary to the customs of a trade, Biringuccio imparted his knowledge to all who would be interested and thus gave the earliest printed work to cover the whole field of metallurgy, the subject of this translation. There were several editions of the work published. This translation is of the first edition published in 1540 after the death of the author. Previous to the appearance of Pirotechnia there was considerable manuscript and printed material, some of which treated on parts of the field of metallurgy. Agricola's first work on mining was published in 1530 and there were several books on alchemy, but of the 30,000 works printed in the fifteenth century, not one was on metallurgy.

Pirotechnia is a classic which should furnish background and perspective to all engaged in the metallurgical profession. The author wrote exactly as if he were speaking to interested parties of his work at the time, a fact which has made the translating especially difficult. The work is divided into ten main topics designated as books. They are headed (1) Every Kind of Mineral, in General. This covers the various ores and includes a description of the practices of making steel and brass; (2) The Semiminerals. Contains a great variety such as quicksilver, sulphur, antimony, vitriol, azure, glass, etc.; (3) Assaying and Preparing Ores for Smelting; (4) The Separation of Gold from Silver; (5) The Alloys that are Formed between Metals. These are the alloy of gold, of silver with copper and of lead and tin; (6) The Art of Casting in General and Particular; (7) Methods of Melting Metals; (8) The Small Art of Casting; (9) The Procedure of Various Works of Fire, which covers the arts of the goldsmith, coppersmith, and pewterer; (10) On Certain Combustible Materials and the Procedures Followed in Making Fireworks to be Used in Warfare and for Festivals. There are 84 illustrations and four interesting appendices.

The work is in terms of practice concerned with carrying out operations on metals for profit and use. The rugged individualism of Biringuccio prevails throughout. A surprising revelation for a 16th century work is that he recognizes ill luck as nothing but ignorance or carelessness. His evaluation of alchemy is astonishingly modern. Modern also is his realization of the advantages of large scale operation and his advice on the use of water power driven machinery in place of hand labor whenever possible. His work reflects an established capitalistic economy, an example of which is his recommendation for short shifts in mining (6 or 8 hours) but only because new and rested men enable the proprietor sooner to achieve profit.

Cyril Stanley Smith and Martha Teach Gnudi have provided here an admirable translation of a book which makes available in English a distinct contribution to culture.

R. H. OPPERMANN.

THE THEORY OF THE PHOTOGRAPHIC PROCESS, by C. E. Kenneth Mees, D.Sc., F. R. S. 1124 pages, illustrations, 16 × 24 cms. New York, The Macmillan Company, 1942. Price $12.00.

This subject has grown to such size and reached such importance that a work which serves as a digest of present knowledge of it is an essential tool. This book does exactly this. It is, in a sense, a summary based on widely scattered literature which is given as reference. Thus, the book reveals the present state of knowledge and tells how, by whom, and when contributions were made which resulted in present knowledge. The photographic process considered here depends upon the light-sensitivity of the compounds of silver only, and the photographic materials discussed are those which are formed by the suspension of halides of silver in a layer of gelatin. There is one other limitation—a chapter on emulsion-making covering various methods of procedure and their effect upon the finished product. The author explains that his knowledge of this was acquired in confidence and he is not entitled to publish such material with the frankness which would justify any publication.

The first part of the book is devoted to photographic material. This is further divided into discussions on light-sensitive material, the sizes of the silver halide grains, and the preparation and properties of gelatin. The action of light is next taken up involving sensitivity, density of the light-sensitive layer, and the effects of Clayden, Herschel, Sabattier and Albert. There is a section devoted to development and the after processes and another on the measurement of sensitivity of photographic materials, including the quantitative measurement of the relation between the image produced on a photographic material and the treatment to which it has been subjected, including exposure and development. Photographic Physics is the heading of part five. It covers the theory of tone reproduction, the physics of the developed image and, in a very interesting way, of the photographic aspects of sound recording. The last part of the book is devoted to optical sensitizing. At the end there is a subject and author index.

The subject is presented in a simple manner making it easily readable. The many illustrations, diagrams, curves and tables add much to the work. The book is the result of an exhaustive search through the literature, expert classification of the material, orderly arrangement, an intimate knowledge of the subject, and an admirable method of approach to the reader. It is a valuable addition to the literature on the technical phases of photography.

R. H. OPPERMANN.

SEMIMICRO AND MACRO ORGANIC CHEMISTRY, A Laboratory Manual, by Nicholas D. Cheronis. 388 pages plus experiments, illustrations, 15 × 22 cms. New York, Thomas Y. Crowell Company, 1942. Price $2.75.

Organic chemistry requires for its understanding a development of skills and techniques of experiment aside from a systematic study. This is true because of the fact that organic chemistry is an experimental science. Emphasis should therefore be made on laboratory work early for every student, and this means the entire laboratory procedure relative not only to the subject matter but to general matters such as exactness, cleanliness, and the development of critical thinking.

From the standpoint of the teacher and the student then, laboratory work is an important part and its presentation should be made simple and impressive.

The author presents here a laboratory manual designed to obtain all of the objectives of laboratory practice in elementary organic chemistry using the semimicro technique. He states that, since it is realized that a sudden and complete shift from traditional macro methods is usually not practicable or desirable in practically all experiments covered by the book, semimicro is paralleled with the macro method. This allows for flexibility for teachers.

There are three general parts to the book. In the first, an introduction to laboratory methods is given which includes the determination of melting points, purification of organic compounds by distillation, determination of refractive indices, and the identification of elements in carbon compounds. This is followed by a study of the preparation and properties of the simpler groups of organic compounds. Examples of these are n-decane and n-octane, ethylbenzene, acetylene, butyl chlorides and bromide, ethers, aniline, nitro compounds, acids, esters, etc. Reactions of hydrocarbons are studied as are hydroxy compounds, and aldehydes and ketones. Part three covers compounds of greater complexity and includes the preparation of chloroacetic acid, urea, substituted anilines, aromatic hydrocarbons by the Friedel-Crafts, etc., reaction. An appendix contains general information regarding the laboratory equipment, such as a list of apparatus and chemicals and reagents, as well as various tables of data useful in the calculation of experimental results.

The book, being a laboratory manual, is divided into seventy distinct experiments. These are divided into sections. Usually these comprise a brief introduction to the material of the experiment and serve to orient the student to the work to be done. For each group of organic compounds there are usually listed several preparations. Some of the experiments, which are marked, are adapted to discussion-demonstrations by the instructor. In the back of the book are various forms which indicate the information desired from each experiment and there are blank spaces for such information. The subject index adds to the value of the work for reference purposes.

This is a useful manual. It definitely shows from many angles, the advantages of the semimicro technique and at the same time provides a good course of study generally.

R. H. OPPERMANN.

COMBUSTION-CHAMBER DESIGN FOR OIL-ENGINES, by Paul Belyavin. 87 pages, diagrams, 13 × 18 cms. Cleveland, Sherwood Press, 1937. Price $1.50.

This little booklet surveys the problems, analyzes experiences, and studies the development of combustion-chamber design, pointing toward the fundamental requirements of proper design. After some 86 pages of detailed treatment, the conclusions reached for the most desirable features to have in a rational combustion chamber are (1) The compressed air in it must be in one volume concentrated as much as possible; (2) The natural turbulence in it should be of sufficient strength and correct direction, preferably not of a rotating bend; (3) Its shape should suit the fuel jets; (4) The air in it must not be cooled during compression by passing through narrow passages.

R. H. OPPERMANN.

A START IN METEOROLOGY, by Armand N. Spitz. 95 pages, illustrated, 14 × 20 cms. New York, The Norman W. Henley Publishing Company, 1942. Price $1.50.

Of increasing importance in everybody's daily life is the weather. It has a bearing on human activities, which is more than ordinarily realized. And now with the advance of such applications of science as is seen in aviation, the weather plays a fundamental rôle. Like other phenomena of nature, the weather offers a fascinating field for observation, but unlike many phenomena, it can be understood to a surprising extent by the human.

This little book is dedicated to young people who, living in a world which is increasingly conscious of the weather, want to know more about it. Examination of it reveals that it is written in a vein which appeals not only to young people but to older people as well. It explains what air is and does, what is meant by atmospheric pressure, the layers of the atmosphere, climate, etc. The weather man's tools are described and their use explained. Separate sections are devoted to the winds, clouds, the behavior of the air, and the causes of temperature changes and storms. Enough information is given to enable the reader to do his own weather forecasting and to practice it continuously with betterment of results. An interesting novelty is the cover of the book. On it has been placed a piece of chemically treated paper which is blue when the humidity is low. When the air is moist the paper will be pink and at time of change, the color will be lavender.

The reader will find the further he reads into the book the more interesting the story, and by the time the end of the book is reached there is a strong inclination to learn still more about the weather. Suggestions are given at this point for a second course in the meteorological feast.

R. H. OPPERMANN.

PUBLICATIONS RECEIVED.

The Theory and Practice of Heat Engines, by D. A. Wrangham, M.Sc. Lond., D.I.C., A.C.G.I., M.I.Mech. E. 756 pages, charts and diagrams, 17 × 25 cms. New York, The Macmillan Company, 1942. Price $10.50.

General Physics for the Laboratory, by Taylor Watson Howe. 107 pages, illustrations, charts, diagrams, 20 × 28 cms. New York, Ginn and Company, 1942. Price $2.00.

Transients in Linear Systems, by Murray F. Gardner and John L. Barnes. Vol. 1. 389 pages, charts and diagrams, 16 × 23 cms. New York, John Wiley & Sons, Inc., 1942. Price $5.00.

Constitution of Alloys Bibliography, by J. L. Haughton, D.Sc. 162 pages, 14 × 22 cms. Suffolk, England, Richard Clay and Company, Ltd., 1942.

The Forest Fights!, by the Timber Engineering Company, Inc. 47 pages, illustrations, 22 × 30 cms. Washington, D. C., Timber Engineering Company, Inc., 1942.

Combustion-Chamber Design for Oil-Engines, by Paul Belyavin. 87 pages, diagrams, 13 × 18 cms. Cleveland, Sherwood Press, 1937. Price $1.50.

CURRENT TOPICS.

Glass Fibers Used for Camouflage.—Glass, ordinarily thought of as a substance used to reveal rather than conceal, today is helping to conceal America's vital war plants against the day when they may become the target of enemy bombers. Because they are light in weight, don't decay, are unaffected by water, fresh or salt, and will not burn, fine, flexible glass fibers thinner than a human hair are being used as the covering, or garnish, for the metal mesh camouflage nets which are employed to hide strategic war production plants and other possible bombing objectives from enemy raiders. The glass fibers, manufactured by Owens-Corning Fiberglas Corporation, are spread over chicken wire and painted with designs that blend with the surrounding terrain, whether it be cultivated fields or orchards, or the houses and gardens of a village or suburb. The fibers can be painted as often as necessary to keep the camouflage design in harmony with seasonal changes in the appearance of the surrounding country side. Since the combination of metal and glass is incombustible, the nets cannot be destroyed by incendiary bombs. While the camouflage nets must be light in weight, they must be strong enough to bear the burden of snow and ice. The nets cannot rest on the roof of a building, but must be supported by a framework, as part of the value of this system of camouflage lies in the effect of depth produced by openings left in the garnish.

R. H. O.

Dry vs. Wet Grinding of Carbide Tools.—(*Iron Age*, Vol. 150, No. 15.) Among the major problems to be decided in tool shops is whether carbide tools are to be wet or dry ground. While it is entirely feasible to hand grind such tools satisfactorily either way, each method has its own peculiar advantages causing the decision as to which procedure shall be followed to rest entirely on the basis of which presents the fewest obstacles in a given plant. The major advantages and disadvantages of each method are well known. Based on field experience over the past 14 years, reported by J. R. LONGWELL, factory manager, Carboloy Co., Inc., Detroit, dry hand grinding is favored, chiefly because it presents fewer difficulties in obtaining properly ground tools. This, of course, would not necessarily hold true when tools are machine ground, as there are other factors to be considered. The difficulty of applying wet grinding to

the refinishing of carbide tools on hand grinders lies primarily in the quantity of water used. There is a decided tendency on the part of the operator to use too little water in order to keep from getting splashed. With carbide tools, using too little water is decidedly worse than using none at all; the extremes of deluge grinding or bone dry grinding are the only satisfactory means of grinding such tools. However from a practical standpoint, field experience has continuously demonstrated that operators do a better job of dry grinding than wet. Irrespective of the method used, correct grinding of carbide tools is not difficult, but centralizing all tool grinding instead of leaving such work to the individual machine operator has proved most satisfactory.

R. H. O.

Portable Ultraviolet Lamp for the Prospector.—(*Compressed Air Magazine*, Vol. 47, No. 8.) The property of certain minerals to become fluorescent when bathed in ultraviolet light is taken advantage of in mining in various ways. It helps in sorting the ore from the gangue as it comes from the workings, and in the mill it is a quick means of testing the tailings from the jigging and flotation operations. Today, it is also of aid to prospectors in their search for such minerals, one of the most important of which at this time is scheelite, a source of tungsten used principally in the manufacture of high speed tool steels. Most of the scheelite found in U. S. fluoresces a characteristic blue under properly filtered ultraviolet radiations and can be readily detected by the latter even when it is associated with other ores and gangue material that make identification with the naked eye difficult. To put this phenomenon to use, there has been developed a portable apparatus in the form of a torch consisting of a mercury arc in a bent quartz tube covered by a suitable filler plate. Current is supplied by a rechargeable 6 volt battery—the complete outfit weighing about 20 pounds. The lamp is said to have an effective range of 12 feet throughout an area of 16 square feet and has been used by the Geological Survey of the Union of South Africa to investigate the scheelite occurrences between Kakamas and Goodhouse south of the Orange River. It is authoritatively reported that tests carried out with the ultraviolet lamp on South African ores have been positive to the utmost degree and that scheelite, when exposed to the surface, becomes apparent even when in its finest powdery form, or in quantities that the assayist would record as a "trace." It has in fact already lead to the discovery of rich ore that, because of its finely disseminated form, has escaped the keen eye of the prospector for more than six years.

Prospecting after dark will reveal scheelite on the surface, whether in situ or as float, because weathering has no obscuring effect on its fluorescence. As only the mineral will glitter the prospector has a visual means of estimating the ore right on the spot.

R. H. O.

Water Pressure Project to Boost Texas Oil Output.—(*Manufacturers Record*, Vol. III, No. 10.) Approval of the first unit of a pressure maintenance project designed to boost the ultimate recovery of crude petroleum from the Nation's most important oil field—the East Texas—by at least 200,000,000 barrels was announced recently by the Petroleum Coördinator for War. The project is to be undertaken by the East Texas Salt Water Disposal Company as the first segment of a comprehensive program under which the water produced from the East Texas field in connection with the production of oil will be injected back into the lower part of the Woodbine sand in order to maintain bottom-hole pressures. The production of water, as well as of oil, has so reduced these pressures in recent years that engineers estimate that unless water is reinjected into the formation the field will yield from 200,000,000 to 800,000,000 less barrels of oil than it would if pressures were maintained at proper levels. Moreover, the flowing life of the wells would be shortened, hastening the day when large quantities of steel and other critical materials would be required for pumping equipment. The Salt Water Disposal Company's plans provide for the daily injection into the Woodbine sand of 90,000 barrels of water. This will be done through six injection wells. Ultimately, the Company's program calls for the construction of injection facilities having a capacity four times that of the initial project. It is also proposed to purchase existing salt water injection facilities having a capacity of 160,000 barrels daily, of which about 80,000 barrels is now being utilized.

R. H. O.

War Standards for Military Radio.—S. K. WOLF. (*Industrial Standardization and Commercial Standards Monthly*, Vol. 13, No. 8.) A project is now under way to set up emergency standards for military radio to help speed production of radio equipment for the Military Services, make replacements of parts easier, and conserve materials. This undertaking is being carried out through the coöperation of the Army, the Navy, the American Standards Association, the Radio Manufacturers Association, the Institute of Radio Engineers, and the War Production Board, together with the prime contractors and subcontractors. In view of the complexity of the

situation it was decided to select the field of Mica Capacitors as a trial assignment before undertaking work on the entire field. As a result of a series of meetings, a draft standard was prepared covering the entire range of Mica Capacitors from 5 to 100,000 micromicrofarads and covering all the various performance characteristics required by the Services. This has necessitated the unification of the requirements of the Services and of the prime contractors and parts manufacturers. Specifications have been developed for each size and grade of Capacitor which indicates the form of case, the capacitance, the tolerance, working voltage, and loss characteristics. As a result of this trial it was decided to use the emergency procedure of the American Standards Association to organize for a thoroughgoing job on the whole problem of materials and parts. It should be emphasized that this job is a revision and unification of existing standards now in use by the Army, the Navy, the Radio Manufacturers Association, the Institute of Radio Engineers, and individual companies, with such additions and corrections as are necessary to make a consistent and thoroughly workable series of standard parts and material requirements. For example, in the work on Capacitors it was found possible to eliminate many items now in use and varying only insignificantly from each other, while at the same time a few types were added in order to make the series sufficiently complete for all practical requirements.

R. H. O.

Non-Static Carpet Weave Is Patented.—(*The Journal of Commerce and Commercial*, Vol. 194, No. 14,967.) A method of weaving rugs and carpets so as to nullify static electricity accumulation has been patented in England by the United States Rubber Co. It provides for the interweaving of a conductive yarn throughout the pile and backing of the carpet which runs into a rubber composition-treated backing that absorbs the static electricity generated through friction. In the description of the process, it is recognized that static generated from rugs is usually increased as the relative humidity is decreased, thus accounting for the more noticeable effect of static during the winter months. The yarn, which is interwoven, may be formed of cotton or other material and it is treated to make it electrically conducting. It is threaded through the rug and along the under side of the backing and again upward to the top surface of the nap or pile. The ends of the treated cord or yarn preferably terminate at the top surface of the rug as formed by the nap. The exposed ends are preferably about two inches apart, although good results have been obtained by spacing the cord ends four or more inches apart. After the cords are drawn through the thickness of

the rug, the under side is treated to render it electrically conducting. For this purpose a coating of a rubber composition containing electrically conducting carbon black is applied to the under side of the backing. As the cords are exposed at the under side of the backing, they engage with the layer of conducting rubber and an electrical connection is formed there between. The layer of conducting rubber composition functions as a condenser and has a sufficiently great capacity to receive and then dissipate accumulation of static by leakage. By spacing the conducting elements or cords throughout the area of the rug, the static is not only discharged from a body contacting the rug but no substantial accumulation of static is possible because of the frequent displacement of the conducting elements which pass through the rug. This type of carpeting has been in use for more than a year on two floors of the Hotel Pennsylvania with successful results.

R. H. O.

New Carrier Current Air Raid Warning Device.—A device which has been developed by J. L. Woodworth in the General Electric Carrier Current Laboratory can be plugged into the house circuit to warn air raid wardens and other civilian defense officials of threatened or actual air raids. This device, which provides audible and visible warning signals, is designed to operate on 720 cycle carrier current systems now in operation on electric power lines in many U. S. cities. (Carrier current equipment is used to send impulses over the power lines to control electric water heaters, street lights, etc.) By using existing power lines to deliver such warnings, the new device would relieve telephone lines for other purposes. The warning device, which looks somewhat like an enclosed type of electric meter used in the home, is operated by a special control board attached to the carrier-current transmitter at the power station. By means of this control board, the four air raid warden signals can be transmitted over the electric power lines. When one of these signals is received by the warning device, a warning buzzer sounds, arousing or attracting the attention of the warden or other civilian defense official. The same signal which starts the buzzer also starts a motor-driven selector which begins rotating a small transparent plastic dial which is divided into four different colored sections—white, yellow, blue and red. This dial turns until the proper colored section (corresponding to the signal sent from headquarters) appears opposite a small window in the cover of the warning device. The signals may appear in any desired order, so that the indicator may go from yellow or blue direct to white, for example. A miniature 110 volt lamp, operating behind the colored dial or window provides the illumination to make visible the colored

signal: yellow for preliminary caution, blue for advance caution, red for air raid, and white for all clear. The special control board can also send signals which will operate sirens, fire-whistles, traffic lights and other warning devices.

R. H. O.

Clogged Gas Lines Cleared With Portable Steamer Units.—F. O. CRAWFORD. (*The Oil Weekly*, Vol. 107, No. 9.) Steaming out of oil lines to remove paraffin deposits and other waxlike accumulations has been used successfully on both lease and trunk oil lines, but it remained for the Illinois-Iowa Power Company to adapt this procedure to the clearing of gas lines. A 4-inch line of this company, used 14 years to transport carbureted water gas 22 miles from the Centralia, Illinois, gas plant to the distribution mains of Mt. Vernon, Illinois, was known to be restricting flow, but as compressors were used and a pressure of 100 pounds per square inch could be maintained at the gas plant, the required volume was delivered at the end of the line. When the system was changed over from carbureted water gas to natural gas with field pressures ranging only up to a high of 35 pounds, the situation became acute. The problem was immediately posed of how to remove the accumulation of coal tar, which had been compressed and sent along the line during the time of transmission through the line. This accumulation was so serious as to demand instant action if the deliveries were to meet Mt. Vernon requirements. Three months after the change-over it was impossible to handle the minimum requirements through 38,000 feet of line. Arrangements were completed for an auxiliary supply, and plans made to attempt to steam out the accumulated tar residue from the line. Portable flash boilers were secured, two units being employed to expedite the work. The clogged line was dug up at 1000 foot intervals and then, due to extreme cold weather and excessive deposits, this interval cut to 500 feet between cuts. Steam was fed into each of these cut sections, in the direction of normal gas flow, under an available maximum initial pressure of 300 pounds per square inch and the blow maintained until the section showed no further flow of tarry residue from the open end. Cut sections were reunited with couplings or the abutting ends welded after completion of the steaming process. Steaming of the line over the period required to melt and force from the cut section the accumulated tarry residues was found to heat it enough to cause marked expansion at the free end, this elongation amounting in some instances to as much as 5½ inches. Provision for shrinkage to former dimensions had to be included in any method of joining the cut sections.

R. H. O.

Flame-Priming Method of Preparing Steel Surfaces for Painting.—Research into the protection afforded steel surfaces by painting indicates that the preparation of the surface is equally as important as the paint itself. So states E. W. DECK in *Iron Age*, Vol. 150, No. 17. While the beneficial effects of painting on a clean, warm, and dry surface have long been realized, it was not until the oxy-acetylene flame-priming process was introduced several years ago that all three of these desired conditions could be achieved. The flame-priming process consists of "scrubbing" steel surfaces with a series of closely spaced oxy-acetylene flames that have an extremely high temperature and velocity. As a result, all mill scale that is not tightly bonded is popped loose by sudden thermal expansion, and physically adsorbed and chemically combined water is driven off from any rust that is present, leaving stable oxides in their place. At the same time other contaminants such as oil and acid salts are consumed or disintegrated by the flames. The surface is then swept or wiped free of loosened foreign material, and painted while still at an elevated temperature. This procedure not only brings about improved corrosion resistance of the paint coating, but also increases cleaning and painting rates and reduces setting time for the paint. As a further advantage, painting can be carried out under conditions of low ambient temperature or dampness which would otherwise cause major delays. The time saved with the process is of particular importance at the present when continuous production without delays in the fabrication and painting of steel is required. The term "flame-priming" is designated for the process at the suggestion of many industrial users. It is felt that the word "priming" best expresses the effect of the process, not only upon the surface to be painted but because it also implies an effect upon the paint coat itself. In addition to cleaning and drying the surface, it heats the metal, thus giving the subsequent paint coat the effect of a low-temperature bake. For this reason, flame-priming would seem a more expressive term than flame-cleaning, descaling, or dehydrating. These latter terms are still widely used for those applications where no paint is applied in conjunction therewith or where it is applied at a later date.

R. H. O.

Radio Parts Tested Under Extreme Temperature Ranges.—(*Refrigerating Engineering*, Vol. 44, No. 4.) Engineers operating a new "cold room" for testing radio parts—located in Kansas City—really have to be "quick change artists." No sooner does the thermometer go soaring up to tropical jungle levels of 150° F. or hotter, than it turns tail and goes skidding down to 40° below zero

or thereabouts. These temperamental temperatures are created to check the performance of precision radio parts under extreme conditions. Such equipment includes sound detection instruments for the Navy, delicate detectors for anti-aircraft use and similar apparatus which must stand up under the diverse climates of various parts of the globe. Solution to the problem is the "cold room" which is an 8 by 12 ft. room lined with 8 in. of cork insulation in the walls and floor, 10 in. in the ceiling. Equipment supplied by Carrier Corporation, Syracuse, N. Y., was used throughout to produce the maximum low temperatures of − 40° F., and consists of a 50 h.p. refrigerating compressor with a diffuser installed in the center roof panel of the room. A boiler and humidifier to produce the high humidity needed to simulate Caribbean conditions are likewise used, with a battery of electric strip heaters to produce temperatures above 150° F. in a few moments time. Equipment undergoing the test is put through the full range of temperatures and checked every ten degrees for operating efficiency, and has included radio equipment ranging from a large transmitter the size of a refrigerator down to microscopic electrical parts. Rubber-gasket pneumatic seals are used on the double door entrance through which all test equipment moves, and seal the "cold room" effectively against cold or heat leakage. Period of test varied with the type of equipment being checked, ranging from an hour for some parts to eight hours for vastly important two-way sets for stratosphere bomber and fighter plane sets. Use of the cold room through this wide range of temperatures has developed several improvements in aerial radio manufacture, notably new insulation and the use of less contractile metals for vital electrical connections and wiring.

R. H. O.